Sowing the seeds of acoustic trapping

Towards rapid isolation of extracellular vesicles

Havers, Megan

2025

Document Version:
Publisher's PDF, also known as Version of record

Sowing the seeds of acoustic trapping:
Towards rapid isolation of extracellular vesicles

Megan Havers

LUND
UNIVERSITY

Doctoral Dissertation

by due permission of the Faculty of Engineering, Lund University, Sweden.

To be defended in Belfragesalen, BMC D13, Sölvegatan 19, Lund

at 9:00 AM on the 9th of May, 2025

Faculty opponent

Professor Richard Oleschuk

Department of Chemistry, Queen's University, Canada

Public defence
May 9th, 2025, 09:00 in Belfragesalen, BMC D13, Sölvegatan 19, Lund, Sweden.

Supervisors
Prof. Thomas Laurell
Dr. Andreas Lenshof
Dr. Thierry Baasch
Department of Biomedical Engineering, Lund University, Lund, Sweden
Dr. Mikael Evander
AcouSort AB, Lund, Sweden

Faculty opponent
Prof. Richard Oleschuk
Department of Chemistry, Queen's University, Kingston, Ontario, Canada

Examination board
Prof. Christelle Prinz
Department of Physics, Lund University, Lund, Sweden
Prof. Aman Russom
Department of Protein Science KTH Royal Institute of Technology, Stockholm, Sweden
Docent Elin Esbjörner Winters
Department of Life Sciences, Chalmers University of Technology, Gothenburg, Sweden

Chairman
Assoc. Prof. Christian Antfolk
Department of Biomedical Engineering, Lund University, Lund, Sweden

Cover illustration
Watercolour interpretation of acoustic trapping *by Alice Bjaaland*

ISBN(s): 978-91-8104-410-2 (printed) & 978-91-8104-411-9 (electronic)
Report No. 3/25
ISRN: LUTEDX/TEEM-1142-SE
Printed by Tryckeriet, E-building, Faculty of Engineering, Lund University, Lund, Sweden

Preface

In 2020, when this thesis was no more than a tiny speck of an idea, the covid pandemic was spreading across our planet. This coronavirus (SARS-CoV-2), although a hundred times smaller than a hair's width, was seemingly everywhere - only nobody could see it without powerful microscopes. At that time, I had not yet been introduced to extracellular vesicles - equally small nanoparticles which are ubiquitous across biological kingdoms. Fascinatingly, they have been found to both facilitate and suppress disease progression. This makes them an excellent target for both diagnostics and therapies. As a nanoscientist, my interest was piqued when Professor Thomas Laurell suggested on a zoom call that I could investigate improving the isolation of these increasingly topical nanoparticles, to aid clinical and fundamental research, by acoustic trapping in a microfluidic chip.

Using the microfluidic platform may be simple, but improving it required considering a broader perspective on acoustic trapping: *How does it work? How can its performance be measured? Which parameters could be changed to improve the performance of nanoparticle trapping? What value can this technique give to researchers in biomedical applications?* Whilst these questions are too extensive to be answered exhaustively in this thesis, I hope that the included work demonstrates some steps towards answering them. As always in research, more questions emerged through observations along this journey, which is reflected in the extensive background and outlook that this thesis encompasses.

For readers less accustomed to the world of science, I invite you to read the popular science article printed on pages iii to v. I hope it gives you a taste of the value and potential of the work captured in this compilation thesis.

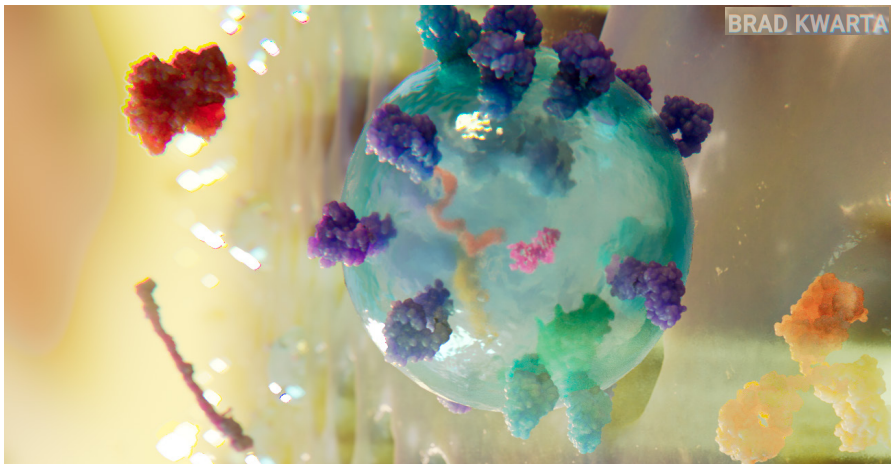

Representation of an extracellular vesicle with surrounding proteins. Reproduced with permission from the illustrator Brad Kwarta.

Trapping packets of health information

In our blood, sweat and tears we all make our own useful nanoparticles. These particles carry information about what is going on in our bodies. They are painless to collect via body fluids and may tell us a lot about our health. The exciting news is that medical researchers have the technology to read the molecular 'messages' that these nanoparticles carry. The challenge is that the particles are very tricky to isolate from a sea of complex biological 'noise'. Now biomedical engineers may have the key to separate the noise and help medical researchers read the messages.

Megan Havers - PhD student of Biomedical Engineering at Lund University.

Scientists call these nanoparticles, 'extracellular vesicles' (EVs) and have shown that they transport a wealth of information between our cells. The biologist's toolbox is well suited to handle cells but not the trillions of EVs in every millilitre of blood, which are 100 times smaller, around the size of viruses. EVs have been isolated by using centrifugation - a traditional cell-separation technique - but scaling these methods down to the nano-scale is not ideal. It means that lots of EVs get lost, whilst the processes take many hours and are labour intensive.

At Lund University, we have found an innovative approach to solve these issues, **acoustic trapping.** The principle is similar to a magnetic field which levitates small particles. However, it uses ultrasound to generate a localised acoustic field which applies acoustic forces on particles.

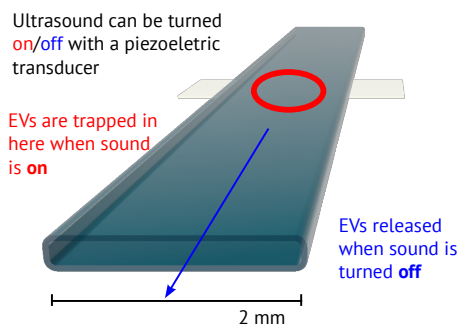

Acoustic trapping *uses ultrasound (sound above the frequency range of human hearing) to generate forces to capture particles from a liquid, within a glass tube. This trapping unit is narrower than sewing thread in its smallest dimension and can be hooked up to syringes to function like a pipette (which transfers small volumes using suction). With the use of micron-sized sound scattering beads (pre-loaded into the red region), even nano-sized particles can be isolated and retained against fluid flow.*

The International Society of Extracellular Vesicles explained that "specific issues arise when working with these entities [extracellular vesicles], whose size and amount often make them difficult to obtain as relatively pure preparations, and to characterize properly".

The promise of acoustic trapping

EV research using traditional techniques is often deprioritised when resources are limited. The powerful thing about acoustic trapping is that it is quick, and it can trap EVs from even a few drops of body fluid. This lowers the bar for EV research to take place with precious samples.

Our research group in Lund which pioneered this new way of working with EVs has led to a small company **'AcouSort'**, who have sent trapping units worldwide. Within the next decade, these trapping systems may be used in personalised medicine, since they could help monitor health of people at a reasonable timescale and with automation.

Eva-Maria Krämer-Albers, Professor of Biology, says "*As a new signalling modality, extracellular vesicles display a diverse role for robust functional regulation of neurons through their protein and nucleic acid cargoes.*"

How EVs tell us about health

Right now, it is research facilities, especially here in Sweden, which are harnessing acoustic trapping in EV studies. The acoustic trapping expertise has been combined with powerful protein detection methods to reveal the cargo of EVs.

Doctors can use new information to diagnose diseases but also monitor patients to allow early intervention and inform treatment. The individual EVs contain DNA, enzymes, fat and a wide variety of proteins which come from the cells from which they originate. Both the number of EVs and the content in any individual will vary depending on health of the organs.

For example, cerebrospinal fluid (CSF) contains EVs from the brain and therefore analysing its content may show early evidence for Alzheimer's and Parkinson's diseases progression in patients.

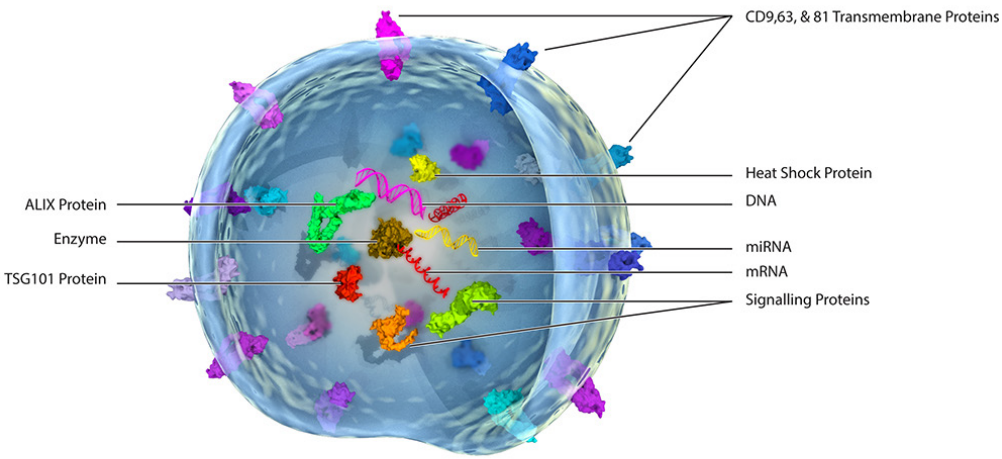

Cross-sectional illustration of an extracellular vesicle. *Various proteins and nucleic acids (DNA and RNA) are encapsulated by a lipid bilayer membrane, which has transmembrane proteins. The expression of these biomarkers depends on the parent cell. Reproduced with permission from the illustrator Brad Kwarta.*

Furthermore, if EVs are isolated from blood this could give evidence of various forms of cancer without requiring invasive surgeries. Even better, the results can be monitored over time for a patient, to personalise the treatment. New techniques to access the information held by EVs, such as acoustic trapping, are key to accelerating these exciting improvements in medical treatments.

The old 'gold standard' - ultracentrifugation

At school, you might remember swinging your bag in a circle and being amazed that nothing fell out - so long as you kept spinning. Similarly, if you spin a bucket of water, it won't spill. This works because the water has momentum away from the swinger, the apparent outward force is referred to as the centrifugal force.

With a bucket of water containing sand, you can sediment the sand grains to the bottom if you spin it fast enough. This centrifugation method is the most popular trick that scientists use to separate particles in a fluid. However, the smaller the particles, the faster you have to spin. So, if you were trying to sediment EVs in a bucket by hand, you would have to spin around thousands of times per second!

Ultracentrifugation uses extremely fast spinning motors and can isolate very small particles from blood. This has been used in most studies of EVs so far, however there are many downsides to this technique when compared with acoustic trapping. Not least of which is the 72 hours processing time required to get access to the smallest EVs, even with extremely fast spinning. New developments mean that acoustic trapping can isolate EVs in less than 10 minutes.

In acoustic trapping, the small size of the system means we can get more information out of small volumes of fluids. The new system is also much more automatable. Replacing ultracentrifugation with a better, faster isolation technique is what gives Alzheimer's researchers hope in investigating EVs from precious patient samples.

The frontiers of isolation

Acoustic trapping to isolate EVs is already providing invaluable medical data. In the Laurell research group, we have isolated EVs from the spinal fluid of people with Alzheimer's. Whilst recent research had found a clinical difference in the levels of certain proteins in spinal fluid, looking at the EVs told a different story.

We still don't know what role these EV cargo proteins have in Alzheimer's disease - the EVs could be a symptom, causing the spread of, or even trying to fight the disease. However, there does seem to be a difference in how these proteins are transported by EVs in affected patients.

We also can combine specific recognition with acoustic trapping to isolate EVs which have a specific surface protein. This works similarly to lateral flow tests used for COVID-19, there were tiny particles coated in antibodies that recognised proteins known to be on the surface of the virus.

In the future, improvements to this technique, such as specifically isolating EVs from neurons in the brain, may clear up some of the questions about Alzheimer's disease. By knowing if and how EVs are helping or hindering disease deterioration, we can design better treatments. Perhaps our own EVs will even be harnessed as vaccines to makes us healthier in the future.

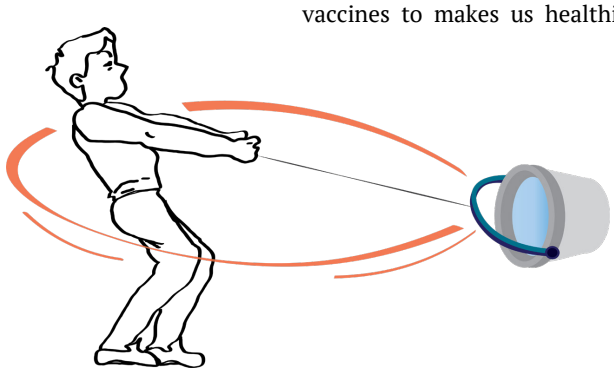

Illustration of the apparent centrifugal force: observed when water does not pour out from a bucket if it is swung around. *The person swinging the bucket pulls it by a string attached to the handle. Centrifuges (or faster ultracentrifuges) are used in many applications, for example to remove yeast after making beer and by scientists separating cells or EVs from blood before medical tests.*

Abstract

Extracellular vesicles (EVs) carry biological information from their parent cell to other cells in the body. To intercept and decipher this information necessitates the isolation of EVs from complex backgrounds such as blood or spinal fluid. Acoustic trapping has been previously demonstrated as a promising technique for EV isolation from cell media, blood plasma and urine. The acoustic fields struggle to directly trap these nanoparticles, however the presence of seed particle clusters can enable sub-micron particles to be trapped. In this work, we combat the limitations of efficiency and throughput in acoustic trapping of nanoparticles by replacing polystyrene seed particles with silica seed particles. The first paper uses 270 nm polystyrene as model nanoparticles to visualise the improved trapping efficiency of 40-2000% from suspensions of $10^{10} - 10^{11}$ particles/ml. Silica-based seed particles experience higher retention forces, allowing faster processing times (less than 10 mins per sample): which is demonstrated for polystyrene nanoparticles (**Paper I**), plasma EVs (**Papers II** and **IV**), and cerebrospinal fluid (**Paper III**). In the second paper, mass spectrometry proteomics data demonstrates that by acoustically trapping EVs we enrich EV proteins and enable detection of proteins too low in abundance in unprocessed plasma. In the third paper, EVs from cerebrospinal fluid of Alzheimer's patients have been found to contain differing phosphorylated tau proteins (via p-tau 181 and 217 assays) when isolated by acoustic trapping. This requires further investigation to elucidate the relationship between the cargo of brain-derived EVs and pathology. The final paper of this thesis presents a novel technique for co-isolating subpopulations of EVs via antibody-functionalised silica seed particles, that we have named immuno-acoustic trapping. Acoustic trapping using silica seed particles shows great promise as a purification step and

has already begun to reveal the protein content of extracellular vesicles. Immuno-acoustic trapping opens up the possibilities to also explore the association between the surface proteins that indicate their origin and the internalised cargo of EVs.

List of papers

Included papers

I. **Silica seed particles improve the efficiency and throughput of nanoparticle acoustic trapping**
M. Havers, T. Baasch, A. Lenshof, M. Evander, T. Laurell
Published in: Physical Review Applied 2024; 21(034016):1-16;
DOI: https://doi.org/10.1103/PhysRevApplied.21.034016.

Author's contribution: major part of planning the experiments, carrying out the experiments, and data analysis. Responsible for writing first draft and editing.

II. **Accessing the proteome of extracellular vesicles via rapid acoustic isolation of a minute human blood plasma sample**
M. Havers, A. Scott, N. Ortenlöf, C. Welinder, S. Ekström T. Baasch, A. Lenshof, M. Evander, M. Gram, T. Laurell
Submitted to: Analytica Chimica Acta.

Author's contribution: major part of planning the experiments, large part of carrying out the experiments, large part of the data analysis, and responsible for writing first draft and editing.

III. Phosphorylated tau in cerebrospinal fluid-derived extracellular vesicles in Alzheimer's disease: a pilot study
R. Sattarov, **M. Havers**, C. Orbjörn, E. Stomrud, S. Janelidze, T. Laurell, N. Mattsson-Carlgren
Published in: Scientific Reports 2024; 14(25419):1-18; DOI: https://doi.org/10.1038/s41598-024-75406-0.

Author's contribution: major part of planning the experiments, major part of carrying out the experiments with acoustic trapping, nanoparticle tracking analysis and microscopy. Part of the data analysis and major part of writing and editing. Not part of carrying out the p-tau assays.

IV. Immuno-acoustic trapping: towards extracellular vesicle sub-population
A. Broman*, **M. Havers***, R. Sattarov, T. Laurell
Submitted to: Analytical Chemistry.

Author's contribution: major part of planning the experiments, major part of carrying out the experiments with acoustic trapping, nanoparticle tracking analysis, and microscopy. Part of the data analysis, major part of writing and editing. Minor part of mass spectrometry preparations.
* Authors 1 and 2 share first authorship

Papers not included in this thesis

V. Advancement and obstacles in microfluidics-based isolation of extracellular vesicles
M. Havers, A. Broman, A. Lenshof, T. Laurell
Published in: Analytical and Bioanalytical Chemistry 2022; 415: 1265–1285; DOI: https://doi.org/10.1007/s00216-022-04362-3.

Author's contribution: large part of literature search, major part of writing and editing.

Acknowledgments

THANKS are due to all those who have made the completion of this thesis possible. I already know this will become an extremely long section and yet it is perhaps the most important - for without the many friends I have made along the way, I wouldn't have enjoyed this process nearly as much.

I think it appropriate to lead with thanks to the person who offered me the privilege of becoming a PhD candidate, my supervisor, **Thomas**. I could say plenty about the 5 years you've supervised me, so I'll *try* to keep it short. You are a fine example of a leader. To see the way you plant academic seeds and watch them grow, with compassion and regular watering, has truly been a lesson I will take with me for life. I know it's not as easy as you make it look. You've taught me to trust the process and to stand up for my ideas. Although sometimes our conversations could do with an intervention to keep them under three hours, I couldn't have asked for a better person to ask questions and spark ideas with.

To my co-supervisors, **Andreas**, **Mikael** and **Thierry**. The ever-present, the trap-father, and the theoretician, you know who you are. You each played an important role in my development as an independent researcher and I am grateful for all the important lessons you have offered me. **Johan**, I reckon your role has been almost a supervisor at times, thank you for many valuable discussions - I wish I had half of your patience and calm. **Ingrid**, thank you for being such a joy to talk to and for trusting me with the position of JäLM representative whilst you have been Head of Department - it came at a perfect time and empowered me to advocate for women and minorities in science.

I want to offer my greatest thanks to my amazing collaborators and lab-gurus in chronological-ish order: **Jen**, **Jakub**, **Roman**, **Niklas**, **Anna**, **Lotta**,

Simon, **Marc**, and **Aaron**. Thank you for sharing your time, your thoughts, and your words with me. Lotta, *du verkade alltid pigg (inte en gris) på morgonen*!

Per and **Pelle**, I met you right at the beginning and you taught me a lot about microfluidics, keep up the great research and enthusiastic teaching. The acoustofluidics family has grown so large and it has been nice to work with you all. The Covid-era was resolutely defined by the international PhD crew of **Richard**, **Felix**, **Franzi** and **Enrico** - you helped me to love snowboarding and beer... but most of all you helped me settle into Lund and were always keen for a laugh and a chat. When **Qing** joined the E-house, I knew I had found solid friend - you can *always* have a hug and you are one of the kindest, strongest people I know. BME time was made especially more fun by **Mahdi**, **Eva**, **Alex**, **Amal**, and **Xing**. **Cecilia** and **Axel** helped me both in the lab and out over these 5 years - both for a listening ear on my harder days and for sharing tears of laugher when the madness struck - *tack så mycket*. I can't list *all* of the **AcouSort** team here, but you were such a warm group and I appreciate you all for welcoming me in for a summer. *Stort tack* also to **Stani**, **Nora**, **Jonathan**, **Simon**, plus **Mira** and **Selma** who came into the world along the way.

Speaking of little people, I want to mention my younger brothers, **Jack** and **Harry**. You may not be so little any more but I hope that one day I can answer all of your biggest questions. Although, I am sorry Harry, I'll never be able count up to infinity! To my dad (**Karl**), thanks for trying to understand these nano-things - here's some more light reading for you to enjoy(!). Thanks also to the rest of my family, and especially to **James**, **Edmund**, Auntie **Claire** and Uncle **Rob** for your enthusiastic support of my research.

Back in England, I have so many wonderful women that inspire me from afar. My mother (**Louise**) and sister **Roma** come first in my life and shaped me completely. I see a lot of your qualities in myself: lively, independent, and hard-working. You inspire me both to keep growing and to slow down when I need to; I wouldn't be the woman I am today if it were not for you both. To 'The Nest' - I was so so lucky to meet you when we were Abbey girls, more than a decade ago. **Alice**, **Anah**, (Sarah) **Arissa**, **Georgia**, **Jasmine**, **Maya**, **Nikita**, **Tanisha** and **Victoria** - what incredible, loving, strong, and intelligent individuals you all are. I could write an essay for you each but I'll keep it to *'ily'* or you'll make me cry again. Alice's contribution is the most tangible, it is her we must thank for the beautiful cover art. Thank you for your talent and

dedication to bringing my vision to life: I would be happy for anyone to judge this book by it's cover!

Rebecca and **Ian**, you are both great scientists and great friends - plus it seems we all shared the great idea to re-join the EU after Uni. You both got me through my undergraduate studies in York and your long-distance calls since then have always been appreciated. Thanks for the support and for coming to visit me in Scandinavia. To my colleagues/friends/housemates from our **Merck**-y year in Chilworth, thanks for teaching me work-life balance!

Achilles, I could joke that you followed me to Scandinavia but that would underplay how happy I am that you've been by my side here. No-one makes me laugh like you do and you can transform even the worst days with a warm hug. I once dubbed 'the Achilles effect' that annoying spike in my profilometer measurements when you hit the lab bench at Merck... but maybe its putting life in perspective when I got the PhD tunnel-vision. Whether we are travelling the world, cycling in Copenhagen or lazing in Lund, life is exponentially more fun with you in it. *Merci, mon meilleur ami*.

Megan Lois Havers
Lund, April 10th, 2025.

Acronyms and abbreviations

AD Alzheimer's Disease

Aβ β-Amyloid

BAW Bulk Acoustic Waves

BCA Bicinchoninic Acid

CSF Cerebral Spinal Fluid

CU Cognitively Unimpaired

DDA Data-Dependent Analysis

DIA Data-Independent Analysis

ELISA Enzyme-Linked Immunosorbent Assay

EV Extracellular Vesicle

FACS Fluorescence Activated Cell Sorting

FFF Field-Flow Fractionation

MS Mass Spectrometry

MSD Meso Scale Discovery

MVB Multivesicular Bodies

NFT Neurofibrillary Tangles

NP Nanoparticle

NTA Nanoparticle Tracking Analysis

PBS Phosphate-Buffered Saline

PCA Principal Component Analysis

PET Positron Emission Tomography

P-Tau Phosphorylated Tau

RIPA Radioimmunoprecipitation Assay

RNA Ribonucleic Acid

SAW Surface Acoustic Waves

TEM Transmission Electron Microscopy

Contents

Part I

Thesis summary (*Kappa*)

Chapter 1
Introduction

Blood tests are extremely useful for diagnosing and monitoring a whole host of health conditions. A life-changing example is daily blood glucose monitoring for people with diabetes. Our circulatory system connects the vital organs and transports all sorts of molecules which can tell us what is going on in our body without the need for invasive surgery. So why can't we easily diagnose and monitor all health conditions with blood tests - like cancers and Alzheimer's disease? In many cases it is because there is not a clear target. Diseases can be localised to an organ, for example in the brain where there is a substantial barrier to the blood, which makes any useful diagnostic targets available in low concentration and with uncertain origin.

Fortunately, scientists have found some useful packages of information which may be traced back to the type of cell which produced them, via some molecular signposts on their surface. There are particles smaller than cells, extracellular vesicles (EVs), so-called because they are found '*extra-*' or *outside of* cells, in all of our body fluids in fact. Due to the ways that EVs bud off from the membranes of cells, they are made up of the molecular components from the original cell. Accessing and decoding these components by purifying EVs from body fluids could help in the challenge of deciphering health indicators without having to directly access the cells.

This thesis concerns an approach that aims to isolate these biological nanoparticles, in order to facilitate access to more information contained within or associated with them. The approach taken here is an isolation technique called acoustic trapping. As it sounds, this uses technology to control the motion of particles with sound. This is performed in miniature systems with ultrasound, at frequencies within the range used for medical imaging.

Much like how charged particles can be moved around by electric fields or magnetic fields act on magnetic particles at a distance, acoustic fields act on particles which have a property we call acoustic contrast. An acoustic trap consists of an acoustic field with a hotspot where particles with acoustic properties different to the surrounding medium can be levitated. Such a system can be generated by vibrating a fluid-filled glass tube at its resonance frequency. Particles made of plastic, glass or organic material (such as cells) which are denser than water get pushed into the acoustic hotspot. Sound waves scatter due to different speed of sound in the particles' material than the media (water or similar), this leads to radiation (acoustic trapping) forces acting on the particles.

These trapping forces can be strong in localised fields that are generated by high frequency sound waves. Larger particles (greater than 1 micron in diameter) may be trapped easily and can be held in place against fluid flowing quickly through the channel. Smaller particles need some help to be trapped, since the radiation forces on individual particles scale proportionally to the particle's volume. It is possible to trap even very small particles when they come in close proximity to larger sound-scattering particles. These helper particles are named *seed particles*, and they have been used to trap extracellular vesicles from blood and other body fluids. Acoustic trapping is performed within a microchannel, meaning the method can handle very small volumes of blood; only a few droplets. The microchannel is mounted like a pipetting robot and fluid control is automated, making it practical to process and dispense samples sequentially.

This approach allows for enrichment and washing of EVs, removing the molecules dissolved in the fluid which would otherwise dominate the signal in many analytical techniques. Pre-processing the samples by isolating the EVs enables downstream analysis to measure the less abundant proteins transported by EVs. The aim is to use this information to identify useful markers of health and disease. By using effective EV isolation methods, targeted research could also help elucidate valuable medical knowledge, since these nanoparticles are currently being investigated as culprits and therapeutic agents in many disease mechanisms.

The idea behind acoustic trapping

Trapping is a technique for separating particles of interest from a mixture. Unlike using a filter or a technique continuously diverting particles away from other content, to trap a particle means holding it stationary whilst the unwanted components can be cleaned away. Trapping particles with acoustic fields can be quite an effective method, but the challenge is in holding the particles of interest tightly enough, whilst washing away the residue as efficiently as possible. This technique is non-contact, meaning the forces act at a distance. With electric or magnetic fields, charged particles can be manipulated and the direction of motion depends on the sign of the charge (positive or negative). In acoustic fields, the direction of the force on a particle depends on the sign of its acoustic contrast.

Somewhat like how a heavy stone will fall downhill to a valley where there is lower gravitational potential energy... a tiny dense particle will fall into a potential well which has lower acoustic energy density - which is also where the pressure is fluctuating the least. Force fields push or pull particles, like magnetic attraction or repulsion of magnetic objects, but specially designed non-uniform fields can trap particles in a levitation hotspot. We create sound fields by vibrating a glass tube at its resonance frequency, where the sound waves constructively interfere, this results in areas of higher pressure fluctuation (*anti-nodes*). Simultaneously, a *node* (the levitation hotspot) can form where there is no pressure fluctuation. In our device, we form a single node in the middle of the fluid-filled capillary. The acoustic fields we use to trap particles can enable us to hold particles which scatter sound at the centre of the capillary. Like light, sound scatters at an interface between different media. For sound, the greater the difference (or *contrast*) in density and compressibility, the greater the difference in sound-speed and the stronger the scattering that results. Particles with these properties can be more easily trapped by acoustic radiation forces.

When particles get smaller, they get more difficult to trap individually. However, if larger sound-scattering particles (seed particles) are in the mix, they can amplify the acoustic forces. We can pre-load the trapping region with a cluster of seed particles that experience strong radiation forces, before introducing the hard-to-trap nanoparticles. Ultimately, this means we can trap *very* small particles, as long as they too scatter sound.

The exact mechanism of nanoparticle trapping is still up for debate and is, in part, discussed in later sections of this thesis. However, it has been demonstrated that biological nanoparticles containing valuable clinical information, known as extracellular vesicles, can be isolated by acoustic trapping.

How can acoustic trapping expedite clinical research?

Clinical research on diseases is increasingly counting on liquid biopsies. Take Alzheimer's disease, where early diagnosis before symptom onset is critical. Monitoring of Alzheimer's patients in the clinic is moving from brain imaging to spinal fluid analysis, and towards blood tests. Finding a specific marker in blood is the ultimate goal, as it would allow widespread screening not feasible with expensive positron emission tomography, magnetic resonance imaging, and invasive lumbar puncture for cerebrospinal fluid collection.

The problem is that blood is *seriously* noisy. To detect a molecular blood biomarker transported in a subset of extracellular vesicles (EVs) which made it through the blood-brain barrier into the cardiovascular system would require extremely specific and sensitive techniques. One way to combat this is to employ purification techniques, such as enrichment of EVs, or a subset of EVs, and removal of free-floating non-vesicular components - as can be achieved with acoustic trapping. This is useful for increasing the detectability of the target for whatever downstream analysis is occurring. This is especially true for a protein analysis technique such as mass spectrometry, where the signal is dominated by components from one extremely abundant protein in blood plasma.

EVs are heterogeneous and although it is thought that different sub-populations may drive independent biological responses or be produced under different conditions - challenges in isolating these nanoparticles mean that the clinical value of EVs has not yet been fully exploited. This thesis tackles the need for better techniques for isolating biological nanoparticles from complex biological fluids. Taking a microfluidics-based approach, acoustic trapping is designed with small volumes in mind. The self-contained set-up described in this thesis has automated fluid handling, making it more reproducible than manual pipetting methods and better suited to handling a few tens of microlitres.

Furthering research via acoustic trapping of extracellular vesicles

Acoustic trapping is not a new technique for isolating EVs from blood plasma and urine, however uptake in the EV research field has been limited. Partly, this was due to the time taken for sample processing before recent developments, that is limited by the flow rates at which the trapped particles can be retained, but it is also due to a lack of understanding of the technique itself.

This thesis takes a holistic approach to developing the field of acoustic trapping towards rapid and clinically relevant EV isolation. The work that follows explores the role of sound-scattering microparticles, which are used to enable nanoparticle trapping. We have pushed the boundary on the maximum flow rates used, to increase the speed of sample processing. The acquired knowledge has been applied to acoustically isolate extracellular vesicles from both blood (of a healthy individual) and cerebrospinal fluid (of a 40-patient cohort including Alzheimer's patients).

1.1 Aim and scope

This thesis aims to expand the understanding of acoustic trapping of nanoparticles, improving the technique and applying it to extracellular vesicle purification for biomedical research. The general goal is to have a rapid purification step for isolating EVs from small volumes of biofluids, that can enable the discovery of the biological functions of these entities and their role in diseases. Here, we focus on isolating EVs collected from cell-free spinal fluid and blood plasma.

- *Hypothesis 1:* Increasing the density of seed particles can improve the throughput and efficiency of acoustic trapping of nanoparticles.

- *Hypothesis 2:* Extracellular vesicles can be isolated by acoustic trapping from less than 10 µL of blood plasma.

- *Hypothesis 3:* Acoustic trapping can aid the investigation of the cargo of extracellular vesicles in the cerebrospinal fluid of Alzheimer's patients.

- *Hypothesis 4:* Immunoaffinity isolation coupled with acoustic trapping enables the isolation of sub-populations of extracellular vesicles.

- *Overarching question:* What are the mechanisms behind acoustic trapping of nanoparticles?

This research was experimental in nature and works towards several broader aims of clinical research. In this work we are aiming to extract useful, specific medical information from *small volumes* of biofluids, with high *throughput*. We refer to increasing throughput, in the sense of increasing the number of technical replicates and patient samples that can be processed in a given time period. Being able to process small volumes of biofluids is valuable for many reasons. First, more information can be gained if more studies can be done on the finite volume gathered from patients. Second, in animal studies, where the aim is always to use fewer and smaller animals, being able to obtain information from the little biofluid available could facilitate valuable research. Third, reducing sample volumes is inevitably favourable for limiting the processing time in microfluidic techniques, moving closer to rapid isolation of EVs. Ultimately, the goal is to develop this technology and increase the valuable information that clinicians can obtain from liquid biopsies. Each hypothesis will be addressed towards the end of this thesis summary.

1.2 Thesis outline

This compilation thesis comes in two parts. This first part is the thesis summary ('kappa' in Swedish), which aims to put the research work in context and also to summarise the main points of the papers. The research manuscripts themselves are reproduced, constituting the second part of the doctoral thesis.

In **Part I**, following this general introduction to the thesis work, **Chapter 2** contextualises this thesis by introducing aspects of nanoparticles and microfluidics pertinent to this research. This background chapter proceeds to provide more detail in sections concerning extracellular vesicles and acoustic trapping. This frames the *what* and the *how* hinted at in the title of this thesis 'Sowing the seeds of acoustic trapping: Towards rapid isolation of extracellular vesicles'. **Chapter 3** introduces important techniques and methods used in the research. The purpose of this chapter is to motivate the choice of methods and to provide understanding of the experimental techniques relevant to this research. This chapter also offers some more technical detail on the acoustic trapping system itself and some experimental considerations.

Chapter 4 briefly outlines the papers included in this thesis. For each of these research publications, the main aims and results are highlighted alongside an illustrative figure. At the end of the thesis summary, **Chapter 5** discusses the significance and future outlook of this work. The limitations and opportunities offered by each outcome are discussed and some remaining questions are highlighted. Finally, the four papers constituting this compilation thesis are included in **Part II**. The titles are also listed on pages ix to x, with statements on the author's contribution.

1.3 Ethics

An ethics review board approved the relevant procedures in **Papers II** and **IV** (Identification number 2020-05818) and **Paper III** (Id. nr. 2013/494), using donor blood and cerebrospinal fluid, respectively. The studies using human-derived biofluids (rather than synthetic particles) were designed to use minimal material whilst having sufficient replicates for biomedical value.

Chapter 2
Background

Acoustic trapping uses acoustic forces to hold particles in position against flow. This technique sits within the wider field of acoustofluidics, where *sound* is used to produce acoustic pressure fields in micro-scale *fluidic* systems. This chapter aims to motivate the use of acoustic trapping applied to isolating extracellular vesicles, as well as highlighting some of the research gaps and challenges in the technique for applications concerning nanoparticle isolation. To properly discuss nanoparticles and microfluidics, it is prudent to first introduce the length scales involved in each, Section 2.1 briefly explores this and some important phenomena in microfluidic systems. The remaining chapter will be divided in two main parts: Section 2.2 will give an overview of extracellular vesicles and Section 2.3 will present relevant technical background in acoustofluidics.

Neither the derivation of theoretical microfluidics, nor the mathematics describing the acoustic-wave propagation and perturbations, is within the scope of this thesis. Many important equations have been comprehensively introduced in the book *Theoretical Microfluidics*, published in 2007 by Bruus [1]. A more general textbook *Fluid Mechanics, course of theoretical physics* translated from the work of Landau and Lifshitz in 1987 [2], is also a good reference point for questions on the mathematics including fluid motion, diffusion and sound. Another useful book is *Microscale Acoustofluidics* [3] by Laurell and Lenshof, published in 2014, which encapsulates both theory and applications relevant to the field. A systematic literature review on microfluidics-based isolation of extracellular vesicles was published in 2023 as part of this PhD work (listed as **Paper V** - not included in Part II) and goes beyond what is discussed in this thesis [4].

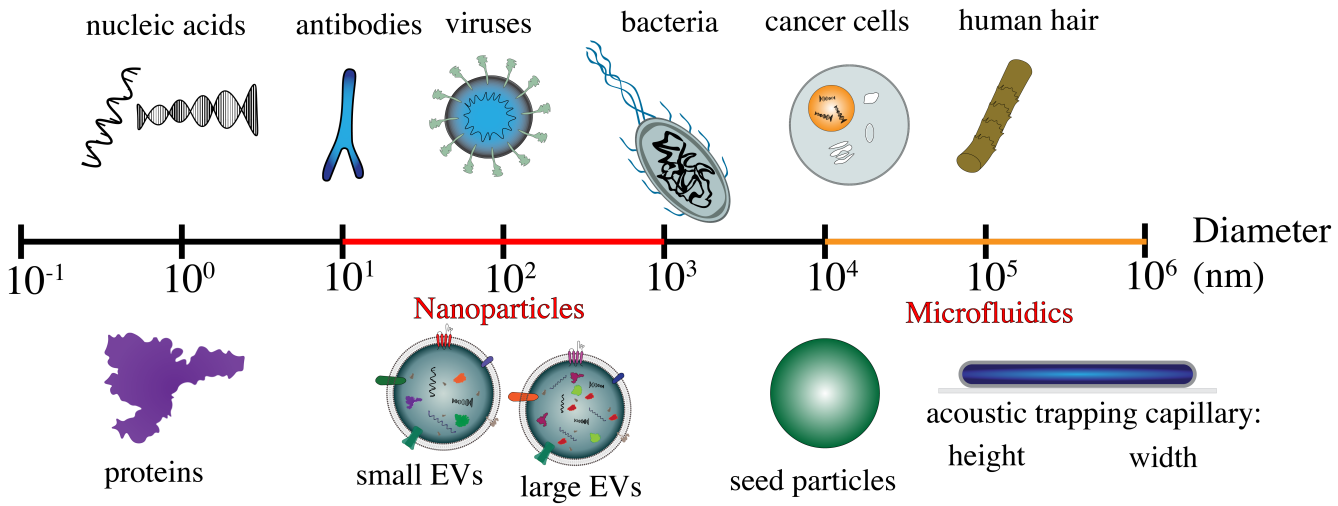

Figure 2.1: Schematic scale from 1 Å to 1 mm, illustrating approximate diameters of biological matter as well as the approximate scale of nanoparticles and microfluidics relevant to this work. Copyright ©2024, The Author(s) [5].

2.1 Nanoparticles and microfluidics

Microfluidics gained traction as a field of research towards the end of the last century, relying on fabrication of micrometre-scale structures which are designed for handling small volumes of fluid [6]. Fuelled by advancements in micofabrication techniques – such as lithography [7], etching [8], and more recently high-resolution 3D printing [9, 10] – complex microsystems have emerged over recent decades. As a symptom of scaling down fluidic channels, their surface area to volume ratio increases and the effect of fluid viscosity dominates over inertia. Thus, laminar flow streams emerge whilst turbulence is suppressed. Laminar flow is characterised by the fluid following predicable adjacent flowlines and thus lends itself to deterministic fluid handling. Many microfluidic devices take advantage of this for applications concerning manipulation and separation of microscale particles [4].

As particles become smaller, their movement becomes increasingly dominated by Brownian motion, leading to diffusion which makes separation challenging. Despite the challenge of diffusion, sub-micron particles have been isolated using microfluidics-based devices with advanced design [11–16] and by incorporating acoustic [17], electric [18], and magnetic [19] fields. The research herein concerns the technique of acoustic trapping in a micro-scale capillary (of cross-section 200 µm x 2 mm), where seed particles (10 µm diameter) can be directly trapped and nanoparticles (40 – 300 nm diameter) both synthetic (such as polystyrene) and biological (such as extracellular vesicles) can be indirectly trapped by scattered ultrasound. These concepts will be described in more detail in the following sections. Figure 2.1 provides context for the approximate scales we are working with when we refer to nanoparticles and microfluidics.

2.1.1 Fluids at the microscale

The equation of motion of a fluid's volume element can be described by Newton's second law: $\boldsymbol{F} = m\boldsymbol{a}$. For a unit element, of mass-density (ρ) and acceleration $\frac{d\boldsymbol{v}}{dt}$, upon the action of a force $-\nabla p$ (the gradient of the pressure over that element) we can write [2]:

$$\rho \frac{d\boldsymbol{v}}{dt} = -\nabla p. \tag{2.1}$$

It is from this simple relation that the more useful Euler's and Navier-Stokes equations were ultimately derived [2]. These equations underlie many phenomena in fluid dynamics; for a more in-depth theoretical background the reader is referred to the textbooks recommended at the beginning of this chapter. In this work, fluid flow is driven by pressure gradients, through narrow channels, at relatively low flow rates (we will be considering volumetric flow rates below one millilitre per minute). Although fluid dynamics can be complex to describe mathematically, the motion of fluids in microfluidic channels can be predicable. Microfluidic systems usually handle aqueous fluids in channels with small geometries, through which fluids tend to creep smoothly in layers, with low Reynolds numbers. Since viscous forces dominate over inertial effects as geometries are scaled down, the flow profile observed will depend on the shape and size of the microfluidic channel. The resulting deterministic nature of flow in microfluidics, allows for predictable, precise, and efficient control of fluid.

Laminar flow

As this thesis deals with microfluidics, where the length scales are much smaller and the viscous forces tend to dominate, the layers of fluid move parallel to each other and the channel walls. This is the phenomenon of *laminar flow*, sometimes called creeping or Stokes flow. In 1883, Osborne Reynolds investigated the transition between steady and unstable flow, controlled by the flow velocity [20]. A beautiful illustration of the scientist performing these experiments can be seen in Fig. 2.2. Photographs obtained using the same apparatus as Reynolds, a century later by Johannesen and Lowe [21], are shown in Fig. 2.3. These flow patterns show that flow between two walls with the same dimensions can be laminar or turbulent depending on the flow rate. These experiments led to the introduction of a dimensionless number that predicts how turbulent flow will be, the Reynolds number $\boldsymbol{Re}$, defined as [2]:

$$\boldsymbol{Re} \equiv \frac{\rho v_0 L_0}{\eta}, \tag{2.2}$$

where ρ and η are, respectively, the density and viscosity of the fluid. The parameters v_0 and L_0 are the characteristic velocity and length scales. So for low fluid velocities and small length scales applicable to microfluidic systems,

the Reynolds number is very small $\boldsymbol{Re} \ll 1$. A low $\boldsymbol{Re}$ (< 1500) corresponds to laminar flow. Whereas, a high $\boldsymbol{Re}$ (> 2500) corresponds to turbulent flow.

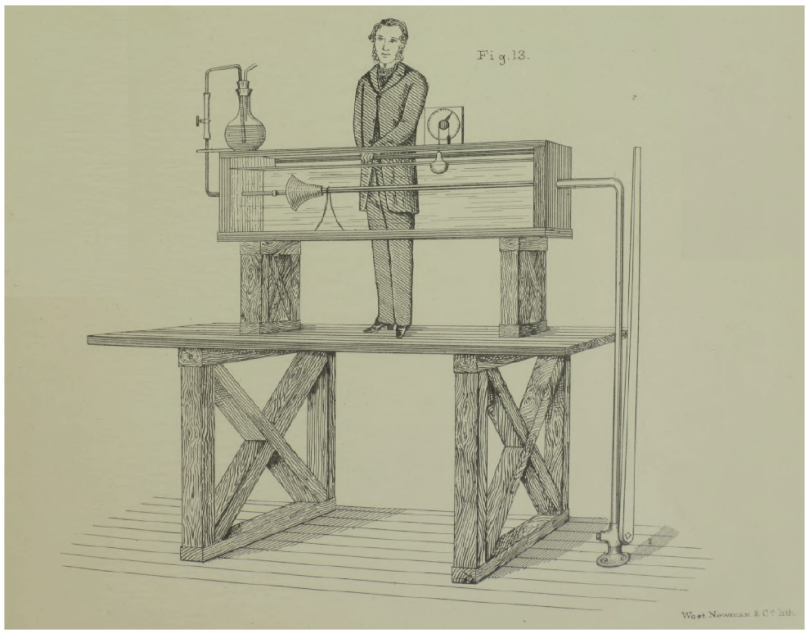

Figure 2.2: Illustration of Reynolds' experimental set up. The glass tube (5 feet long with a diameter of 1 inch) is shown, in which he observed the phenomenon where fluid exhibits steady flow or eddies depending on the flow velocity. Used with permission of The Royal Society (U.K.), from [20]; permission conveyed through Copyright Clearance Center, Inc.

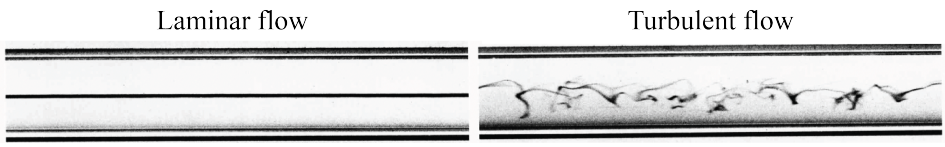

Figure 2.3: Laminar flow can be observed by an undisturbed filament of coloured water, which is disrupted as the flow speed is increased and transitions to turbulent flow. Photographed by N. H. Johannesen and C. Lowe, reproduced from [21].

Microfluidic flow profiles

When flow is driven in a microfluidic channel by applying pressure, such as with syringe pumps, constant laminar flow can be generated. Although flow-lines are parallel, the magnitude of the velocity of fluid close to walls tends to differ from fluid at the centre of the channel. This has been explained mathematically by the no-slip boundary condition (for a steady-state flow through a straight channel) meaning that an a element of fluid touching the wall will have the same velocity as the wall (often zero) [22]. This *Poiseuille flow* results in geometry-dependent flow profiles. In general, we observe that fluid progresses faster through the centre of a microfluidic channel than at the sides, as shown in Fig. 2.4.

The flow of incompressible Newtonian fluids (such as water) can be predicted by the Hagen-Poiseuille law. Fluid flow through a straight channel depends on the hydraulic resistance, which can be determined by the cross-section geometry of the channel [22]. In 2D, the flow profile between two very close walls is approximately parabolic, as depicted for a narrow tube in Fig. 2.4b and across the height for the glass capillary in Fig. 2.4c. The hydraulic resistance for a rectangular channel with high aspect ratio (i.e. where the channel width is much larger than the channel height) results in a parabolic flow profile across the smallest dimension, Fig. 2.4c. The flow profile is flatter across the width.

In our microfluidic channel, the new fluid enters in the centre of the capillary first, Fig. 2.4a. A keen eye may observe that the flow profile implied by this sample front is steeper than predicted, across the capillary width in Fig. 2.4c. The exaggerated sample front we observe here is likely the consequence of the steeper flow profile in the narrow circular tubing, that the sample passed through prior to entering the capillary.

The inhomogeneous flow velocity is important to consider, when determining the force experienced by particles at different locations in the capillary. The channel cross-section is also important when calculating the maximum flow velocity $v_{\max}$ from an applied volumetric flow rate $\boldsymbol{Q}$, as the fluid velocity in the very centre of a capillary will depend on the geometry of the cross-section. In the capillary used for acoustic trapping in this work, approximately a rectangular channel as depicted in Fig. 2.4c, the flow velocity in the centre of the channel is given by [23]:

$$v_{\max} = \frac{\beta}{hw}\boldsymbol{Q}\,, \tag{2.3}$$

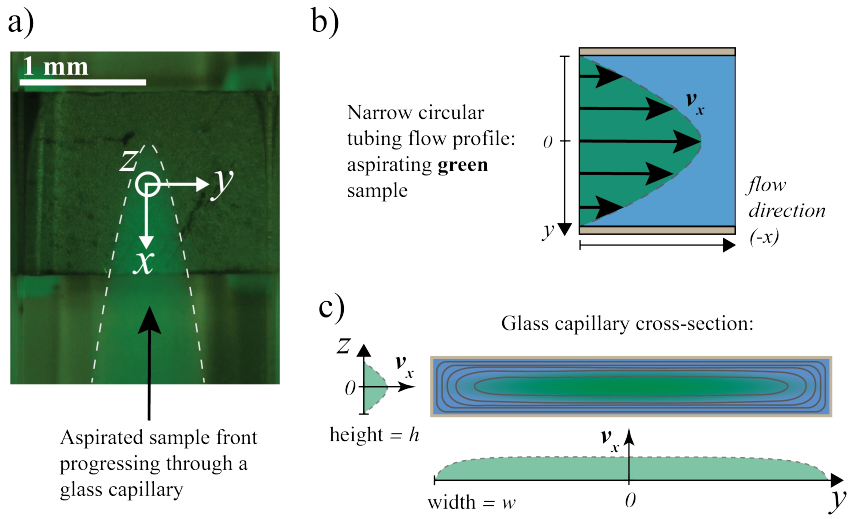

Figure 2.4: a) Image showing the upwards syringe-pump driven aspiration of fluid containing green fluorescent nanoparticles from a narrow tubing into a glass capillary. Here the width of the capillary is 2 mm and the sample front (highlighted by the dashed white line) is travelling slightly faster in the centre than at the walls. b) Schematic of a non-linear flow profile in a narrow tubing with a circular cross-section, depicted in 2D. The y direction separates the walls of the tubing, whilst x is the channel length direction and the direction of flow. The velocity of the flow is indicated by the length of the flow-lines. c) The rectangular cross-section of the glass capillary with approximate contour lines and plots showing that the flow velocity (v_x) increases more steeply across the height direction than across the width, inspired by [22].

where β is an aspect-ratio-dependent constant: $\beta = 1.74$ in the case of a rectangular capillary with the dimensions 200 µm (h, height) by 2 mm (w, width). This is used in **Paper I**, to determine the local fluid flow velocity at the centre of the capillary where particles are trapped [24].

2.1.2 Particle motion in fluids

When a particle is suspended in a fluid, its motion will be determined by many forces. Gravitation and buoyancy usually play a role, although for neutrally buoyant particles (where the mass-density of the particle and fluid are the same)

these forces balance and the particle neither sinks nor floats. Drag forces oppose the motion of particles relative to the surrounding fluid, preferring for a particle to be *dragged* along in a moving fluid. Diffusion, on the other hand, drives particles away from each other due to random collisions, resulting in a more *homogenous* distribution within the fluid. Both drag and diffusion are dependent on particle size, or more specifically on hydrodynamic radius - which is the effective size of a particle if it is assumed to be a perfect sphere, taking into account its shape and interactions with the surrounding fluid. These forces are extremely important for microfluidics-based separation of nanoparticles.

Stokes' drag force

When there is fluid flow, such as in the case of pressure driven flow through a microchannel, a particle at rest relative to the fluid will experience a force in the direction of flow [1]. The force experienced by a stationary particle of hydrodynamic radius a in a fluid of viscosity η and flow velocity v, is given by [2]:

$$\boldsymbol{F_D} = 6\pi\eta a\boldsymbol{v}. \tag{2.4}$$

The result is that, for spherical particles, the magnitude of the drag forces are proportional to the particles' radii. This is important to bear in mind when trying to trap particles against flow, as is the aim for the work within this thesis. Drag forces act along the channel direction for the simple case of laminar flow, although the non-linear flow velocity profile across in a microfluidic channel will mean that the magnitude of this force depends on the location of the particle relative to the walls. In some cases, such as when acoustic streaming is active (see Section 2.3.3), these forces drag particles around in the streaming vortices.

Diffusion

Brownian motion was first observed by Robert Brown in the early 19th century, when looking under a microscope at the random motion of grains of pollen suspended in water. These observations led to the understanding that the random walk of small particles is dependent on their size, see Fig. 2.5. The equalisation of concentration gradients in a fluid mixture, due to Brownian motion, is an irreversible source of energy dissipation [2].

In microfluidics, this phenomena of diffusive species flowing down a concentration gradient can be observed as mixing in laminated fluids. Diffusion becomes increasingly relevant if the diffusivity (rate of diffusion) of the particles is increased and as channel geometries shrink. The diffusion coefficient D describes the expected random motion of a particle, which directly relates to its size [25], as defined by the Stokes-Einstein relation [26]:

$$D = \frac{k_B T}{6\pi a \eta} = \frac{< d^2 >}{6t}, \tag{2.5}$$

where k_B is the Boltzmann constant, T is the temperature, a is the hydrodynamic radius of the particle, and η is the viscosity of the medium. This determines the mean squared distance $< d^2 >$ travelled by the particle in time t [2]. Diffusion occurs slower than many other processes, but over small distances, such as in microfluidic channels, its effect becomes noticeable. This phenomenon can also be used to measure the size of nanoparticles, such as in nanoparticle tracking analysis, described in Section 3.2.2.

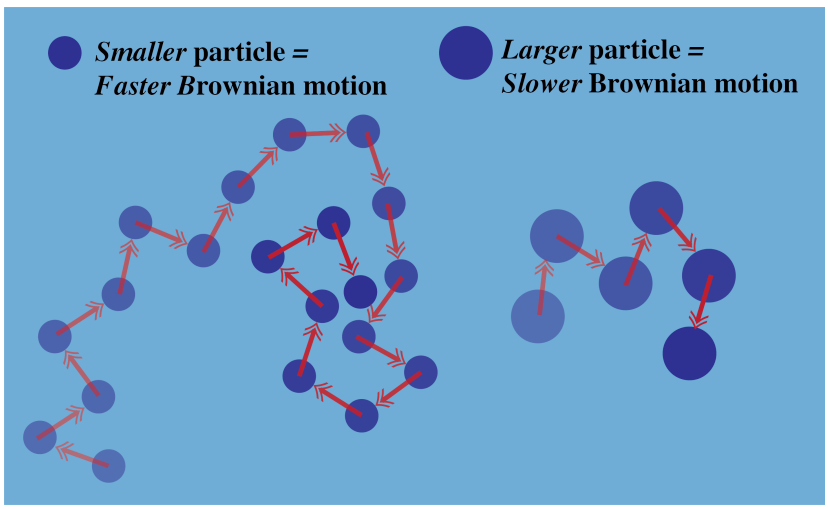

Figure 2.5: Illustration of the random motion of particles in a fluid due to diffusion. The red arrows show each discrete step that a particle takes before a random microscopic collision causes a change in its direction. The gradient in particle opacity signifies time passing; the smaller the particles are, the faster and further their random motion.

2.1.3 Early microfluidic separation techniques

In 1966, Giddings *et al.* described field-flow fractionation (FFF), a technique that was later used in a pioneering microfluidic chip design which implemented deterministic fluid handling to separate colloids of different sizes or materials [12, 27]. As Fig. 2.6 illustrates, components with different properties pass through a microfluidic channel at different distances from the lower wall due to diffusion or an external field. The parabolic flow profile across the channel height (Poiseuille flow, discussed previously in Section 2.1.1) leads to different flow velocities at different distances from the wall. Thus, there are higher drag forces on the component with a mean distance further from the wall and this can result in a separation in the elution times of the two components.

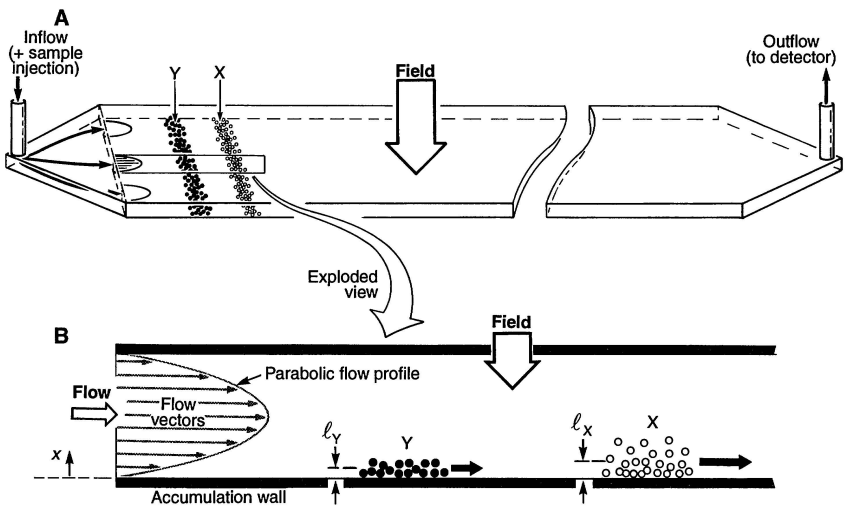

Figure 2.6: Schematic of field-flow fractionation operated to separate some components X and Y in a microfluidic channel. a) The perspective view shows the narrow channel with an inflow of mixed sample from the left and an outflow where the components exit one after the other. b) The side view shows that the two components have different mean distances above from the lower wall (l) and the parabolic flow profile of the fluid results in separated migration through the channel. Reprinted with permission from the American Association for the Advancement of Science. Used with permission of AAAS, from [12]; permission conveyed through Copyright Clearance Center, Inc.

FFF comes in many flavours; sedimentation (the normal mode), thermal, steric, electrical, lift-hyperlayer, and flow [12, 16, 27, 28]; the principle is the same but each variation has a different set-up and field driving the separation. An impractical problem with the elution strategy is that particle fractions are sequentially collected and thus must be separated in the direction of flow by time [12], limiting throughput and often requiring long channels. Another strategy was developed by Springston *et al.* to separate particles by height in a microfluidic channel and have a flow splitter to collect particles that have been forced into each parallel flow-line [29], Fig. 2.7a. One of the first applications of these types of techniques was to sort cells by their physical properties for analysis.

Cell separation was a major driver of technical development of acoustophoresis in 2004 [30, 31], Fig. 2.7b. Acoustophoresis is a method that uses sound fields to move particles, as will be discussed in Section 2.3. The flow splitters allow continuous separation of cells that are pushed into different flow-lines in an acoustic field, due to their different acoustic properties. For details on the physics behind particle manipulation using acoustic fields, see Section 2.3.2. Born out of the development of acoustophoresis, in 2007 acoustic trapping of live cells was demonstrated by Evander *et al.* [32], Fig. 2.7c. Acoustic trapping of bacteria and synthetic nanoparticles was first demonstrated in 2012, following the development of the seed particle method [33], see Section 2.3.3. It was not until 2015 that this technique was extended to isolating what the authors referred to as 'microparticles' from blood plasma, these sub-micron particles would now be referred to as *extracellular vesicles* [17].

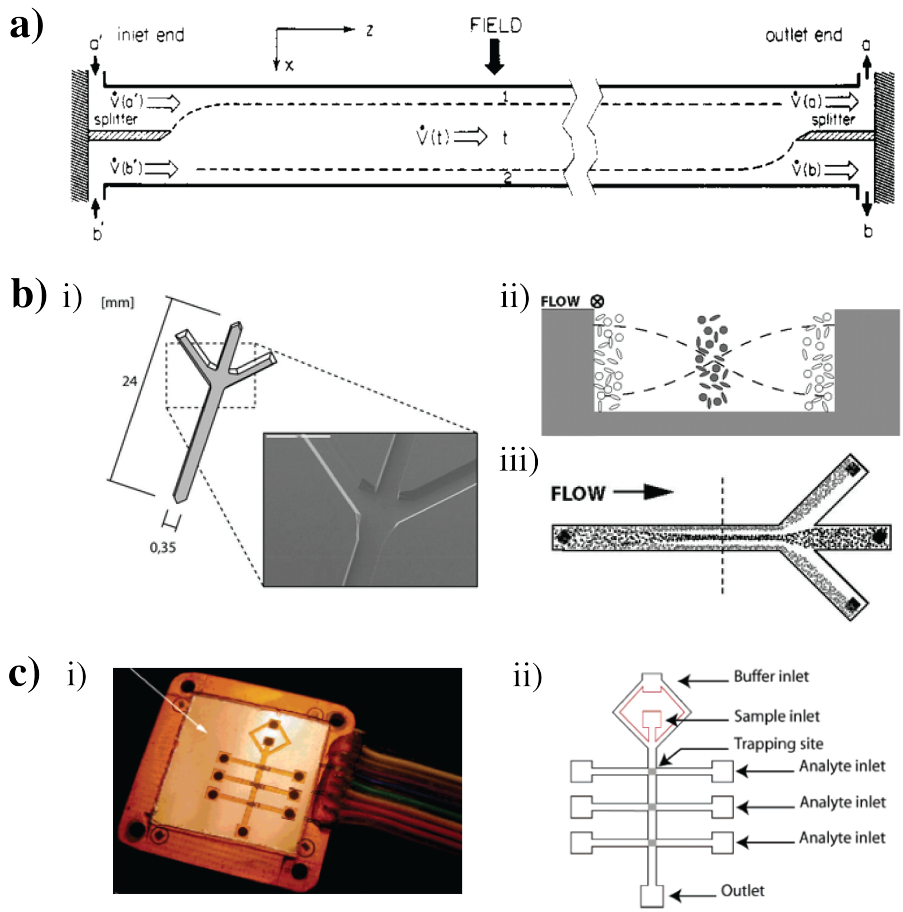

Figure 2.7: a) Particle fractionation based on gravitational sedimentation, implementing an H-filter design, here the channel had a width of 2 cm and a depth of 380 µm. Reprinted (adapted) with permission from [29]. Copyright 1987 American Chemical Society. b) An acoustophoresis separation chip with i) flow splitter 350 µm wide and 125 µm deep. Separation of lipids from blood occurs due to ii) acoustic forces and iii) into central or outer flow splitters. Reproduced from Ref. [30] with permission from the Royal Society of Chemistry. c) An early acoustic trapping chip capable of trapping cells at three sites, the channels were etched 600 µm wide and 61 µm deep. i) Photo of microfluidic chip and ii) sketch of the chip design. Reprinted (adapted) with permission from [32]. Copyright 2007 American Chemical Society.

2.2 Extracellular vesicles (towards rapid isolation from biofluids)

Extracellular vesicles (EVs) are a class of biological nanoparticles originating from cells. In observations in the 1980s, these particles were found to be produced from animal cells and possess both the receptors [34] and the phospholipid composition [35] inherited from the membranes of the parent cells. EVs are heterogeneous, but are thought to be most commonly produced by one of the two mechanisms illustrated in Fig. 2.8: selective budding of the plasma membrane or secretion from intracellular stores called multivesicular bodies (MVB) [36]. The following section will begin by explaining the importance and value of studying the content of EVs, before exploring their physical properties and how they can be isolated from biofluids.

The intraluminal vesicles that are released from the MVB of all cells are generally smaller than 100 nm and are referred to as *exosomes*: a name proposed by Johnstone in 1987 [35]. *Ectosomes* formed by outward vesiculation are heterogeneous and generally larger than exosomes; however, they cannot always be distinguished by size if the mechanism of formation is unknown. Historically, these nanoparticles, found in body fluids, were dismissed as cell debris; however, in 1996 Raposo *et al.* [37] suggested a role of exosomes in antigen presentation, which drew attention to a new mode of biological information transfer [38]. The majority of research has been focused on EVs produced by animal cells, such as those found in blood. EVs can be produced by many different cells, from neuronal cells to red blood cells, and their components often reflect the cell of origin. EVs may also be produced by other means: from bacteria [39], plants, and fungi cells. There is even evidence of interspecies EV uptake, such as in host-parasite interactions [40] and within the intestinal tract microbiome [41].

2.2.1 Content of EVs

Since their discovery, characterisation of extracellular vesicles and their cargo has led to growing insight into their role in intracellular communication and the mechanisms of diseases [42]. EVs have been found in every biological fluid (biofluid) tested so far and they carry nucleic acids (both messenger and inhibitor RNA), proteins (tetraspanins, internal protein cargo and associated

protein corona [43–45]), lipids, and metabolites from their parent cell [46], Fig. 2.8. The tetraspanins are a family of proteins with four transmembrane domains [47]. Several have been identified on the membranes of EVs including CD9, CD81 and CD63 [48–52].

Section 3.3 will introduce some of the methods used in this work to analyse the protein content of EVs. Analytical tools such as immuno-chemical techniques, mass spectrometry, and genetic sequencing are being used to identify disease-related components in EVs. With the aim to use the information to diagnose, understand, and ultimately combat the progression of threats including but not limited to cancers, neurological diseases (such as Alzheimer's and Parkinson's), and cardiovascular disease.

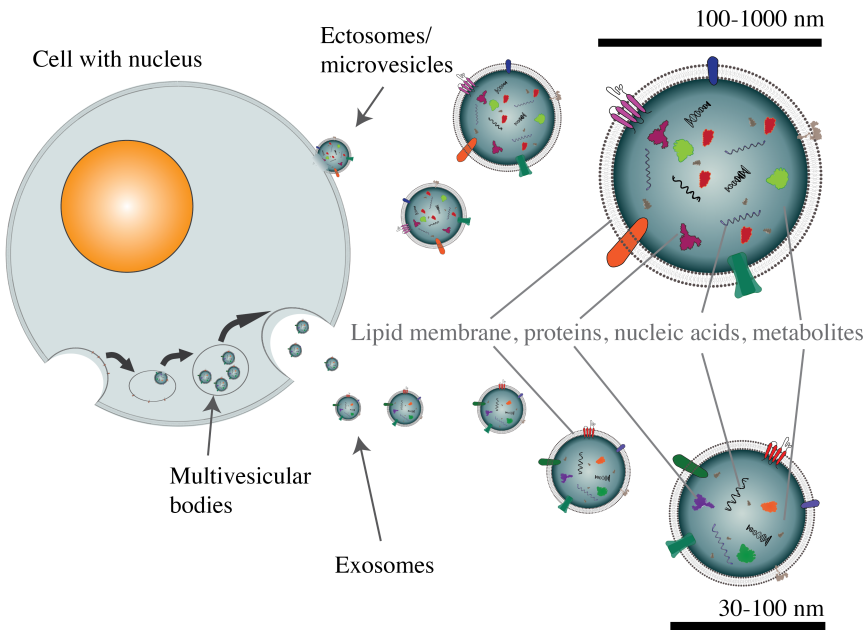

Figure 2.8: Illustration of the origins of extracellular vesicles from an animal cell. The upper pathway via shedding from the plasma membrane forming what are sometimes referred to as ectosomes/microvesicles, usually large EVs (100 – 1000 nm). The lower pathway is preceded by the inward budding of small domains in the membrane of late endosomes and then exocytosis release of what are sometimes referred to as exosomes, usually small EVs (30 – 100 nm).

2.2.2 Disease and diagnostics with extracellular vesicles

Roles of EVs in health and disease

EVs are important in maintaining homeostasis - a state of balance among all the body systems needed for the body to survive and function correctly. Functions of EVs include promoting coagulation [53] (important for wound healing) and immune modulation [37, 43, 54–56] (suppressing and activating T-cells) as well as having roles in healthy metabolism [57], pregnancy [58, 59], and stress response [60–62]. Furthermore, the cargo of EVs is transferred between cells. In the case of genetic material, the uptake of EVs can result in a change in protein expression in the recipient cell. Valadi *et al.* demonstrated that RNA contained in mouse mast cell EVs can be transferred to other mouse and human mast cells [38]. The therapeutic value of EVs in this manner was shown when mesenchymal stem cell derived-EVs were found to have therapeutic effects on neurological impairment in stroke mice [63].

On the other hand, EVs and their cargo have also been found to be associated with harmful processes in a vast number of diseases [64]. Some processes where EVs play a role are shown in Fig. 2.9. Cancer research has revealed numerous complex roles of EVs, for example EVs produced by primary tumours can be transported in the bloodstream and aid the creation of a pre-metastatic niche for a secondary tumour site [65]. Extensive research has linked EVs to inflammation, including the triggering of cardiovascular diseases [66] and diabetes [67]. Even obesity [68] and diseases of the central nervous system [69, 70] appear to be worsened by mechanisms driven by extracellular vesicles.

EVs in biofluids

Urine, cerebrospinal fluid (CSF) and blood are particularly rich biofluids in their diagnostic potential, but they each pose unique challenges for EV isolation. Even cell-free blood plasma is challenging to handle, since it has high viscosity and free protein concentrations. This means that purifying EVs from blood for downstream analysis requires not just the removal of cells, but also ideally the removal of contaminating proteins and other non-vesicular components. CSF is a scarcer biofluid as well as being more dilute, with a lower concentration of EVs, than plasma so it can be challenging to gather sufficient material for analysis. Section 2.2.5 will address advancements in EV isolation methods.

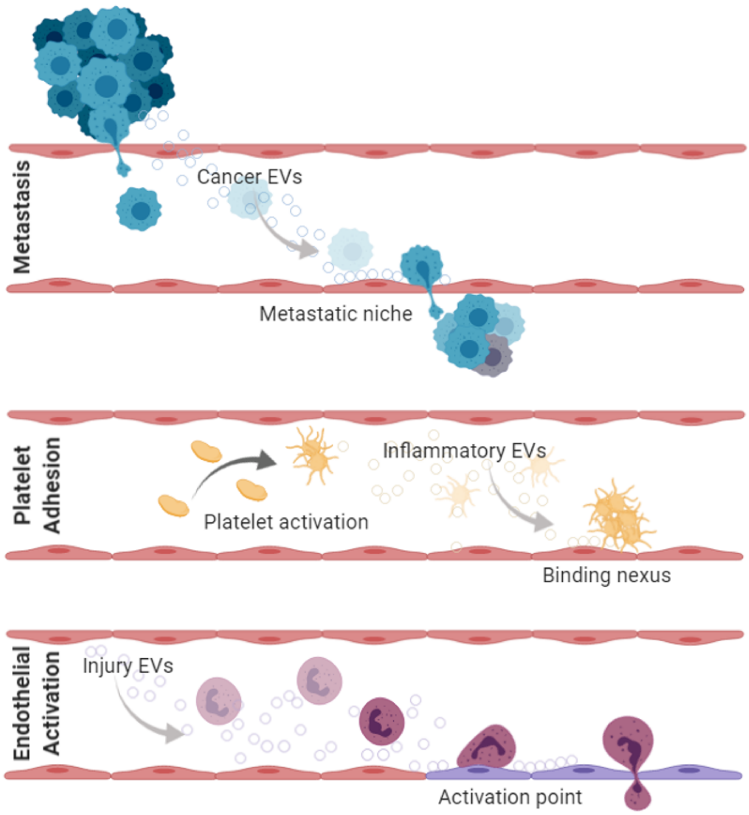

Figure 2.9: In the vasculature, EVs may play a role in creating a pre-metastatic niche, platelet activation and adhesion, and inflammatory response activation in the endothelium. Reproduced from [64] according to the (CC BY-NC-ND 4.0) licence.

What is a biomarker?

A *biomarker*, from *biological marker*, is broadly a measurable characteristic which can be '...evaluated as an indicator of normal biological processes, pathogenic processes, or pharmacologic responses to a therapeutic intervention' [71]. Biomarkers are extremely useful for disease detection and health monitoring as well as clinical trial evaluations of efficacy and safety. EV transported biomarkers could even give insights into the mechanism of disease progression which are not accessible when purely measured in the biofluid. **Papers II** and **IV** investigate proteins in blood that are associated with EVs, via mass spectrometry.

2.2.3 EVs in Alzheimer's disease

The following section briefly introduces Alzheimer's disease (AD) and the potential role of extracellular vesicles in its progression. This aims to provide context for **Paper III** and motivate the study of phosphorylated tau as a biomarker via liquid biopsies. For more detail, the reader is referred to the review by Gomes *et al.* [72] on EVs and their implications on diagnosis and treatment of AD.

The scale of Alzheimer's disease

Over 30 million people worldwide had Alzheimer's disease in 2020 [73] and unless breakthrough cures are found soon the number in the United States of America alone is expected to reach 14 million by 2060 [74]. It is the leading cause of disability and poor health in the elderly population - reflecting a growing burden on the patients and their caregivers [74]. The process leading to cognitive decline in AD is introduced in Fig. 2.10.

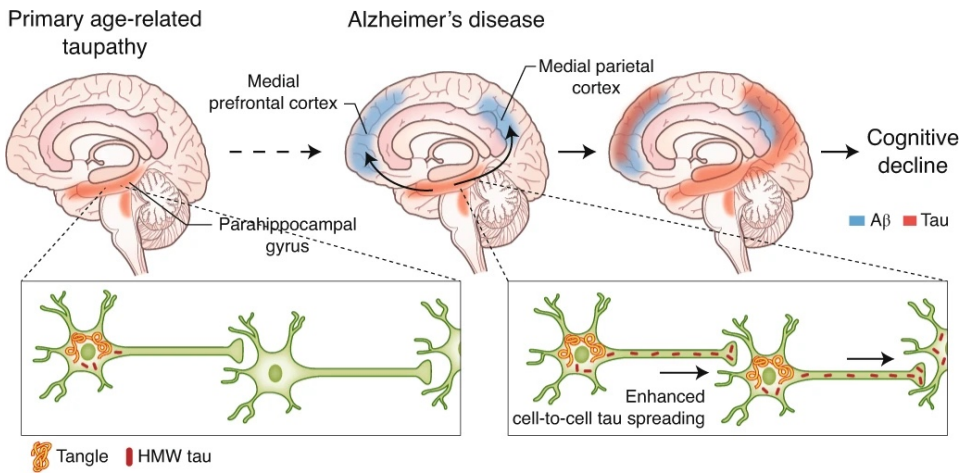

Figure 2.10: Illustration cognitive decline in human Alzheimer's disease (AD) and the associated pathology of of Aβ (amyloid-β) plaques accelerating tau spreading. Abnormal tau, tangles and HMW (high molecular weight, bioactive) tau, are indicative of the primary age-related taupathy. In the progression of AD, the presence of Aβ plaques in the cerebral cortex correlates with the propagation of neuronal tau to more areas of the brain. From [75]. Reproduced with permission from Springer Nature.

AD pathology

Alzheimer's disease is definitively characterised post-mortem by tau deposition neurofibrillary tangles (NFT) as well as amyloid-β (Aβ) deposition in senile plaques [75], Fig. 2.10. In life, AD diagnosis is based on clinical symptoms and cognitive investigation. However, the early-stage pathologic changes in AD patients can be monitored by positron emission tomography (PET) and cerebrospinal fluid (CSF) biomarkers, such as the proteins Aβ1-42, total tau, and phosphorylated tau (p-tau) [76], Fig. 2.11.

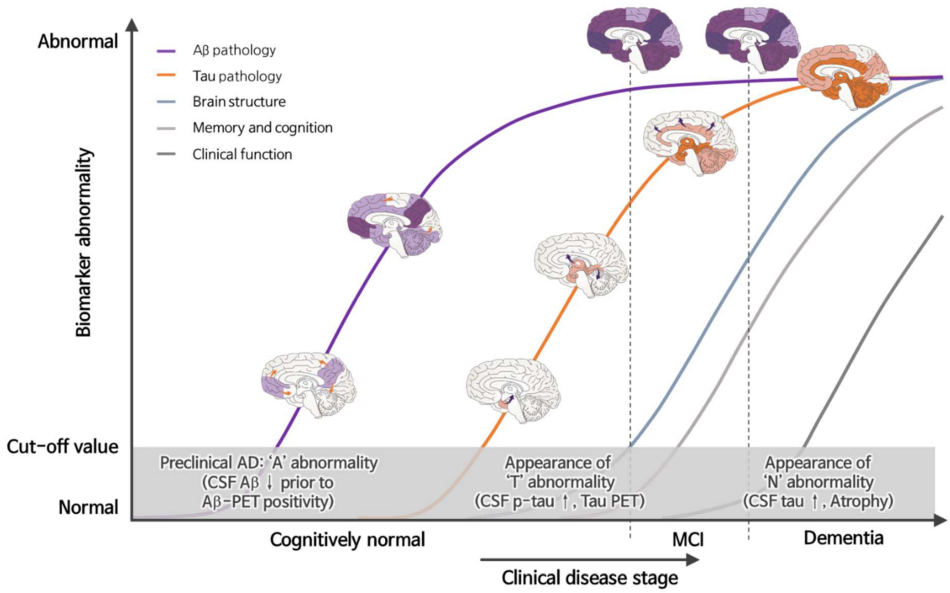

Figure 2.11: The Alzheimer's disease (AD) cascade illustrated by clinical disease stages, in terms of biomarkers and changes in the spatiotemporal pattern of Aβ (amyloid-β) and NFT (neurofibrillary tangles) deposits. Positron emission tomography (PET) of the brain and cerebrospinal fluid (CSF) liquid biopsies are used alongside functional tests to determine the progression of the disease. Abnormality in CSF Aβ42 and Aβ-PET ('A' abnormality) are biomarkers in pre-clinical stage AD, followed by abnormality in CSF p-tau or tau-PET ('T' abnormality) and finally increased CSF total tau and hippocampal atrophy ('N' abnormality) are detected in late-stage dementia. Reproduced from [76] according to the (CC BY 4.0) licence.

Ultimately, the mechanism of AD development is still debated but Aβ and tau both appear to play a critical role over the course of the disease [75]. Critically, these biomarkers show changes in pre-clinical AD which makes them ideal for diagnosis and may drive combination therapies in the future [75], Fig. 2.11. Tau may be phosphorylated at several locations and phosphorylation at threonine 217 (p-tau217) and 181 (p-tau181) have recently emerged as particularly promising biomarkers for AD [77].

Current evidence for EVs role in AD

EVs may propagate misfolded proteins which aggregate and cause neurodegeneration, although this has not been thoroughly investigated *in vivo*. Various isoforms of tau proteins have been found inside EVs, both in AD patients and tauopathy mice models [78–82]. In mouse models, tau fibrils have been found to be mediated by EVs [79, 83]. Tau pathology has been induced in naive mice via EVs derived from familial Alzheimer's induced pluripotent stem cells [69]. Figure 2.12 illustrates potential roles of EVs in transporting Aβ, tau, mRNA and miRNA from neurons and glial cells [72]. Pathological forms of tau and Aβ from diseased cells could be taken up by healthy cells, potentially spreading AD pathology. EVs can traffic these proteins out of the brain into the blood [84].

Accessing brain biomarkers

Two problems make treating AD challenging. The first is the lack of knowledge about the mechanism of AD progression and how different factors synergise. The second is frequent misdiagnosis of symptomatic AD in specialised clinics. This is driving the need for blood biomarkers which can accurately diagnose and monitor the progression of the disease [85]. Conditions of the brain are especially difficult to monitor and treat due to the impermeability of the barriers in the central nervous system. Information from the brain may not be transferred into the blood or CSF, evading detection via liquid biopsies, and targeted therapies need to be able to cross the other way, into the brain. However, extracellular vesicles can cross these barriers, Fig. 2.12, in both directions [86–89], making them promising for both diagnostics and therapies in neurodegenerative conditions.

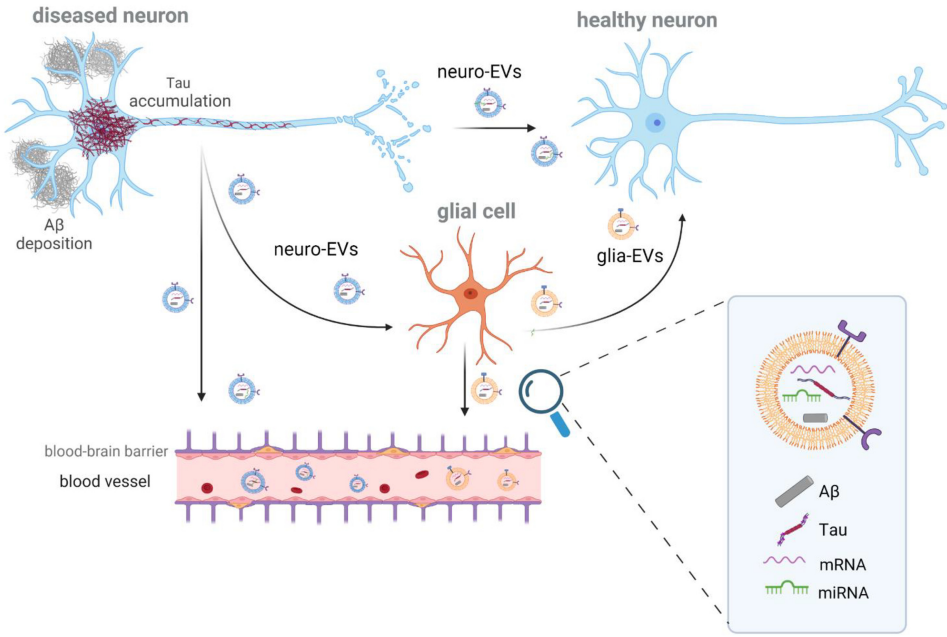

Figure 2.12: The proposed roles of extracellular vesicles in the spreading of Aβ and tau pathology between neuronal and glial cells, as well as miRNA and mRNAs that can induce cellular responses. Neuron-derived EVs (neuro-EVs) and glia-derived EVs (glia-EVs) may carry forms of Aβ and tau proteins which originated from a diseased neuron (donor cell), triggering Alzheimer's disease pathology in healthy neurons (recipient cells). Glial cells may act as an intermediate, taking up neuro-EVs and releasing glia-EVs. Both types of EVs could cross the blood-brain barrier and be found in the peripheral blood. Reproduced from [72] according to the (CC BY-NC-ND 4.0) licence.

Section 2.2.5 will outline methods used to isolate EVs from biofluids, including blood and CSF. In some cases, surface markers on the EVs are targeted to drive their separation. Otherwise, EV isolation methods rely on the physical properties of the EVs, primarily their size and density. If biofluids are left for a long time, their components will naturally separate out by sedimentation under gravity, depending on their mass and size. Both bulk and microfluidic methods exist which fractionate components in fluids by these properties. However, effective separation based on these techniques require careful consideration of the physical properties of the targets and the potential contaminants.

2.2.4 Physical properties of EVs

EVs were previously reported to have densities in the range of 1.13 to 1.19 g/ml [90], although it has since been reported that the range of densities (some high-density EVs populations were found in the range of 1.26 to 1.29 g/ml) and the heterogeneity of sub-populations is wider than this reflects [91]. The sizes of EVs have been reported to range from 30 nm to 1 µm [92]. Whilst the size depends to some degree on biogenesis, Fig. 2.8, there is a continuum making size-based isolation unable to isolate distinct sub-populations [93]. Figure 2.13 summarises the sizes and densities of EVs compared to common contaminants.

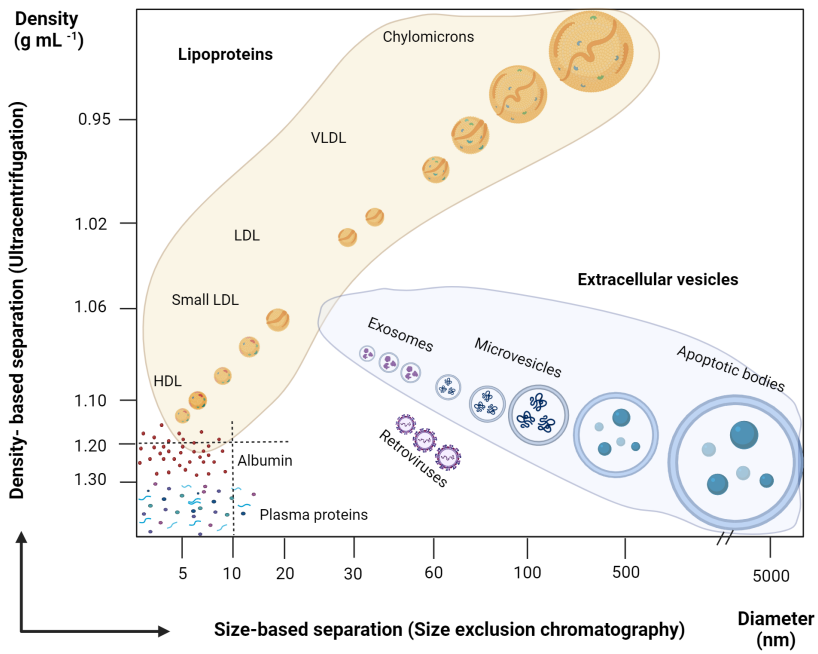

Figure 2.13: Schematic of separation capacity based on size and density of blood components. The properties of EVs overlap with lipoprotein particles if only size or density is considered, but combining the two allows distinction between the particles by physical properties. Lipoproteins are smaller and/or less dense than EVs, whereas free proteins are denser and smaller. Originally adapted from [93] by Kitka, D. (2024) BioRender.

The molecules expressed on EVs result in a net negative surface charge, zeta potential < -20 mV, contributing to their colloidal stability [94]. However, it is important to note that the electrostatic surface properties can depend on the surrounding environment, such as salt, pH, presence of detergents, and buffer concentrations [94].

The concentration of EVs *in vivo* varies widely depending on the biofluid and individual. Several publications report correlations with disease and increased EV concentration [95], but there is also variation due to other factors such as more EVs in blood following vigorous exercise [50, 60]. Auber *et al.* estimated the EV secretion rates of different human blood cell types: on average per minute the secretion rates range from nearly 100 EVs per monocyte, to less than 1 EV per 100 erythrocytes [96]. There are approximately 10^{12} extracellular vesicles per mL of blood [96], whereas in CSF there are typically around 10^9 EVs/mL.

2.2.5 Advancement and obstacles in EV isolation

A major obstacle in disease prognosis in medicine is that sub-micron targets, such as extracellular vesicles in biofluids, are very difficult to isolate in a reliable way [51]. Isolating EVs from complex biological backgrounds is important in order to increase signal-to-noise ratio of transported molecules where diagnostics have a limited dynamic range. Isolating EVs may also help researchers to interrogate mechanisms of disease progression. For future therapeutic applications of EVs, purity will be critical for efficacy and safety.

This thesis focuses on isolating EVs for diagnostic purposes rather than therapeutic ones, due to the difference in scale of fluid handling needed in these applications. For therapeutic applications, like using EVs as vaccines, large volumes (tens of litres) of extracellular milieu must be processed. On the other hand, diagnostic applications are ideally performed with minimal volumes of biofluids. Biobanks, repositories storing biological samples for medical research, often contain small (<1 mL) aliquots of human samples from many patients which are used sparingly. For particularly challenging medical research into disease mechanisms or new therapies for in cancer, diabetes, and stroke, sometimes animal experiments are the only way to gain insight.

Techniques improving the ease of processing small volumes of biofluids from mice without pooling samples or using large animals could enable more efficient animal use. Furthermore, studies on CSF as in **Paper III** are hard to set up. CSF is quite invasive to collect and only 1-10 millilitres can be safely extracted because each individual only has 150 mL in circulation. Clinicians therefore favour techniques where the most information can be gained from the smallest volume of biofluid.

Ultracentrifugation

The principle of differential centrifugation as a separation technique is that particles sediment at different speeds, depending on their density, size, shape, and the media they are suspended in. The sedimentation coefficient s of a particle is given by:

$$s = \frac{m}{6\pi\eta r}, \tag{2.6}$$

where m is the mass of the particle, η is the viscosity of the medium, and r is the radius of the particle. If the particle is spherical and has density ρ, its mass is given by $m = \frac{4}{3}\pi r^3 \rho$. In practice, this means that sedimenting (forming a pellet of) one particle, whilst leaving another particle population in suspension (the liquid called the supernatant) is possible if they are sufficiently different in size and density, provided that the appropriate centrifugation speeds are used. Particles which have higher sedimentation coefficients need less time to reach the bottom of a given container. The sedimentation time of particles with smaller s values can be accelerated by faster centrifugation.

Figure 2.14 outlines a strategy for isolating two populations of EVs (large and small) from dead cells, apoptotic bodies and cell debris or other solutes in a sample. Centrifugation is convenient for separating some cells from small dye molecules in a staining protocol, requiring only a few hundred $\times\, g$ and 10 minutes or so. On the other hand, separating nanoparticles in a similar way takes many more manual steps, hours of time, and up to 100 000 $\times\, g$ *ultra*-centrifugation speeds [97], which exposes the particles to high shear forces [98]. Isolating EVs by ultracentrifugation requires hundreds of microlitres of sample, thus EV samples are often pooled together [99].

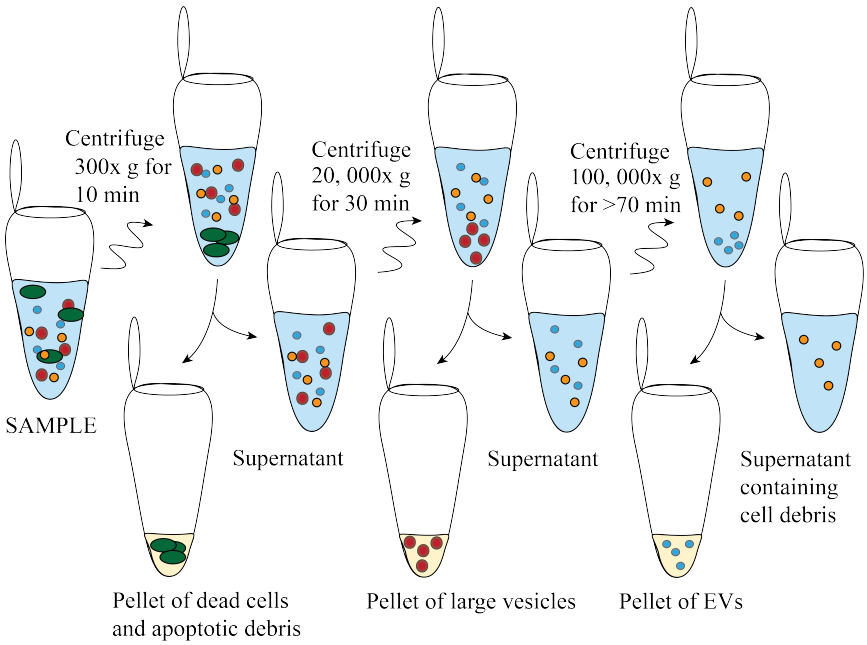

Figure 2.14: Ultracentrifugation multi-step protocol for isolating EVs from body fluid or conditioned medium, taking several hours. Three steps are shown to purify a pellet of small EVs from a complex mixture, the two fractions shown are the supernatant and the purified pellet isolated for the approximate centrifugation $\times g$ and time. Sequential separation highlights larger cell debris (green ellipses), large vesicles (red circles), small EVs (blue circles), and smaller, less dense debris (orange circles). Reproduced from [4] according to the (CC BY 4.0) licence.

Immunoaffinity

In medicine, *immuno-* relates to the immune systems and processes in living organisms and *affinity* describes the attraction between an antibody (or *immunoglobulin* protein) and an antigen. The tips of these Y-shaped proteins can bind specifically to an epitope on a specific antigen. This mechanism can be utilised in purification technologies, such as chromatography, magnetic-bead capture [100], and extensively in microfluidics-based platforms [101–103]. Antibodies can be coated onto surfaces or beads to *functionalise* them, for example to capture an EV possessing the target antigen on its surface, Fig. 2.15.

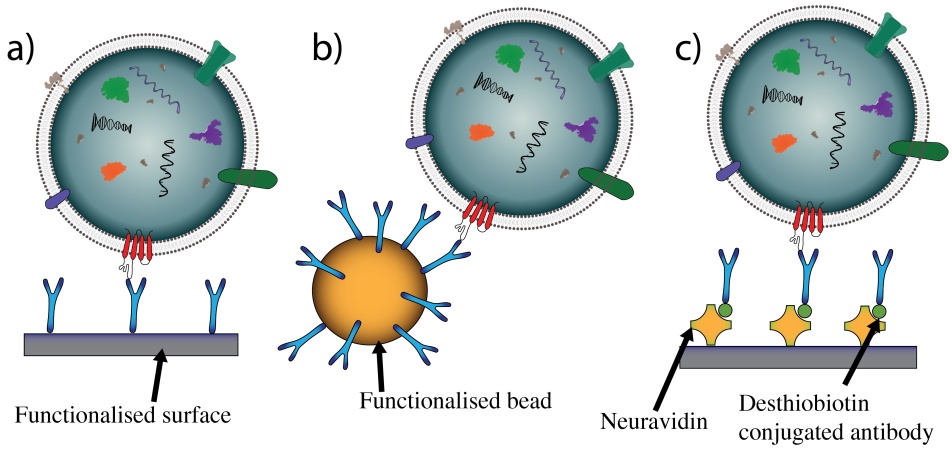

Figure 2.15: Schematic of three different iterations of immunoaffinity based isolation methods: a) functionalised surface, b) functionalised bead and c) an example of more complex functionalisation to also allow EV release. Here, the targeted EV (membrane enclosed particle containing various proteins and nucleic acids) is assumed to possess the surface marker (indicated by a red tetraspanin protein) for the complementary antibody (represented by a blue Y-shape protein) used for capture. Reproduced from [4] according to the (CC BY 4.0) licence.

This is a very specific isolation process and enables highly pure isolation, however the heterogeneity of EVs extends to its surface markers and thus immunoaffinity-based techniques will only be able to isolate a subset of EVs possessing the targeted antigen. This may be sufficient for many applications, but cannot paint a full picture of the EV population. Furthermore, antibodies are expensive, as are the magnetic beads commercially available, which makes this technique difficult to scale up. Using a microfluidic system can mitigate this by reducing the volumes of fluids required but also by integrating mixing modalities which increases the chance of collision, and thus rate of binding between the antibody and its target.

Immunoaffinity capture is the special ingredient in immuno-acoustic trapping, introduced in **Paper IV**, and its integration seed particle acoustic trapping is discussed in Section 3.1.2. In addition to the integration with acoustic trapping, other microfluidic isolation techniques have incorporated this method.

Microfluidics-based EV isolation

The review paper by Havers *et al.*, entitled 'Advancement and obstacles in microfluidics-based isolation of extracellular vesicles' [4], describes some of the microfluidics-based techniques which show promise in isolating EVs from biofluids. The graphical abstract, reproduced in Fig. 2.16, gives an overview of these techniques. The techniques are diverse, but intrinsic benefits of microfluidic isolation methods lie in their small volume and deterministic fluid handing. As discussed in Section 2.1, at the microscale fluids tend to obey laminar flow and small volumes of fluids can be controlled predictably. EV isolation techniques on microfluidic platforms can be divided into two types: passive and active methods.

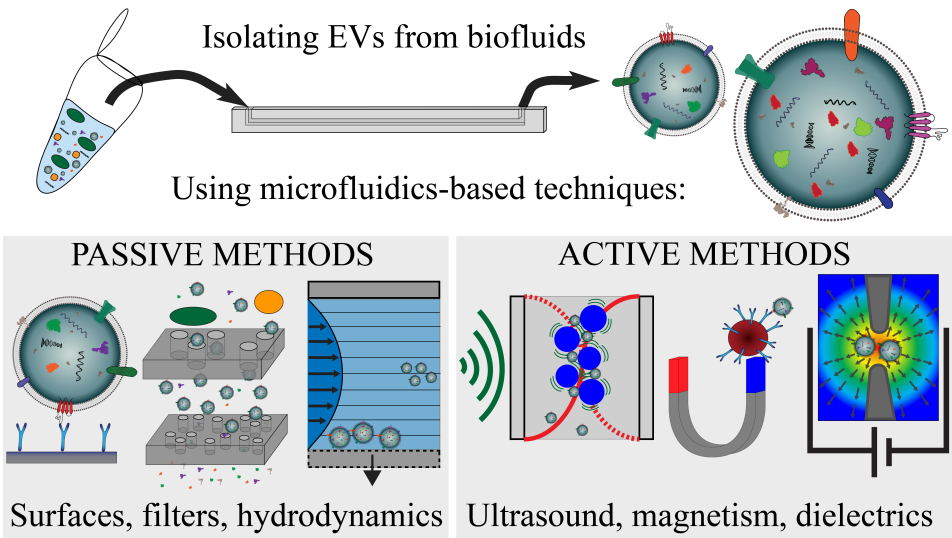

Figure 2.16: An illustration of microfluidics-based isolation of extracellular vesicles from biofluids, highlighting techniques which have been incorporated into such devices. From left to right: passive devices consisting of functionalised surfaces, mechanical filters, and hydrodynamics; active devices incorporating acoustic, magnetic, and electric fields. Reproduced from [4] according to the (CC BY 4.0) licence.

Passive methods tend to be immunoaffinity or size-based devices, EV isolation is driven by functionalised surfaces [101, 102, 104–109], mechanical filters [14,110–113] or field flow fractionation [16,28,114,115]. More complex devices include deterministic lateral displacement [13,116,117] and viscoelastic separation [11, 118–121].

Active methods require external forces: acoustic, magnetic or electric fields are applied in some way to manipulate particles in microfluidic channels. Magnetic fields have been utilised to isolate EVs via affinity capture on functionalised magnetic beads [19, 102, 103, 122–124] as well as by label free particle manipulation [15, 125]. Dielectrophoresis uses electric field gradients to separate or trap EVs [126–128]. The focus of this thesis, acoustic trapping, is an active technique which relies on acoustic fields generated with ultrasound. In some EV isolation devices ultrasound is produced by bulk acoustic waves (BAW) [17, 33, 60, 129–133] or surface acoustic waves (SAW) [134–137].

Acoustic trapping of EVs

In the previous decade, acoustic trapping has emerged as a novel and powerful technique for nanoparticle enrichment in fluids [33]. Acoustically enriched extracellular vesicles (EVs) have provided diagnostic and prognostic information such as miRNAs [130], surface markers [129], and protein expression [132]. Acoustic trapping functions as a fluidic platform able to retain particles and cells against flow in an acoustic field in a BAW (bulk acoustic wave) device [32, 138]. Compared to other popular label-free techniques like ultracentrifugation, acoustic trapping is relatively rapid and gentle [129]. Acoustic trapping also allows washing, removing non-trapped species like free proteins [132]. Unlike many other microfluidic techniques, acoustic trapping has been commercialized (AcouSort AB, Lund, Sweden) and can process biological samples at flow rates exceeding 30 µL/min. The rest of this chapter will set out important theory to understand this technique.

2.3 Acoustofluidics (Sowing the seeds of acoustic trapping)

Acoustofluidics refers to ultrasound-driven manipulation of particles in microfluidic systems. These are often simple systems using a piezoelectric transducer to vibrate a hard-walled rectangular channel at a resonance frequency [139]. If the channel is vibrated to produce a half-wavelength standing wave then there will be a single pressure node at the centre of the channel [1, 139, 140], see Fig. 2.17. By designing a system with in-plane separation, this technique was applied for focusing cells into the pressure node in continuous flow [31]. This provided an alternative method for cell-medium exchange without needing centrifugation [141]. Acoustic trapping similarly relies on bulk acoustic standing waves, albeit with a localised acoustic field, see Fig. 2.18. We will only discuss single-node systems here, as is the case for the small acoustic trapping units used in this work, however many acoustofluidic systems are operated with multiple pressure nodes [31, 132, 133, 141]. This subsection will discuss the theory behind acoustic trapping - from acoustic resonance to radiation forces on particles - and introduce current hypotheses on seed particle trapping. Table 2.1 defines some important parameters used in this section.

2.3.1 Standing waves and resonance

Although the acoustic fields in acoustofluidic systems are 3-dimensional, valuable insight can be gained from looking at the cross-sections of the microfluidic channels, in Fig. 2.18. Understanding concepts such as acoustic impedance and resonance frequency underlies the development of acoustofluidic techniques. In brief, sound is reflected at boundaries between materials of differing acoustic impedance, defined as $Z = \rho c$ for plane waves; dependent on the mass density ρ and speed of sound c in the medium [142]. Note that the speed of sound through a medium can be written as $c = \sqrt{\frac{1}{\kappa\rho}}$, where κ is the adiabatic compressibility of the medium. The resonance frequency of a system is defined by the dimensions of the boundaries.

Table 2.1 Summary of symbols for parameters concerning the force acting on a small particle placed in a standing wave generated in a fluid-filled channel.

Parameter	Definition	Unit
λ	Wavelength	m
k	Wavenumber	m^{-1}
f	Frequency	Hz
ω	Angular frequency	rad s^{-1}
Z	Acoustic impedance	Pa s m^{-1}
c	Speed of sound	m s^{-1}
v	Velocity	m s^{-1}
p	Pressure	Pa
E_{ac}	Acoustic energy density	J m^{-3}
F^{rad}	Primary acoustic radiation force	kg m s^{-2}
U^{rad}	Radiation potential	kg m^2 s^{-2}
F_r	Lateral retention force	kg m s^{-2}
F_{Sec}	Secondary acoustic radiation force	kg m s^{-2}
$<>$	Mean (time-averaged) notation	-
∇	Vector differential operator	-
f_1	Monopole scattering coefficient	
κ_0	Compressibility of fluid	Pa^{-1}
κ_p	Compressibility of particle	Pa^{-1}
$\tilde{\kappa} = \frac{\kappa_p}{\kappa_0}$	Compressibility contrast	
f_2	Dipole scattering coefficient	
ρ_0	Mass density of fluid	kg m^{-3}
ρ_p	Mass density of particle	kg m^{-3}
$\tilde{\rho} = \frac{\rho_p}{\rho_0}$	Mass density contrast	
Φ	Acoustic contrast factor	
a	Particle radius	m
V_p	Particle volume	m^3
(x, y, z)	Cartesian coordinates	m

For example, a confined geometry with two hard walls will have a resonance frequency at $f = \frac{2h}{c}$, so the wavelength is equal to half the height h. Harmonics (multiples) of this fundamental frequency will also exist. If the half-wavelength resonance mode is generated, the pressure oscillation is zero at the centre of the capillary and maximum at the walls. A standing wave approximation can be defined for a 1-dimensional sinusoidal plane wave, propagating in the z-direction where $z = 0$ at the centre of the capillary, Fig. 2.17. The pressure field in a 1D standing wave can be written as:

$$p(z,t) = p_0 \sin(kz)\cos(\omega t). \tag{2.7}$$

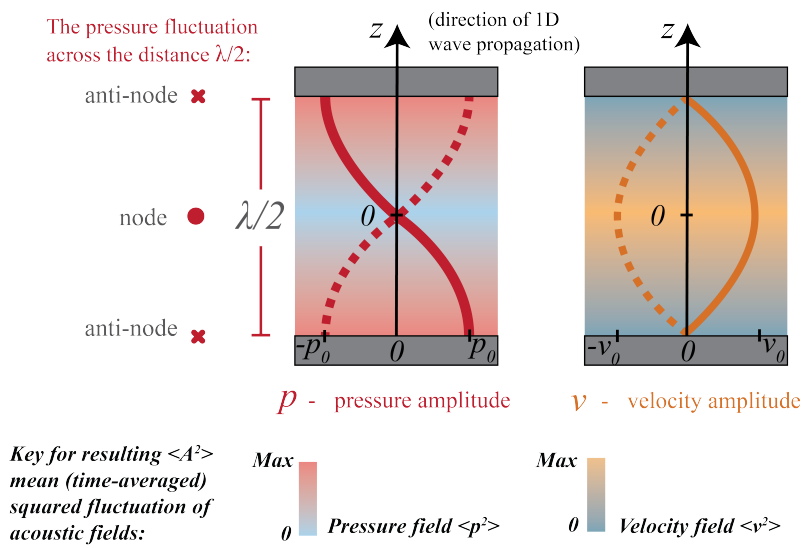

Figure 2.17: Schematic representation of a one-dimensional half-wavelength resonance mode where the wave is propagating in the z direction. The half-wavelength sound wave results in a pressure node in the centre and anti-nodes near at the walls. The grey walls represent rigid boundaries: the waves propagate between them and are reflected at the boundaries due to a difference in acoustic impedance. The pressure amplitude p and the velocity amplitude v are indicated in red (left) and orange (right), respectively. The background colour gradients (see key) illustrate the resulting mean squared fluctuation of the pressure and velocity components of the 1D acoustic field.

The pressure oscillates overtime, with a fixed amplitude p_0 and wavenumber $k = \frac{2\pi}{\lambda}$. As illustrated in Fig. 2.17, the fluctuation in pressure in time depends on the position along the wave propagation direction. The pressure and velocity fields in the fluid which result from these waves are illustrated in 1D, where the velocity field is zero at the walls (at $z = \pm\frac{\lambda}{4}$) and the pressure field is zero halfway between the two walls (at $z = 0$). Figure 2.18 extends this to 2D fields, and relates these fields to their use in acoustophoresis.

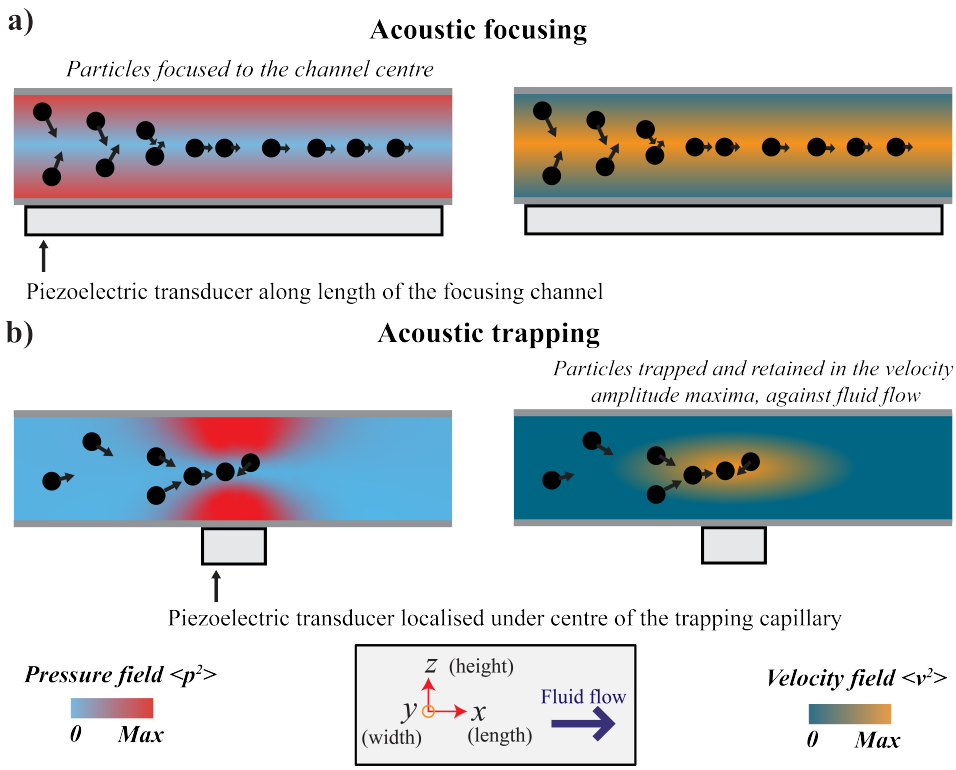

Figure 2.18: Illustration in 2D, comparing a) acoustic focusing with b) acoustic trapping, where the approximate motion of particles is indicated with arrows. Both acoustofluidic techniques involve a rigid fluid-filled channel mounted on an ultrasound transducer which is driven at the half-wavelength resonance. In acoustic trapping, the smaller transducer leads to localised acoustic fields, shown both in terms of the pressure (left) and velocity (right) fields. The origin $(0, 0, 0)$ lies at the centre of each capillary.

Figure 2.18 shows the acoustic fields in 2D in ideal cases corresponding to where the sound is either produced continuously along the length of a microchannel (as in the case in acoustic focusing of particles) or from a more localised point (for acoustic trapping of particles). These acoustic fields can be used to manipulate particles via acoustic forces, as detailed in the sections that follow. In this depiction of acoustophoresis, the pressure and velocity gradients lead to particles being focused to the mid-height of the channel ($z = 0$) but continuing to progress with the fluid. In acoustic trapping, particles are still focused in the z direction, however the localised velocity field introduces lateral radiation forces which trap particles against flow in the x direction, see Section 2.3.2.

2.3.2 Particle manipulation in acoustic fields

When a particle (or cell) is placed in an acoustic field, the particle's movement will depend on its volume as well as its density and compressibility compared to the fluid [143, 144]. Figure 2.19, summarises several relevant physical mechanisms affecting a particle in an fluid that result from an incident acoustic wave. Gor'kov presented the theory for the force acting on a small particle placed in a standing wave. The acoustic radiation force depends on the gradient of the acoustic potential at that location in the field as [144]:

$$\boldsymbol{F^{rad}} = -\nabla \boldsymbol{U}^{rad}. \tag{2.8}$$

In the case of a spherical particle in an acoustic field, the acoustic radiation potential can be written as [145]:

$$U^{rad} = \frac{4\pi}{3}a^3\left[f_1\frac{1}{2}\kappa_0 < p^2 > -f_2\frac{3}{4}\rho_0 < v^2 >\right]. \tag{2.9}$$

The monopole scattering coefficient f_1 is given by the compressibility contrast:

$$f_1(\tilde{\kappa}) = 1 - \tilde{\kappa}. \tag{2.10}$$

The dipole scattering coefficient f_2 is defined by the density contrast:

$$f_2(\tilde{\rho}) = 2\frac{\tilde{\rho} - 1}{2\tilde{\rho} + 1}. \tag{2.11}$$

The other variables are as previously defined, see Table 2.1. The mechanisms of monopole and dipole radiation on a single particle are described in Fig. 2.19a and c, respectively.

By consequence of this acoustic radiation force, Eq. 2.8 - 2.11, a particle with positive scattering coefficients will move towards a pressure node (velocity anti-node), whereas a particle with negative scattering coefficients would move towards the pressure anti-node (velocity node) [30]. Most particles and biological species of interest, for example cells, have positive scattering coefficients in water since they are generally more dense and less compressible than the fluid (large $\tilde{\rho}$ and small $\tilde{\kappa}$ in water) [146]. In acoustophoresis, acoustic radiation forces can be used to focus cells or particles away from the walls of the channel, see Fig. 2.18, where they can be transported along a flow-line and be separated from a mixture [30, 31, 139].

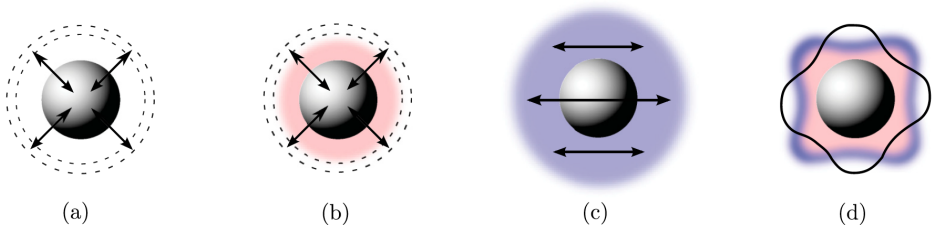

Figure 2.19: Simplistic representations of some physical mechanisms describing multipole components, resulting from an acoustic wave incident on a particle in a fluid. Shading represents thermal (pink) or viscous (blue) boundary layers, which can arise due to different particle properties. (a) *Compressibility contrast* $\tilde{\kappa}$ leads to monopole radiation, as the incident periodic pressure field compresses the particle relative to the fluid. (b) *Thermal contrast* also gives rise to monopole radiation as well as development of a diffusive thermal boundary layer, as the incident periodic temperature field leads to thermal expansion of the particle relative to the fluid. (c) *Density contrast* $\tilde{\rho}$ gives rise to dipole radiation as well as a viscous boundary layer, as the difference in inertia between the particle and fluid causes the particle to oscillate relative to the fluid. d) *Particle resonances* can cause complex thermoviscous boundary layers and multipole radiation, when acoustic wavelengths are comparable to the particle size. Reprinted figure with permission from [147] Copyright 2015 by the American Physical Society.

Primary acoustic radiation force

For a standing one-dimensional pressure wave in the z direction, as illustrated in Fig. 2.17, the radiation force (Eq. 2.8) acting on a spherical particle can be reduced to [143, 145]:

$$\boldsymbol{F_{1D}^{rad}(z)} = -4\pi\Phi\left(\tilde{\kappa},\tilde{\rho}\right)a^3 k E_{ac}\sin\left(2kz\right)\boldsymbol{e_z}, \tag{2.12}$$

where the mean acoustic energy density in the fluid is E_{ac}. The acoustic contrast factor $\Phi\left(\tilde{\kappa},\tilde{\rho}\right)$ combines the scattering coefficients in this 1D case:

$$\Phi\left(\tilde{\kappa},\tilde{\rho}\right) = \frac{1}{3}f_1\left(\tilde{\kappa}\right) + f_2\left(\tilde{\rho}\right). \tag{2.13}$$

The resulting force felt by the particle will push a particle with positive Φ into the pressure node [148], where $z = 0$ in Fig.s 2.17 and 2.18. A particle with negative Φ, not the case in this work, would instead be pushed towards the pressure anti-nodes at the channel walls [30, 149]. The acoustic radiation forces on smaller particles are weak, as $F^{rad} \propto a^3$. Hence, acoustophoresis is not generally used for separating sub-micron particles. Some developments have shown that focusing of sub-micron particles is possible [150–153], but generally very high acoustic energy densities and/or low flow rates are required.

Acoustic fields simulated in three dimensional capillaries

Ley *et al.* presented 3D simulations for an acoustic trapping capillary actuated at its half-wave resonance frequency [23]. This actuation model was designed to mimic a pushing and pulling motion on the glass capillary (with a wall displacement of around 0.1 nm) and simulated pressure and displacement fields, as well as the resulting lateral acoustic radiation forces. They analysed various geometries, chiefly the 0.2 by 2 mm glass capillaries regularly used for acoustic trapping [5, 24, 33, 154, 155], Fig. 2.20. In practice, the capillaries are connected with tubing at each end, therefore the acoustic waves are not reflected at the end of the capillaries. This was modelled as an artificial perfect absorber of outgoing travelling bulk acoustic waves [23].

The resulting fields, presented in terms of pressure and displacement in Fig. 2.20b-c, show a standing wave above the actuation plane plus a travelling wave moving away from the transducer region. The pressure amplitude drops by an

order of magnitude just past the transducer, which gives rise to the lateral forces that define the trapping region, Fig. 2.20d.

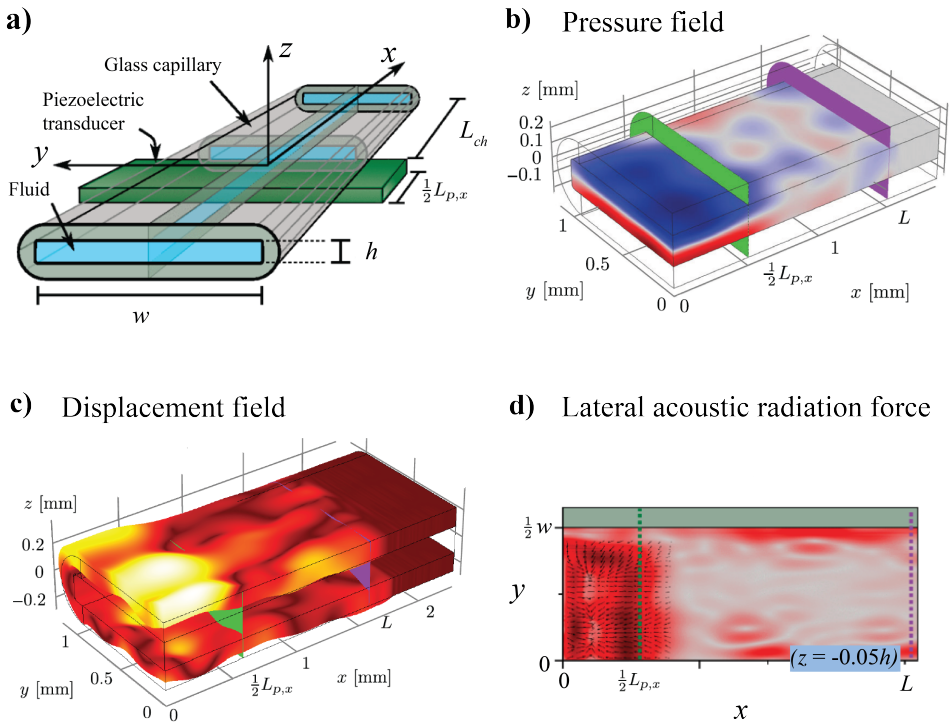

Figure 2.20: 3D model and (one-quarter) simulations of a simple glass capillary with dimensions as used in this work (h=200 µm and w=2 mm) actuated for the simulations at 3.906 MHz. The green boundary indicates the edge of the actuation region and $(0, 0, 0)$ is the centre of the capillary. The purple boundary indicates the position of the artificial perfect absorber in the models, added to dampen outgoing travelling bulk acoustic waves. a) Sketch of the full 3D capillary filled with water and mounted on a transducer. b) The pressure field p indicated by blue (-0.18 MPa) and red (0.18 MPa) in the fluid. c) The displacement field $\boldsymbol{u}$ of the glass capillary ranging from dark red (0 nm) to white (1.2 nm). d) The lateral acoustic radiation force acting on 12 µm polystyrene beads in the x-y plane at $z = -0.05h$, light gray is 0 pN and dark red is 0.44 pN. Reprinted figure (adapted) with permission from [23] Copyright 2015 by the American Physical Society.

Lateral forces on particles

In acoustic trapping, as in acoustic focusing, the primary axial acoustic radiation force (in the z direction) levitates particles in the acoustic field, Fig. 2.18b. However, since the acoustic field is localised, the velocity fluctuation magnitude drops at the edge of the transducer [156]. This additionally introduces lateral radiation forces (see black arrows in the negative x direction in Fig. 2.20), enabling the system to trap particles against fluid flow, Fig. 2.21.

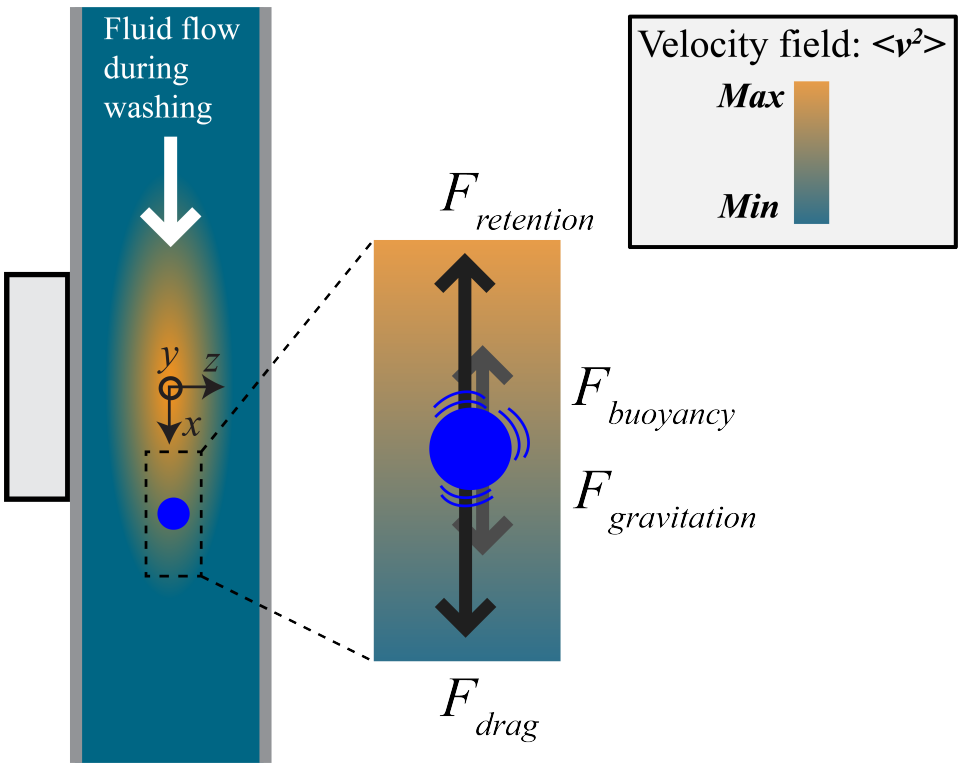

Figure 2.21: Schematic side-view in the $x-z$ plane in the centre of a vertical acoustic trapping unit, where a single particle is trapped against flow. Inset highlights the forces acting on the particle trapped in an acoustic field where orange glow represents the area with highest mean squared velocity fluctuation.

This localized acoustic field is used to suspend a pancake-shaped cluster (a thin disc) of particles in the capillary above the piezoelectric transducer. The use of such a seed particle cluster will be explained in Section 2.3.3, when we approach the trapping of nanoparticles. A seed particle cluster may be retained at this point, against the drag force induced during washing in the x direction, when there is a local strong Gor'kov minimum [23, 144, 156]. The retention force $\boldsymbol{F_r}$ for a single particle of volume V_p at point $(x, 0, 0)$ in the capillary actuated with pressure amplitude P_0 and angular frequency ω [24, 156]:

$$\boldsymbol{F_r}(\boldsymbol{x}) = -V_p \frac{3\, f_2 p_0^2}{8\, \omega^2 \rho_0} k_x k_z^2 \sin\left(2k_x x\right) \boldsymbol{e_x}. \tag{2.14}$$

In the capillary used in this work, the resonance frequency f of the water-filled capillary was 4 MHz. The angular frequency, ω is $(2\pi f)$ of the applied ultrasound. The wavenumbers in the x and z directions are given by:

$$k_x = \frac{2\pi}{\lambda_x} = \frac{2\pi}{2l} \text{ and } k_z = \frac{2\pi}{\lambda_z} = \frac{2\pi}{2h}, \tag{2.15}$$

where the piezoelectric transducer length l is approximately 2000 µm and h = 200 µm is the height of the capillary. λ is the corresponding wavelength for each wavenumber k, in the x and z directions.

According to Eq. 2.14, the retention force which a particle experiences in an acoustic trap depends on its density relative to the fluid. In order to achieve a high throughput in nanoparticle trapping, the seed particle cluster needs to withstand strong drag forces and be stably trapped. This requires a strong retention force which can be enabled by both strong acoustic fields and the microparticles having a large density contrast ($\tilde{\rho}$), as demonstrated by the transition to silica seed particles in **Paper I** [24]. The seed particles are particularly useful if they can be acoustically trapped at a wide range of voltages and flow rates, see Section 2.3.3 for detail on the transition to silica seed particles on this basis. Increasing the acoustic field strength can be achieved by increasing the voltage of the ultrasound transducer, however an unfortunate side effect is excessive heating, which is to be avoided for biological samples.

Secondary acoustic radiation force

In practice, the acoustic forces on a particle depend on more than just its own physical properties, the surrounding fluid, and the applied acoustic field. Usually there will be more than just a single particle in the acoustic field. If the other particles also scatter sound then their presence will introduce interparticle forces, sometimes called secondary acoustic radiation forces [157, 158]. One consequence of interparticle forces, combined with the primary acoustic radiation force, is that microparticles or cells in an acoustic field are pushed close together to form a tightly packed cluster levitated in the pressure node [156, 159].

To understand this mathematically, a simple case is illustrated in Fig. 2.22, where we consider the forces on a probe particle which is in the vicinity of a large source particle. The interparticle forces between the probe and source particle can be attractive or repulsive depending on the position of the particles relative to the acoustic pressure node as described by Baasch *et al.* [159].

Equation 2.16 presents a simplified expression for the magnitude of the secondary acoustic radiation force F_{Sec} between two particles (given subscripts $_{p1}$ and $_{p2}$) dependent on their radii (a_{p1} and a_{p2}), densities (ρ_{p1} and ρ_{p2}), and compressibilities (κ_{p1} and κ_{p2}) [157]:

$$F_{Sec} = 4\pi\, a_{p1}^3 a_{p2}^3 \Bigg[\frac{(\rho_{p1}-\rho_0)(\rho_{p2}-\rho_0)(3\cos\theta^2-1)}{6\rho_0 d^4} < v^2(z) > - \frac{\omega^2 \rho_0 (\kappa_{p1}-\kappa_0)(\kappa_{p2}-\kappa_0)}{9d^2} < p^2(z) > \Bigg]. \quad (2.16)$$

This is a short range force which increases significantly with decreasing distance d between the particles, and the sign depends on the angle θ describing the particles' positions relative to the pressure node. Upon closer inspection of the first part of Eq. 2.16, it can be seen that, in the pressure node where $< p^2(z) >= 0$, the interparticle force scales with the distance as d^{-4}. Therefore a strong force can arise even when one of the particles is very small (a is small), so long as the particles are very close together (d is also small).

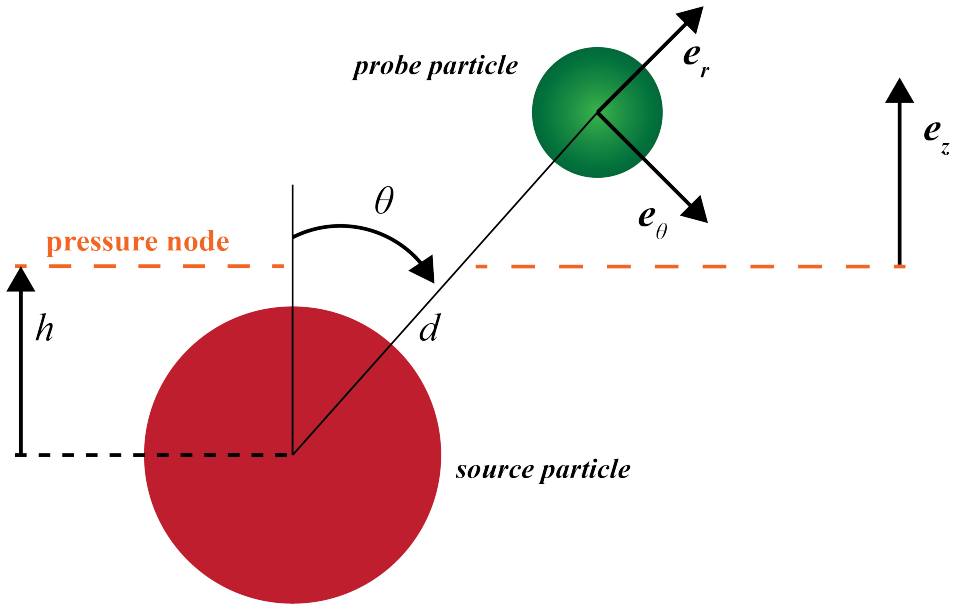

Figure 2.22: Schematic representation of source and probe particles near an acoustic pressure node. Secondary acoustic radiation forces occur for multiple particles in an acoustic field, which generates attractive or repulsive forces between the particles. The interparticle force experienced by the probe particle will depend on the angle θ and distance d from the source particle. Schematic inspired by Baasch *et al.* [159].

2.3.3 Acoustic trapping of nanoparticles

So far, the acoustic forces responsible for trapping a cluster of microparticles in an acoustic pressure node have been described. It can be seen from both Eq.s 2.14 and 2.16 that the acoustic radiation forces scale with the volume of the particle, thus $F^{rad} \propto a^3$. From Eq. 2.4, drag forces scale as $F_d \propto a$, thus they begin to overcome trapping forces as particles get smaller. In general for our system, operated at a peak to peak voltage of 10 V_{pp}, the trapping limit is approximately 1 µm for polystyrene particles. Particles larger than that limit can be trapped (including cells, polystyrene and silica), whereas sub-micron particles cannot be directly trapped. Of course, this is a generalisation because both acoustic and drag forces may be controlled to some degree. However, with any practical flow rate in our system, the acoustic forces on a small number of

sub-micron particles are insufficient to retain them.

The first hint at a solution to enable acoustic trapping of sub-micron particles was found seemingly by accident. Instead of the intended dilution, a very high concentration of polystyrene nanoparticles was used in a trapping experiment and began to aggregate together and be trapped. In the results, published in 2012, Hammarström *et al.* showed that there was a threshold [33] of particle concentration above which they could even trap particles with diameters close to 500 nm. Still, many particles were caught up in acoustic streaming rolls which will be discussed in the next subsection.

This finding led to the introduction of seed particle trapping, whereby microparticles are preloaded in the trapping region and then nanoparticles can be trapped in the interstitial space within the cluster of microparticles. These particles are called *seed particles*, microparticles from which a cluster of trapped particles can grow: in some ways like how a seed crystal can support the growth of large crystals in a solution. The exact mechanism which makes it possible to trap nanoparticles in this way is, however, less well established. Figure 2.23 illustrates some of the factors which may play a role in holding nanoparticles close to seed particles, and enabling them to be retained against flow.

Historically, $\boldsymbol{F}_{Sec}$ interparticle forces were thought to be the sole drivers of nanoparticle trapping [33]. When particles are close to the pressure node, this acoustic interaction force would be dependent on the dipole scattering coefficients and sizes of all the particles involved, Eq. 2.16. Although attraction as well as repulsion due to secondary acoustic forces has been observed experimentally [159–163], the role of these forces in acoustic trapping is unclear. A better understanding of these effects could allow improved efficiency and control of acoustic trapping. It may be important to also consider electrostatic forces if the particles are charged. Furthermore, there is increasing attention towards the potential roles of hydrodynamic shielding and micro-streaming in helping nanoparticles to be trapped in the vicinity of seed particles, rather than getting pulled away by drag forces. The following section will first discuss acoustic streaming, a relevant phenomenon observed when trapping smaller particles, and then address each of the mechanisms summarised in Fig. 2.23.

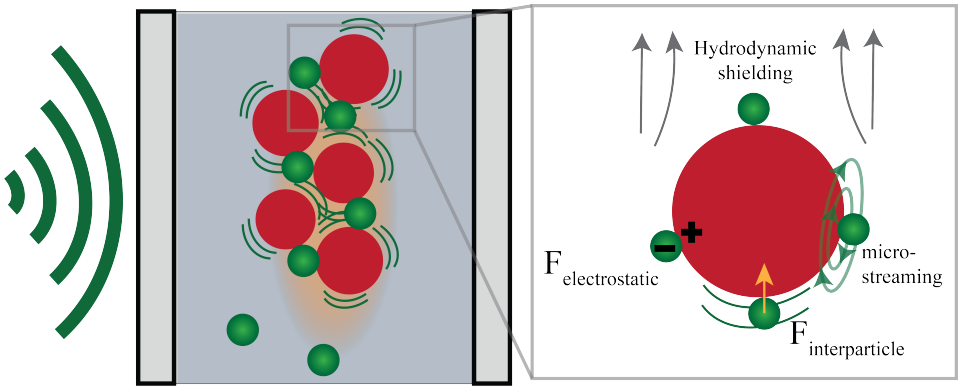

Figure 2.23: Schematic representation of forces which may play a role in acoustic trapping of nanoparticles (represented in green) inside seed particle clusters (red circles). Part of figure inspired by [4]. i) Nanoparticles may be hydrodynamically shielded by the seed particles, experiencing lower drag forces and allowing retention in the cluster whilst external flow is applied. ii) Electrostatic attraction can be relevant to consider, depending on the surface charge on each particle, for example between a positively charged seed particle and a negatively charged nanoparticle. iii) Interparticle forces caused by the sound scattering of seed particles increase significantly at short distances and can lead to particles being attracted to each other. iv) Microstreaming close to the seed particle surface may drive vortices capable of trapping nanoparticles.

Acoustic streaming

Acoustic streaming has been observed when transducers are actuated below trapping capillaries, introducing drag forces that recirculate fluid in the vicinity of the trapping region [33], Fig. 2.24a. With dilute concentrations of nanoparticles, Hammarström *et al.* [33] observed that the motion of the particles was dominated by streaming rolls, evading trapping. The characteristic streaming rolls can be observed in the plane parallel to the transducer in the centre of the trapping capillary, whilst the transducer is being actuated, Fig. 2.24a. Incoming sub-micron particles are pushed by fluid towards the centre, but then rapidly pushed towards the walls and around away from the transducer before recirculating back again. This streaming is thought to be largely induced by thermoviscous effects due to the thermal gradient above the transducer (Fig. 2.24b) and to a less extent boundary driven streaming (Fig. 2.24c) [164].

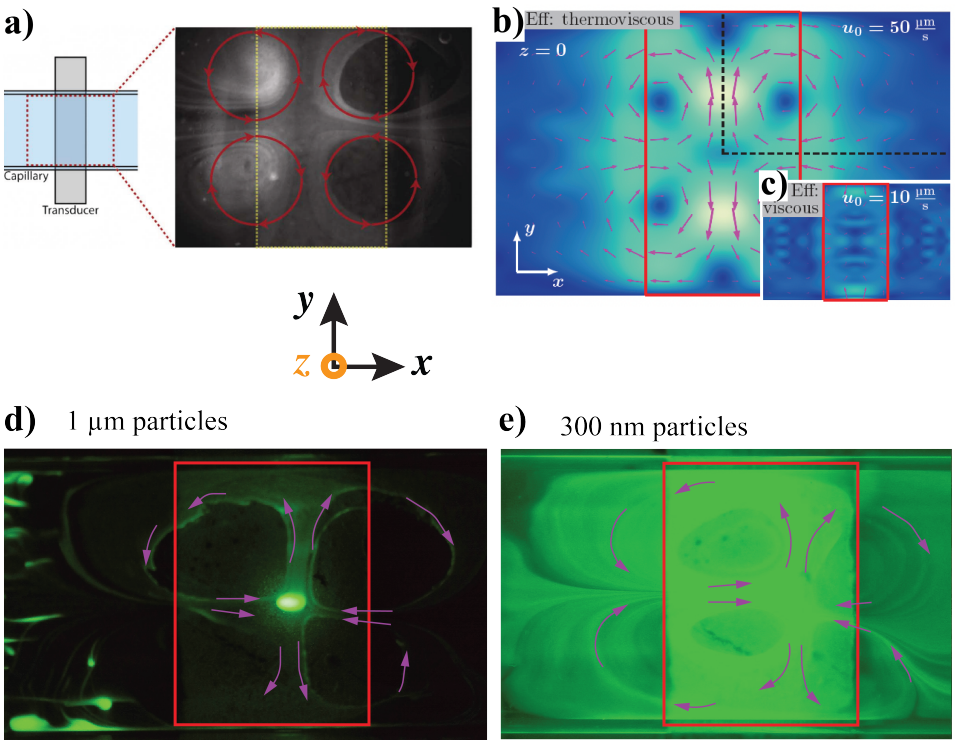

Figure 2.24: a) Experimental observation of acoustic streaming in a trapping capillary, figure used with permission of Royal Society of Chemistry, from [33]; permission conveyed through Copyright Clearance Center, Inc. The acoustic streaming pattern in the trapping capillary is shown using 500 nm particles at a concentration of 0.1%wt. The capillary is horizontally aligned and the transducer is outlined in yellow. Four characteristic streaming rolls are observed for this setup at resonance, as indicated by the red arrows. b) Theoretical simulation of thermoviscous acoustic streaming. The streaming velocity in the central plane $z = 0$ is indicated by the size of the magenta arrows. The dashed black lines show the symmetry planes, and the red lines the edge of the actuation region. c) The same simulation neglecting thermal effects. b-c) are adapted and reprinted with permission from [164]. Copyright 2021, Acoustical Society of America. d-e) Show the acoustic streaming rolls observed with 1 µm and 300 nm green polystyrene particles. Magenta arrows roughly show the four vigorous streaming rolls are present in both cases.

The simulations by Joergensen *et al.* suggest that, in theory, only 1 °C difference in temperature above and outside of the actuation region is sufficient to produce 50 µm/s streaming rolls [164]. Preliminary results show that the pattern and velocity of these streaming rolls can be modified by external temperature gradients. Streaming rolls observed in a trapping capillary are shown for polystyrene particles of 1 µm and 300 nm in Fig. 2.24d and e, respectively. In Fig. 2.24d, a bright spot in the centre is observed, indicating the 1 µm particles beginning to be trapped, however as the streaming rolls build in speed this cluster was also disrupted by the streaming. The four characteristic streaming rolls can be seen to dominate for 300 nm, Fig. 2.24e, whereas no trapping is seen even in the absence of an external flow. However, it is still unknown to what degree this streaming phenomenon aids or hinders nanoparticle trapping when seed particles are present. One argument is that the recirculation should be advantageous because it increases the chance of nanoparticles coming in close to the seed particles. Without recirculation there might be more nanoparticles close to the wall which follow a flow-line too far from the seed particle trapping cluster. On the other hand, rapid streaming rolls could overcome trapping forces in some locations around the cluster and thus have a detrimental effect on trapping. It's worth noting that several microfluidic devices have been designed to use streaming rolls themselves as a mechanism of trapping [165–167].

The importance of seed particles

Whilst Fig. 2.24 showed that 300 nm polystyrene particles recirculate in streaming rolls in the absence of seed particles, those same nanoparticles can be enriched in the interstitial space between seed particles. Seed particle clusters are pre-loaded into the trapping region to allow the acoustic trapping of nanoparticles, Fig. 2.25. This technique was first demonstrated in 2012, enabling acoustic trapping of particles as small as 100 nm [33]. The acoustic trapping seed particle concept is similar to earlier work by Gupta *et al.* [168], where a chamber packed with glass beads (3 mm) was actuated with an acoustic standing wave to trap 2 - 15 µm polystyrene against flow.

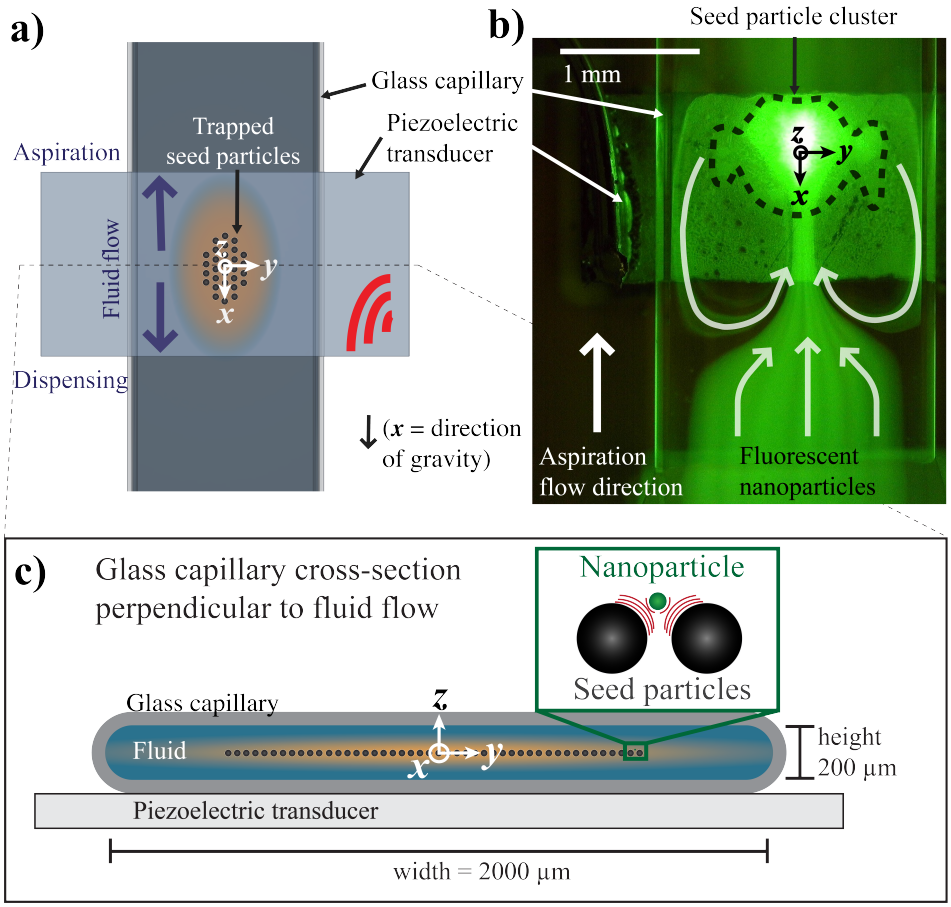

Figure 2.25: A glass capillary actuated with a piezoelectric transducer at 4.1 MHz, used for acoustic trapping of nanoparticles. a) Schematic where the acoustic field is represented by the local $< v^2 >$ maximum (orange shading) in the centre of the capillary. The velocity gradient traps seed particles (10 µm, dark spheres), between which nanoparticles (< 300 nm, green sphere) are trapped. b) Image of trapping region during aspiration of high concentration NPs (around 10^{12} particles/ml) into the seed particle cluster. Arrows indicate how the sample is aspirated and acoustic streaming focuses and recirculates nanoparticles into the seed particle cluster. c) Schematic of a cross-section of the capillary where a nanoparticle is being trapped between seed particles. Adapted and reproduced from [24] according to the (CC BY 4.0) licence.

A visual demonstration of the value of seed particles is presented in Fig. 2.26. Nanoparticles of 150 nm cannot be trapped directly even if they are made of an extremely dense material such as gold nanoparticles (AuNPs). However, seed particles can enable trapping of these previously untrappable nanoparticles as well as significantly increase trapping of the slightly larger sub-micron particles (250 nm AuNPs).

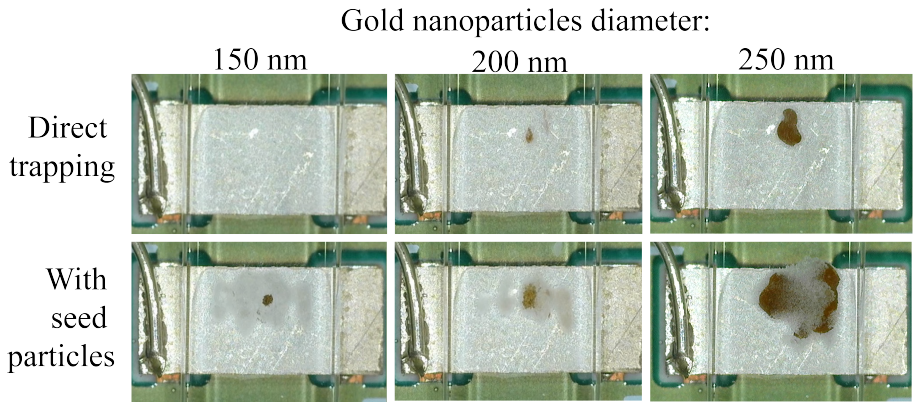

Figure 2.26: Direct and seed particle trapping of gold nanoparticles (AuNPs). AuNPs were grown to 150, 200 and 250 nm, trapped nanoparticles can be seen in brown. The seed particles in the bottom row of this image were 12 µm polystyrene and they can just about be seen as a grey cloud in front of the transducer (white rectangle).

Since its inception, there have been a number of publications using this seed particle method to trap sub-micron particles from biofluids, for various diagnostic and research applications. Acoustic trapping of bacteria using seed particles has been performed in several studies [33, 169, 170]. The addition of seed particles was critical in this case, because the concentration of bacteria in blood culture (approximately 10^7 bacteria/mL [169]) was lower than the concentration at which direct capture would have been possible [33]. Following from that work, acoustically trapped EVs from blood plasma [17, 129, 131, 133, 171, 172], conditioned media [129] and urine [129, 132, 173] have been studied. The work in **Paper III** adds cerebrospinal fluid to that list. As discussed in Section 2.2, the concentration of EVs in these biofluids range from $10^9 - 10^{12}$ particles/mL and the majority of those EVs are smaller than 100 nm.

Silica-based seed particles

Although seed particle enabled nanoparticle trapping has been utilised for over a decade, most studies used the same size (10 - 12 µm) plain polystyrene microparticles [33, 132–134]. The work in this thesis focuses mostly on transitioning to silica-based seed particles. As shown in Fig. 2.27, an acoustically trapped cluster of silica seed particles with 10 µm diameters can be used to effectively trap 1 µm-sized particles, overcoming the streaming rolls which dominated in Fig. 2.24. Another notable use of silica seed particles was while trapping bacteria for mass spectrometry in 2014, by Hammarström *et al.* [169]. In that case, the choice of material was motivated by the hydrophilic surface properties of silica beads, anticipating that silica seed particles would have less non-specific binding of proteins than polystyrene seed particles. However, they did not compare trapping performance versus polystyrene seed particles.

There are two acoustic advantages of using silica seed particles instead of polystyrene seed particles. These advantages stem from the fact that silica is twice as dense as polystyrene; this has significant consequences for the retention and interparticle forces (Eq.s 2.14 and 2.16, respectively), generated with silica seed particles. The dipole scattering coefficient, Eq. 2.11, of silica in water is an order of magnitude greater than polystyrene in water, see **Paper I**. This leads to high acoustic radiation forces retaining silica seed particles in the trap. The advantage of a high retention force is that the seed particle clusters can be trapped against higher flow rates and allow more rapid processing during nanoparticle trapping, without the risk of losing the cluster [24]. After this was demonstrated, Costa *et al.* [174] also used silica seed particles for their advantageous acoustic properties: using silica seed particles enabled microplastics to be acoustically trapped from water, at flow rates of 5 mL/min. From previously presented theory, we would expect that the secondary acoustic radiation forces should be stronger on nanoparticles, if the density contrast of the seed particles (source particle in Fig. 2.22) is increased.

The use of silica seed particles to trap 270 nm polystyrene nanoparticles was investigated in detail in **Paper I**. **Paper II** also demonstrates that the trapping of extracellular vesicles can be achieved with silica seed particles. Furthermore, we investigated whether neutrally charged seed particles can still be used to trap EVs by using zwitterionic silica seed particles **Paper II**, as electrostatic attraction could be expected to play some role.

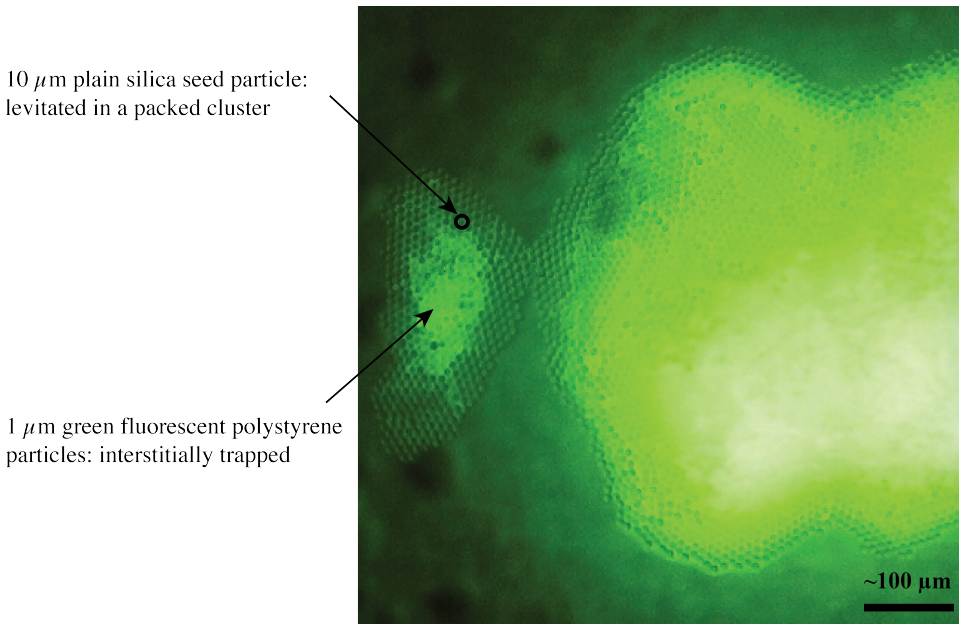

Figure 2.27: Image of fluorescent polystyrene 1 μm particles trapped inside a seed particle cluster. 10 μm silica seed particles are just about visible, one is circled in black, and the green glow shows enriched polystyrene particles within the seed particle cluster. The scale bar is approximately 100 μm.

Electrostatic attraction

As the acoustic trapping process involves two different types of particles (the nanoparticles and the seed particles) getting close to each other, the charge on the surface of these particles can become important. For example, if microparticles have an amino (-NH_2) or carboxylic acid group (-COOH) termination on the surface, these particles become positively and negatively charged in water, respectively. This can lead to electrostatic attraction between microparticles and nearby oppositely charged nanoparticles, or else repulsion if they are similarly charged. Even without such terminal groups, as for the plain polystyrene and silica microparticles used in this work, there may be chemical forces (such as a hydrophobic or Van der Waals force) between neighbouring particles in an aqueous medium. For example, in the absence of stabilisers, plain polystyrene particles in pure water have been seen to aggregate [175]. The effective charge

on the surface of these particles can change with pH and the attraction/repulsion experienced by a charged particle can also be shielded by salt concentration, since ions attracted to charged surfaces produce a double layer and a diffuse layer. Preliminary experiments showed that the adsorption properties of seed particle surface were noticeable when trapping in Milli-Q®(ultrapure water from Merck KGaA), where carbon dioxide from the air can make the solution acidic.

Zwitterionic silica seed particles were used in **Paper II**, with the aim to remove electrostatic effects. *Zwitterionic* silica (SeQuant®ZIC-HILIC^{TM} now owned by Merck KGaA, Darmstadt, Germany) is often used in liquid chromatography [176, 177]. The silica surface is functionalised with sulfoalkylbetaine zwitterionic groups, designed to be a hydrophilic, highly polar stationary phase that can enter into simultaneous attractive and repulsive electrostatic interactions, yet has zero net charge [176, 178, 179]. Using zwitterionic silica seed particles would therefore be expected to reduce electrostatic effects, in nanoparticle trapping.

Hydrodynamic shielding

In a fluid with laminar flow, the flow will divert around an obstacle, such as can be seen in Fig. 2.28. A small particle may thus be shielded from the flow by a larger obstacle, and the smaller particle would not experience the same drag force as it would have done without the obstacle. Several microfluidics-based techniques have used hydrodynamics to trap cells [180] and extracellular vesicles [181]. Hydrodynamic focusing via pinch-flow fractionation [114] and deterministic lateral displacement [13, 116, 117] are other techniques which rely on the features of laminar flow to divert nanoparticles into different flow-lines, made possible by the geometry of the microfluidic channels and the way flow moves around obstacles.

For the case of acoustic trapping within a seed particle cluster, modelling the hydrodynamic effects for thousands of microparticles in the fluid would be extremely challenging. As previously discussed, acoustic streaming can also divert the flow, although it is unknown exactly how this is affected by the presence of seed particles. The overall contribution of hydrodynamic effects to nanoparticle trapping is therefore undefined.

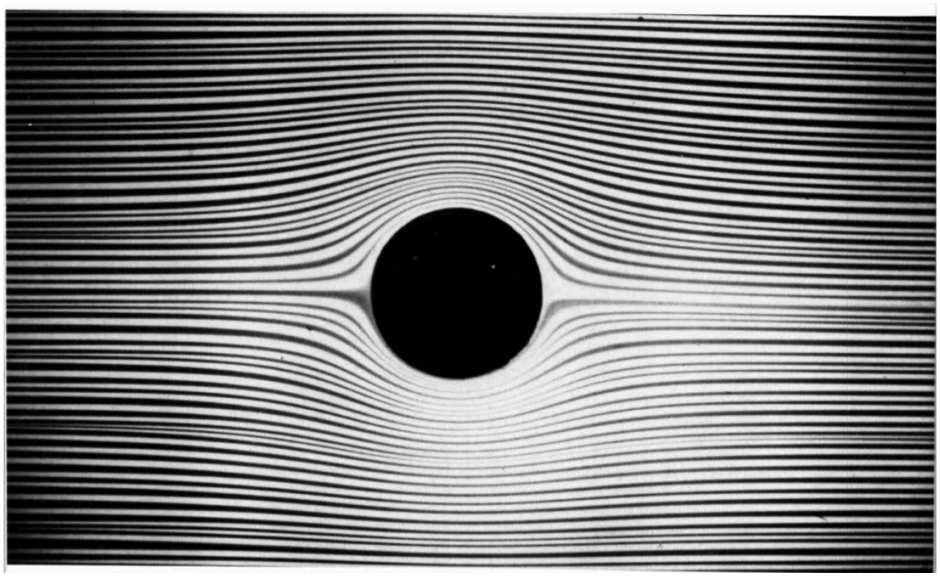

Figure 2.28: Creeping flow streamlines moving around a circular object, dominated by viscous forces in water flowing at 1 mm/s between glass plates spaced 1 mm apart. Photograph by D. H. Peregrine, reproduced from [21].

Microstreaming

Microstreaming around particles in an acoustic field has been theoretically predicted [182–184]. Small, slow vortices localised near the microparticle surface are predicted to occur when in an acoustic field, much like has been seen around an oscillating cylinder, Fig. 2.29. This idea has been utilised for trapping sub-micron particles around micro-pillars, with similar micro-vortices that are actuated by acoustics [185]. Seed particles oscillating relative to the fluid may therefore generate microstreaming. If there are micro-vortices, these could also assist in the trapping of nanoparticles close to the seed particle surfaces.

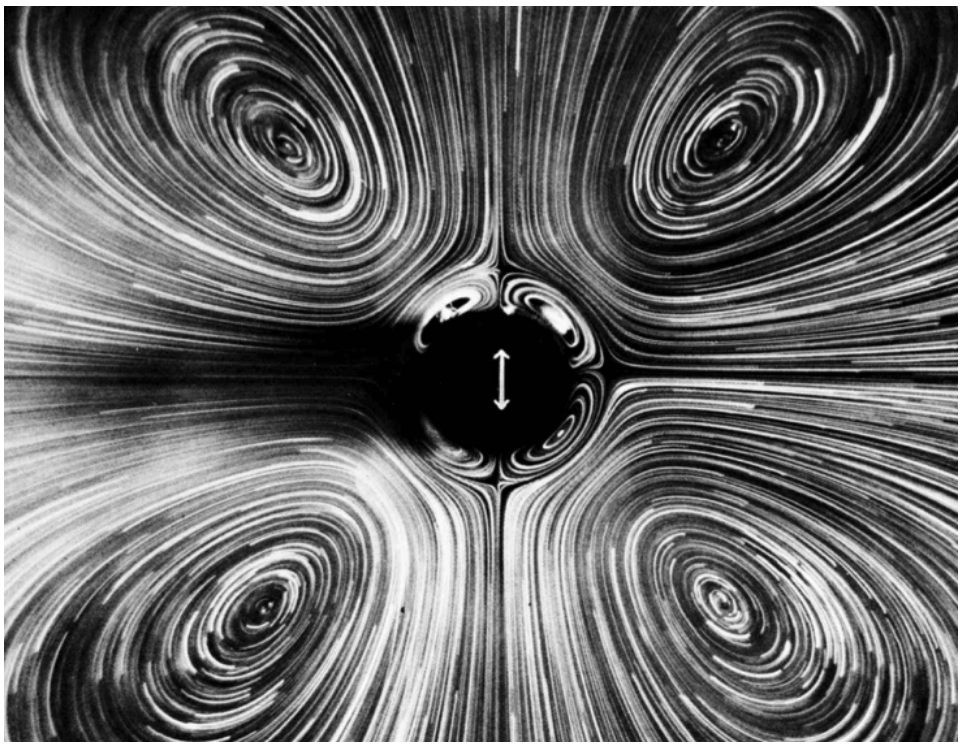

Figure 2.29: Secondary streaming induced by an oscillating cylinder. Photograph by Masakazu Tatsuno, reproduced from [21].

Chapter 3
Techniques and Methodology

Techniques for nanoparticle capture and characterisation face many challenges, especially in specificity and resolution. This chapter provides some more detail on the instruments and techniques used in the papers included in this thesis. As already addressed, acoustic trapping and immunoaffinity are promising tools for isolating EVs or subsets of EVs from background contaminants, the practical use of these techniques is introduced in Section 3.1. Figure 3.1 highlights the main approaches taken to extracellular vesicle downstream analysis, which are addressed in Sections 3.2 and 3.3.

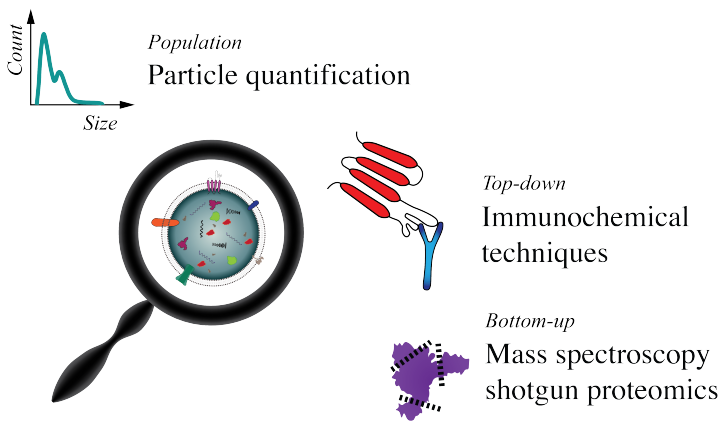

Figure 3.1: Schematic overview of the methods used in EV analysis. On a population level, particle quantification can give concentration and size distributions. Top-down protein analysis can be performed by immunochemical techniques. Bottom-up proteomic analysis is achieved with shotgun mass spectrometry.

3.1 Nanoparticle isolation

Nanoparticle isolation by acoustic trapping occurs inside a glass capillary mounted on a piezoelectric transducer, as described in Section 2.3. To be practical for biomedical applications, the trapping unit has been integrated into a system as a pipetting robot with automated control of the position and fluidics: the AcouTrap 2 (AcouSort AB), Fig. 3.2.

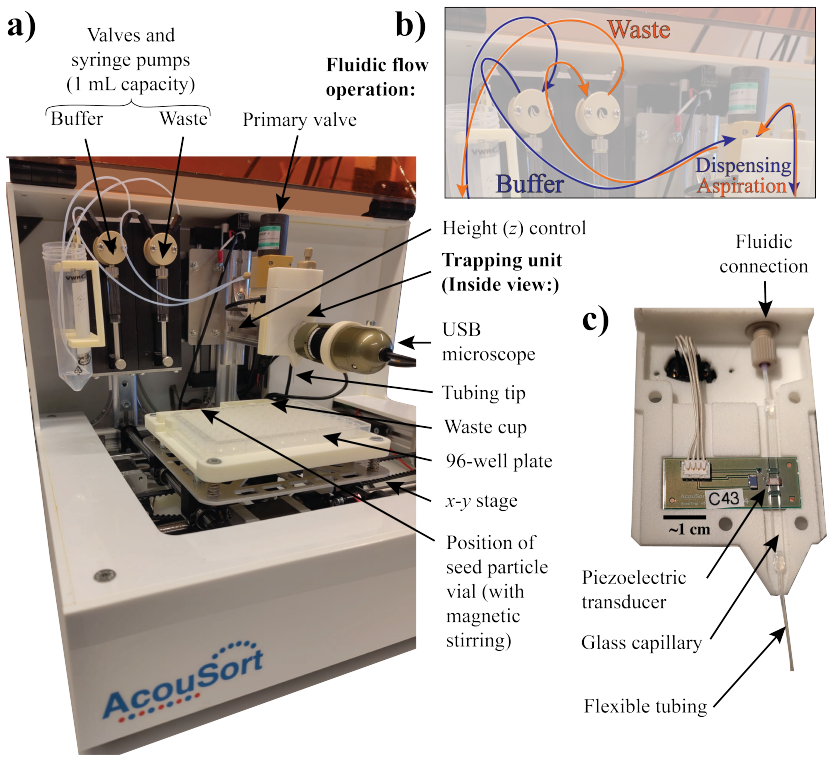

Figure 3.2: a) Annotated image of the AcouTrap 2 system used in this work, equipped with a Dino-Lite USB microscope directed at the trapping region. The locations of the *x*-*y* stage and *z* height control mechanics are indicated. b) Inset shows the direction of fluid flow modes: dispensing in blue (used when washing with buffer into the waste cup or sample release into the 96-well plate) and aspiration in orange (used when pulling in fluid from the 96-well plate). c) The inside view of the trapping unit used in this work - with the transducer, capillary and tubing annotated.

3.1.1 Operating the AcouTrap

To operate the AcouTrap, the software reads scripts which provide commands to operate the valves, syringe pumps, and stage shown in Fig. 3.2, as well as controlling the ultrasound actuation and frequency tracking. Figure 3.3 is an example of a script used to trap 25 µL of sample (biofluid or nanoparticle solution) using pre-loaded seed particles and dispense the seed particle cluster in 75 µL. The 6 main steps that constitute this process are highlighted, namely **1.** trapping the seed particle cluster, **2.** washing the seed particle cluster, **3.** aspirating the nanoparticle sample, **4.** aspirating buffer so that all of the sample reaches the trapping region, **5.** washing the sample, and **6.** dispensing the cluster containing the isolated nanoparticles.

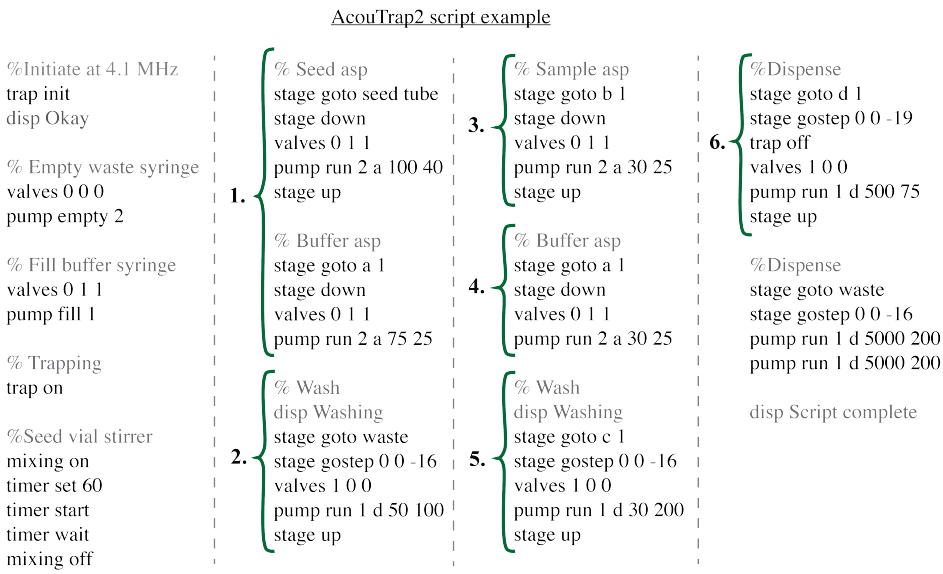

Figure 3.3: An example script for use in the AcouTrap 2 software as a text file, the commands have been split into 4 columns to be read sequentially from top to bottom. Pump number 1 and 2 refer to the buffer and waste syringes, respectively. Aspiration (*asp*) is controlled by the command *pump run 2* ***a*** *[flow rate] [volume]*. Dispensing is controlled by the command *pump run 1* ***d*** *[flow rate in µL/min] [volume in µL]*. Display (*disp*) and commented (%) commands are shown in grey and used to mark each key step in the process.

Frequency tracking

As explained in Section 2.3.1, the resonance frequency of a confined geometry is dependent on the speed of sound c in the fluid medium. Therefore, an exchange of media or a change in the physical properties of the existing media, can result in an altered resonance frequency. As the trapping procedure progresses there are inevitably changes speed of sound due to temperature (which affects the fluid density), exchange of medium (during washing), and the introduction of particles with different properties. Keeping a pressure node in the centre of the capillary overtime means ensuring that the ultrasound is actuating at the resonance frequency. An important consequence of operating at the resonance frequency, as shown in Fig. 3.4, is that it will result in the highest retention forces on the particles.

Hammarström *et al.* [155] developed a method to maintain the stability of the trapping during aspiration of particles and buffer exchange, by frequency tracking by sweeping within 10% of the resonance. In the work presented in this thesis, a frequency scan of $\pm 1\%$ was repeated every second to find the frequency at which the power input is maximised. This enables the system to continuously adapt to gradual changes in the content of the capillary. As detailed in Appendix B of **Paper I**, the resonance frequency of the system shifts with temperature and seed particle load, Fig. 3.5. Depending on the broadness of the resonance peak, if tracking is not activated then a slight change in acoustic impedance of the medium could mean that the seed particles are lost.

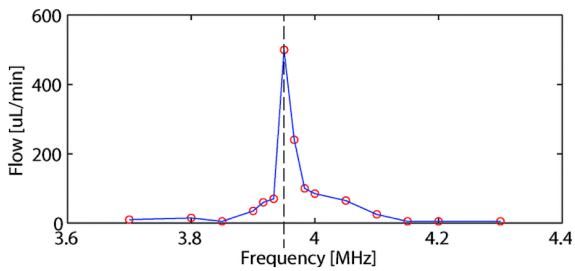

Figure 3.4: The maximum flow rate at which a cluster of beads could be trapped at different frequencies. Used with permission of Royal Society of Chemistry, from [155]; permission conveyed through Copyright Clearance Center, Inc.

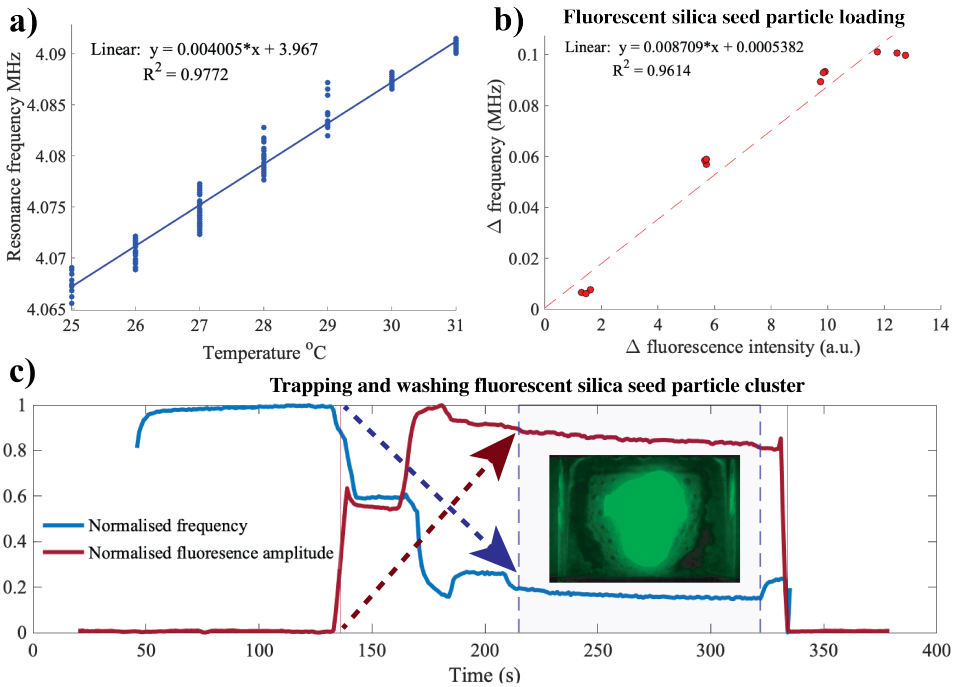

Figure 3.5: a) Resonance frequency of a 200 µm-high water-filled trapping capillary, compared to the measured temperature on the circuit board near the piezoelectric transducer. The temperature change occurred due to the piezoelectric material heating up during actuation. This set-up only recorded temperature to the nearest 1°C. Reproduced from [24] according to the (CC BY 4.0) licence. b) Correlation between frequency change and the fluorescence intensity change, following the trapping of increasing numbers of fluorescent silica seed particles. c) Normalised frequency (blue) and fluorescence (red) changes overtime during a silica seed particle trapping protocol. After washing at a flow rate of 50 µL/min, the flow was stopped for 1 min (see image of stable cluster) and then the sound was turned off to release the cluster.

For this reason, tracking is usually active when trapping nanoparticles. On the other hand, the sweeping of frequencies during frequency tracking can cause a trapped seed particle cluster to jump slightly as the acoustic force may be lost while the frequency is off-resonance for a short time. In **Paper I**, frequency tracking was switched off when testing critical flow rates of clusters at flow rates higher than 200 µL/min, as in some cases this momentary loss of acoustic force

was enough for the cluster to be moved outside the trapping region.

3.1.2 Immunoaffinity beads

The immunoaffinity beads used in this work were protein A coated silica seed particles of size 10 µm, Fig. 3.6. Protein A has long been known as an anti-antibody [186], binding to the Fc region on immunoglobulins without causing large conformational change, this makes it ideal for conjugating various antibodies onto bead surfaces. Microparticles are available with various antibodies functionalised on their surfaces, but using protein A gives us the flexibility to choose any antibody of interest. This could also work for a mixture of antibodies if desired.

As described in Section 2.2.5, immunoaffinity beads such as these have been used to isolate EVs in various microfluidic systems. **Paper IV** integrates this with the AcouTrap platform to benefit from sub-population of EVs. This work targeted CD9, a common tetraspanin on the surface of EVs, as discussed in Section 2.2.1. Although antibodies are expensive, this label-based technique has potential to retrieve more biologically important information on the origin of EVs and disease mechanisms, to inform future targeted therapies.

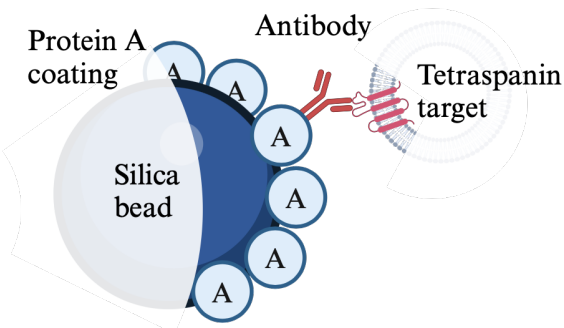

Figure 3.6: Schematic of immunoaffinity capture of tetraspanin positive target vesicle using a Protein A coated silica bead. The antibody is represented by the red Y shape bound at its base to protein A on the bead surface. The tetraspanin protein is illustrated as a pink transmembrane structure with an exposed loop. Illustration not to scale - bead is 10 µm and vesicle is 100 times smaller. Created in Biorender.com.

3.2 Nanoparticle characterisation

3.2.1 Fluorescence microscopy

Fluorescence microscopy was primarily used for acoustic trapping method development, using synthetic nanoparticles. Fluorescent particles, such as the green polystyrene nanoparticles used in **Paper I**, were detected with a fluorescence microscope, mounted as in Fig. 3.2. This was sufficient to visualise the relative concentration of nanoparticles throughout the trapping process, see Fig. 3.7. Videos were recorded and processed frame by frame to quantify average green fluorescence intensity overtime. This method was developed and realised in **Paper I** to compare the process of acoustic trapping of nanoparticles with different seed particles.

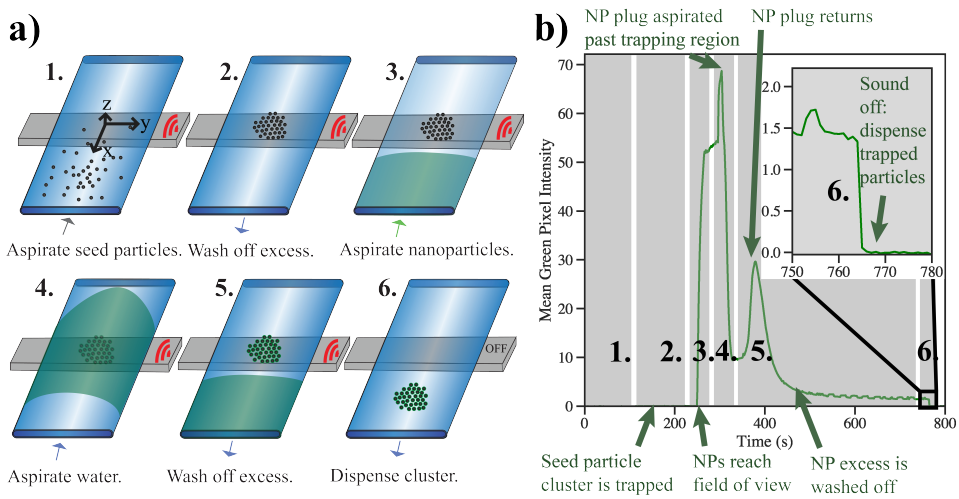

Figure 3.7: a) Schematic of process for acoustic trapping of nanoparticles with seed particles. b) Fluorescent profile overtime during the process of trapping an excess of fluorescent nanoparticles. Numbers correspond to the steps detailed in Fig. 3.3. The peaks show when the plug of nanoparticles passed over the trapping region. The change in fluorescent intensity at **6.**, when the sound was turned off, was used to quantify relative acoustic trapping. Reproduced from [24] according to the (CC BY 4.0) licence.

3.2.2 Nanoparticle tracking analysis

Nanoparticle tracking analysis was used to quantify the size distribution of nanoparticles, both synthetic and biological, before and after trapping. Nanoparticle tracking analysis (NTA) is a technique which relies on the Brownian motion of small particles as they randomly collide in a fluid, which was discussed in Section 2.1.2. The NTA instrument used in this work (LM10, Malvern Panalytical) functions by shining a sheet of laser light through the sample fluid. Particles passing through the laser path will scatter light up to the camera and be detected, see Fig. 3.8. The particles can be indirectly observed through the resulting diffraction patterns and their movement can be monitored from frame to frame. Software in the instrument calculates the distribution of particle sizes based on individual tracking events. The random motion of a particle directly relates to its size and can be calculated from its observed motion according to Eq. 2.5 [187]. The size in this case is the mean diameter, from the hydrodynamic radius, which assumes the particle is a perfect sphere.

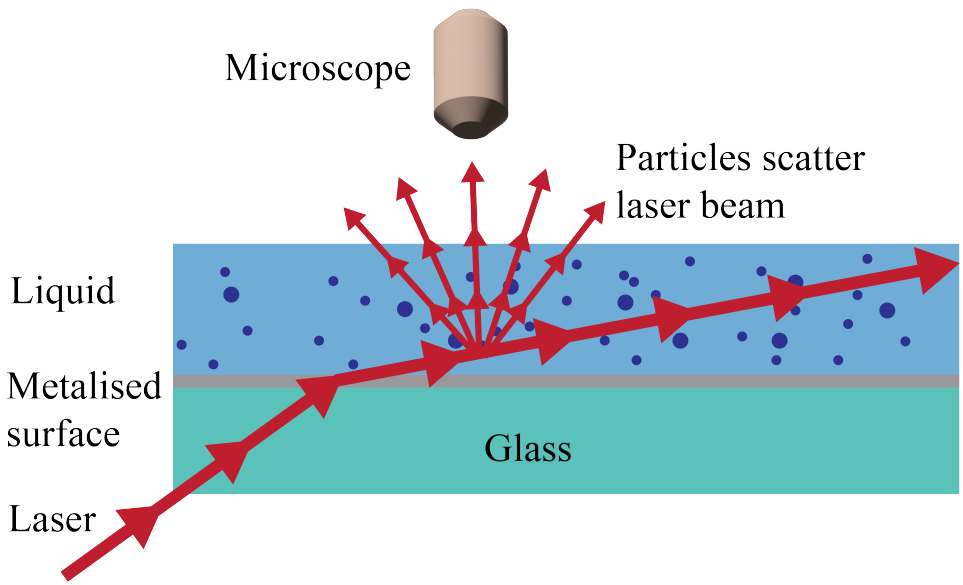

Figure 3.8: Illustration of the laser set up for observing scattered light from nanoparticles in the NTA Malvern Panalytical. Inspired by Malvern Panalytical.

The result is a distribution of particle sizes, which is limited to between around 50 nm and 1 µm. The lowest detectable particle size is dependent on how much the particles scatter light, so the lower size limit of detection is smaller for gold nanoparticles than for EVs. This method is much better suited to measuring heterogeneous samples than dynamic light scattering, as the bulk technique struggles to resolve multiple populations [187, 188]. Particle concentrations derived from NTA measurements are approximate, as they are based on the known volume in the field of view and the average number of particles in a frame. However, NTA has been reported to give variable nanoparticle concentration [189] and it is also limited to samples in the range of 10^7–10^9 particle/mL. The technique was used throughout this work, **Papers I-IV**, to determine the size distribution of nanoparticles (including EVs) in samples.

3.2.3 Transmission electron microscopy

Transmission electron microscopy was employed in the EV trapping studies where the surface markers were of interest. Transmission electron microscopy (TEM) is a powerful imaging tool, Fig. 3.9. Unlike optical microscopy, in TEM the focused beam is made of high energy *electrons* that can have a wavelengths as small as 1 nm. The extremely small wavelength means the resolution is good enough to image EVs as small as a couple of tens of nanometers in diameter. TEM is much higher in resolution than nanoparticle tracking analysis and directly quantifies the particle diameter and morphology rather than inferring the hydrodynamic diameter from particle motion. On the other hand, TEM is a challenging, low throughput characterisation technique with extensive preparation to bind and stain EVs on a grid, Fig. 3.9a. Immunoaffinity, covered in Section 2.2.5, is often paired with TEM via immunogold labelling. This is applied in **Papers III** and **IV**, where gold nanoparticles conjugated with secondary antibodies bind to primary antibodies targeting, for example, tetraspanin epitopes, Fig. 3.9b.

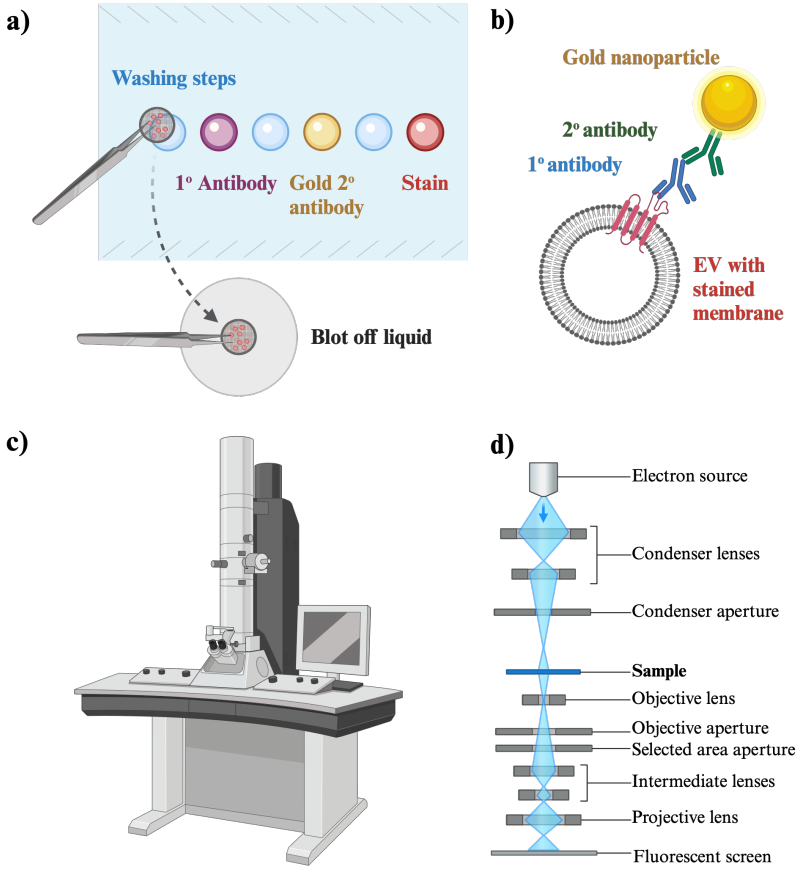

Figure 3.9: Schematic representation of the TEM process. a) Simplified illustration of the staining and washing of the TEM grid, detailed protocols are found in **Papers III** and **IV**. Before staining, the grid is prepared and a droplet of sample is added and left to nearly dry. At each step in this illustration the grid is floated sample-side down for a certain amount of time. Blue droplets indicate washing steps between reagent additions, and blotting on filter paper is performed in between steps to remove excess liquid. Primary (1°) and secondary (2°) antibodies are used where the secondary antibodies are conjugated to gold nanoparticles. b) Immunogold indirect labelling of tetraspanin on an EV. Illustration of c) TEM system and d) the electron beam: the focused electrons are transmitted through the sample and onto a fluorescent screen for detection. Created in Biorender.com.

3.3 Extracellular vesicle protein analysis

Immunogold labelling in conjunction with transmission electron microscopy is a protein analysis technique that targets surface proteins exposed on the membranes of intact EVs. There are many other protein analysis tools that we can use for looking at proteins both inside EVs and on their surfaces. This has been the subject of many investigations and is applied in **Papers II-IV**. Analysing proteins is of particular interest as they have been extensively characterised and they are made up of known amino acid sequences which relate to their structure and function. There are vast databases containing information on each human protein [190]. Some proteins are particularly common, like albumin, whereas others are rarer and are differently expressed in healthy individuals compared to those with a specific disease [99].

3.3.1 Extracellular vesicle lysis

To access EVs cargo, the vesicle membrane must be ruptured. There are a number of techniques which have been employed, a popular method in mass spectrometry preparations is to add radioimmunoprecipitation assay (RIPA) buffer and sonicate the EVs with the Bioruptor (Diagenode SA) [133]. Commercial Bioruptors use 20-60 kHz sound and 100-230 V to generate mechanical stresses by cavitation. In **Papers II** and **IV**, EVs were lysed in this way before protein purification and digestion to peptides for analysis by mass spectrometry.

The RIPA buffer contains sodium dodecyl sulfate (SDS), which is considered a harsh surfactant, that can denature many proteins. Therefore, for immunochemical techniques where the proteins should be intact and functional, gentler lysis methods were explored. The role of detergents in lysis is to solubilise the lipid bilayer membrane of vesicles [191]. In **Paper III**, the rupture of EVs was investigated with non-ionic detergents TritonX and Tween 20X, Fig. 3.10, compared to using the Bioruptor alone. Tween 20X was found to effectively break down EVs whilst not interfering with downstream immunoassay performance [5].

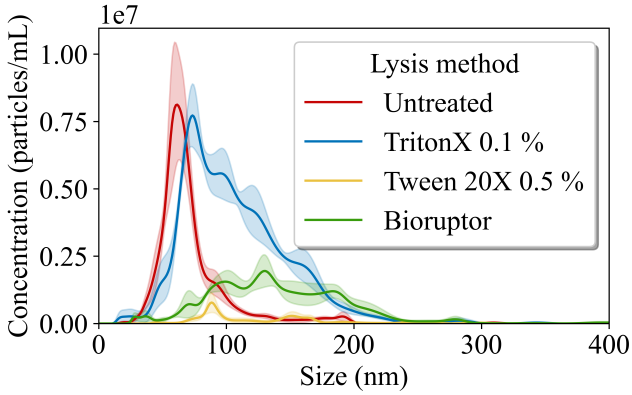

Figure 3.10: NTA size distributions of EVs from trapped CSF following treatment with three lysis methods. The untreated sample shows a typical size range of EVs, mostly below 100 nm. TritonX appears not to lyse the EVs sufficiently. The Bioruptor method reduces the number of EVs to a great degree. The Tween 20X treatment appears to be very effective at breaking apart the particles so that very few are detected by NTA. Reproduced from [5] according to the (CC BY 4.0) licence.

3.3.2 Total protein quantification

The bicinchoninic acid (BCA) assay quantifies total protein. In the assay, residues in proteins (amino acids in a chain) cause a reduction in alkaline Cu^{2+}, to form an intense purple complex [192] which can be quantified with a plate reader. A micro-based BCA assay can be used to improve the sensitivity to detect protein concentrations of 1-25 µg/ml. This method was used in **Paper II** to ensure that there was sufficient protein in each sample for mass spectrometry to be performed.

3.3.3 Mass spectrometry

Mass spectrometry (MS) is a method for measuring the mass-to-charge ratio of molecules [193]. This versatile tool has advanced significantly over the last century. Today, MS is an essential tool in proteomics where proteins can be quantified from a complex sample [194]. Top-down proteomics, meaning

analysing intact proteins, is challenging as these large, folded entities are difficult to ionise evenly. In bottom-up proteomics, amino acid sequences of peptides, the building block of proteins, can be deciphered and used to identify relative abundances of different proteins in a sample [195], Figure 3.11. It is easier to analyse peptides than intact proteins, thus we use the bottom-up method. Details of the sample preparation, running the mass spectrometer, and data analysis used in this work can be found in **Papers II** and **IV**. For more information about MS-based proteomics and where this field is headed, the reader is referred to the thorough review by Guo *et al.* [194].

Figure 3.11a illustrates that mass spectrometry determines the mass-to-charge ratio of molecules by their paths through an electric field, whereby a spectrum of the intensity (or abundance) of each fragment can be produced [193]. This technique is for small molecules, thus proteins must first be cleaved (digested by an enzyme at specific locations) into peptides, Fig. 3.11b. The peptides are then separated by liquid chromatography before gradually entering the mass spectrometer and the abundance of each peptide sequence is analysed [195].

For a single mass spectrum (MS1), multiple sequences of amino acids which make up the peptides can have overlapping signals. Therefore in complex mixtures with many peptides, tandem mass spectrometry 'MS/MS' is used, whereby the scanned peptides are further fragmented and a second set of mass spectra (MS2) is acquired [195].

The acquisition of MS/MS can be either by data-dependent (DDA) or data-independent (DIA) methods [196, 197]. In DDA, only some peptide ions are selected for further fragmentation and analysis. In DIA, all peptide ions within specified mass range are fragmented, leading to more complicated data analysis but less bias in acquisition. In both cases, the amino acid sequences are then correlated with protein databases to determine the protein content [198]. In **Paper II**, a neural network based software - DIA-NN [199] - was used with an experiment-specific spectral library that was first compiled from DDA runs on pooled samples from a small volume of each technical replicate. In **Paper IV**, DIA was used and the mass spectra were compared against a predicted library.

One limitation of mass spectrometry proteomics is the limit of the dynamic range of such measurements. This is especially a problem in blood plasma where there are many common proteins such as albumin that dominate the

signal [99]. EV marker proteins, and potentially EV cargo, are often much lower in abundance than common plasma proteins [200], over 10^5 times lower as highlighted by the red dots in Fig. 3.12 - note the $\log_{10}$ scale. As can be seen by the hundreds of proteins in this plot, the broad identification of proteins makes MS a powerful tool in biomarker discovery. If a large cohort is studied, patterns of differential expression can identify which proteins could be worth further investigation.

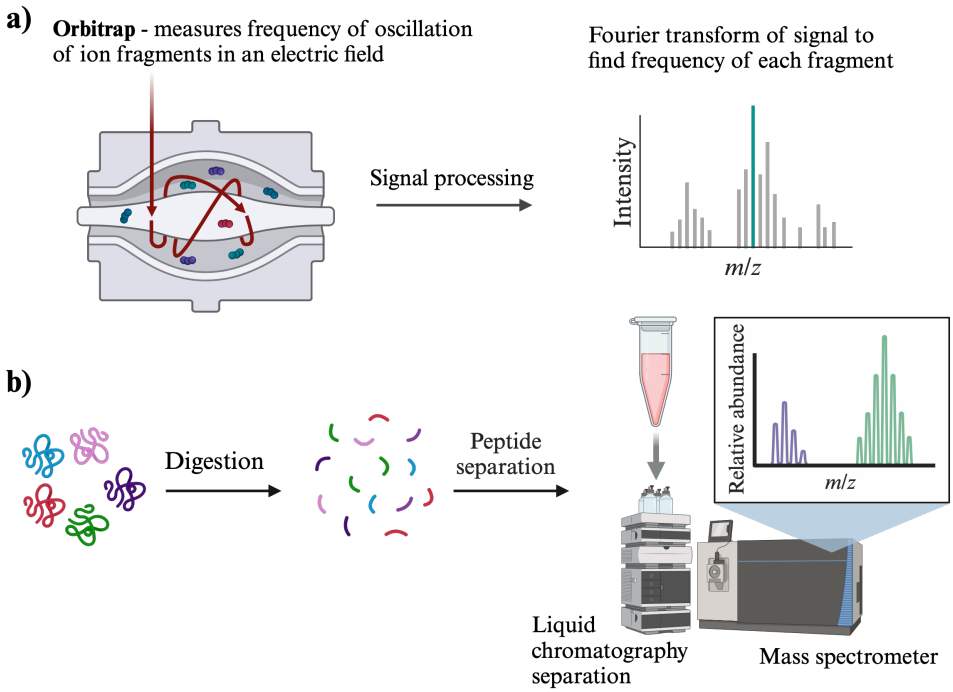

Figure 3.11: a) In general, mass spectrometry involves charged fragments accelerated in an electric field, where the motion of the molecules is used to determine the mass-to-charge ratio (*m/z*) of each event. In the Orbitrap, it is the frequency of oscillations in an electric field which allows the fragments to be distinguished. b) Purified proteins can be digested into peptides and the dissolved peptides can be separated by liquid chromatography before detection and MS analysis of relative abundance of *m/z* peaks. Created in Biorender.com.

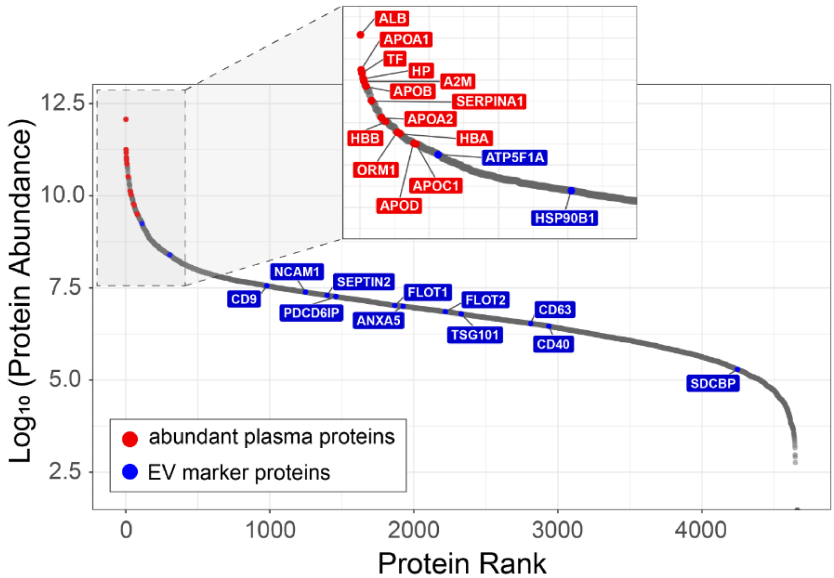

Figure 3.12: Protein rank plots showing the $\log_{10}$ abundance of proteins detected in raw plasma. Some abundant plasma proteins are highlighted (in red) as well as a number of EV marker proteins (in blue) that are identified to be around 5 orders of magnitude lower in abundance. Reproduced from [200] in accordance with the (CC BY 4.0) licence.

In **Papers II** and **IV**, MS was used to analyse the protein content of isolated EVs compared to raw blood plasma. The aim of EV isolation is to increase the abundance of EV proteins (blue) to move further up the ranks, whilst reducing the abundance of plasma proteins. The idea is to boost the signal of these EV associated proteins and to identify more proteins that were too low in abundance to be detected in plasma, as demonstrated in **Paper II**.

3.3.4 Meso Scale Discovery Platform

In **Paper IV**, our target was to detect specific phosphorylations on p-tau from lysed EVs. Assays had previously been developed to detect these specific p-tau forms in CSF [77, 201, 202]. The Meso Scale Discovery Platform (MSD) is shown in Fig. 3.13. The target molecule - in this case p-tau 181 or 217 - is

captured by a primary antibody. A secondary antibody containing a SULFO-TAG^{TM} then binds and allows sensitive detection through a bottom electrode. The imager applies a voltage, causing a series of electrochemically initiated reduction and oxidation reactions which result in luminescence [203], this allows quantitative detection of analytes.

This system was used, instead of a standard enzyme-linked immunosorbent assay (ELISA), because MSD can handle sample volumes of 10-25 µL in microwells within a 96-well plate format (allowing multiple readouts from a single acoustic trapping run) and has a much higher dynamic range than ELISA. Two clear limitations of this technique are: the targets need to be known and the specific antibody must be available. It is impractical for broad biomarker discovery, however it can be very sensitive and specific for quantitative detection and targeted diagnostics.

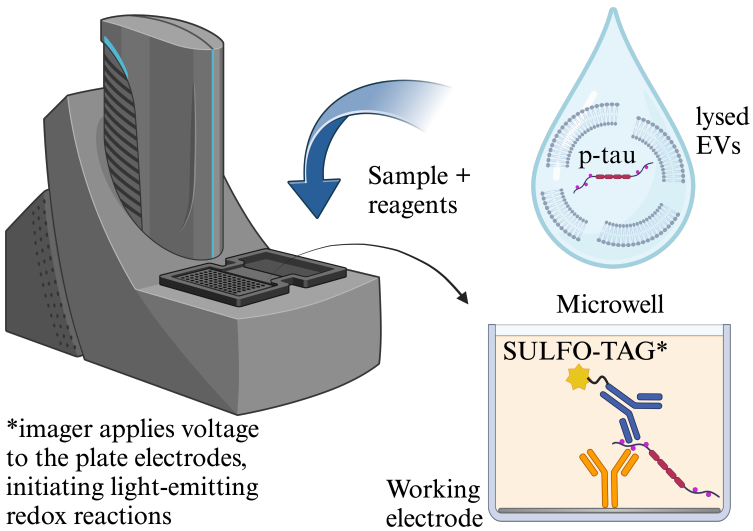

Figure 3.13: Schematic of the use of the MSD platform to detect p-tau targets from a sample of lysed EVs. The sandwich assay using a SULFO-TAG in a microwell of the MSD system enables sensitive detection of a specific phosphorylation of the tau protein. Each microwell in the array is filled with around 25 µL of sample and analysed in the same run, with calibration references. Created in Biorender.com.

Chapter 4

Summary of included papers

The papers included in this thesis follow a progression of improvements and valuable applications of acoustic trapping of nanoparticles using seed particles. As summarised in Fig. 4.1, **Paper I** uses fluorescent nanoparticles to investigate the use of silica seed particles. **Paper II** and **III** apply the improved method to investigate EV content, looking at general protein cargo in the first case and specific targets in the second. Finally, **Paper IV** introduces immuno-acoustic trapping to isolate a targeted EV subpopulation.

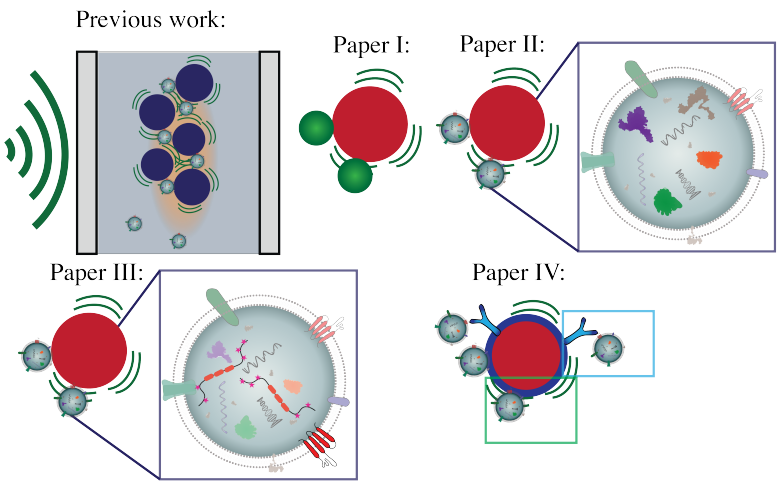

Figure 4.1: Summary of included papers. Seed particles of polystyrene (blue) and silica (red) are illustrated trapping polystyrene nanoparticles (green) or extracellular vesicles (bluish-grey). Parts of the figure are inspired by [4].

Paper I: Silica seed particles improve the efficiency and throughput of nanoparticle acoustic trapping

Aim: Does increasing the density of seed particles improve the throughput and efficiency of acoustic trapping of nanoparticles? *(Addressing Hypothesis 1)*

A limitation of acoustic trapping with seed particles is that the fluid flow rate cannot be too high, such that the drag force on the particles exceeds the acoustic forces. **Paper I** demonstrates that silica seed particles can improve the performance of acoustic trapping efficiency and throughput. Our experimental results aligned well with the theory that predicted silica seed particles should experience much higher acoustic retention forces than polystyrene seed particles. This was simply demonstrated in a method suggested by Ley and Bruus [23]: increasing the flow rate until particles can no longer be retained in the acoustic field and calculating the retention force experienced from the maximum drag force applied. Silica seed particles have a 10 times higher dipole scattering coefficient than polystyrene seed particles, we show that when actuating at 10 V_{pp} the acoustic forces result in a maximum flow rate of 2100±200 µL/min for silica compared to only 200±50 µL/min for polystyrene particles, both with 10 µm diameters, see Fig. 4.2a-b.

Critically, we demonstrate nanoparticles may be trapped into seed particle clusters with greater efficiency and throughput if polystyrene are replaced with silica seed particles, Fig. 4.2c. More specifically we show that, for polystyrene nanoparticles (270 nm diameter) aspirated in a concentration of less than 10^{11} particles/mL, 40-2000% more nanoparticles can be trapped with silica seed particles than polystyrene seed particles. Furthermore, the paper demonstrates that washing flow rates can be increased from 30 µL/min to 200 µL/min without compromising nanoparticle trapping efficiency, Fig. 4.2d. This was only achievable in this system by using silica seed particles rather than polystyrene seed particles which would be lost at such a high flow rate. In this instance the total processing time was halved, paving the way for more efficient processing of nanoparticles.

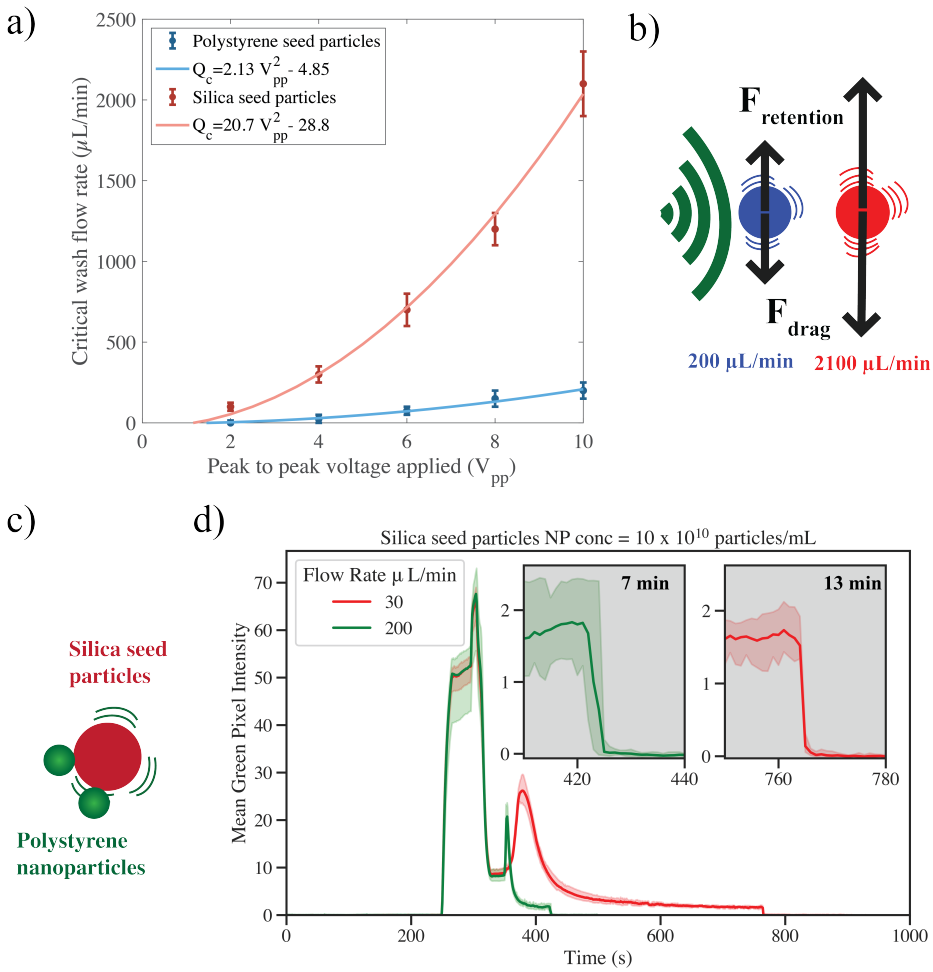

Figure 4.2: a) The quadratic relationship between the critical mean wash flow rates and voltage, for seed particle clusters. b) Schematic illustrating that the equilibrium point between the drag and retention forces, and the corresponding flow rate for silica and polystyrene 10 µm particles at 10 V_{pp}. c) Schematic of acoustic seed particle trapping of polystyrene nanoparticles. d) Graph of fluorescence-time profiles generated by trapping nanoparticles with silica seed particles, where the flow rate was either 30 µL/min (red) or 200 µL/min (green), N=6 for each. The trap off fluorescence change can be seen from the insets, the bounds of the slow wash (red) are well within the bounds of the fast wash (green). Adapted from **Paper I** [24], in accordance with the (CC BY 4.0) licence.

Paper II: Accessing the proteome of extracellular vesicles via rapid acoustic isolation of a minute human blood plasma sample

Aim: Can extracellular vesicles be isolated by acoustic trapping from less than 10 µL of blood plasma? *(Addressing Hypothesis 2)*

In order to address this question, we explored acoustic trapping of small volumes of human blood plasma. Carrying forward the knowledge that silica seed particles were effective at trapping synthetic nanoparticles and allowed higher throughput, we used both polystyrene and silica-based seed particles. **Paper II** compares the proteomic profile of trapped EVs with raw plasma, via mass spectrometry. The findings from this work confirmed that silica seed particles allowed acoustic trapping at higher flow rates, processing biological samples in as little as 6 minutes. In the mass spectrometry proteomic analysis, there appeared to be no significant effect of seed particle density or charge on the EVs isolated from 8 µL of plasma.

Critically, we demonstrated the analytical value of acoustic trapping as a pre-purification method to enrich for less abundant proteins, Fig. 4.3, whilst washing away plasma proteins. Many of proteins which were highly enriched by trapping, have previously been associated with EVs. There was not only an enrichment in the abundance of EV associated proteins in plasma, but also 51 unique proteins were consistently detected only in trapped samples, not in raw plasma. This shows great promise for acoustic trapping as a rapid pre-processing step, to aid the identification of less abundant biomarkers in future large cohort studies.

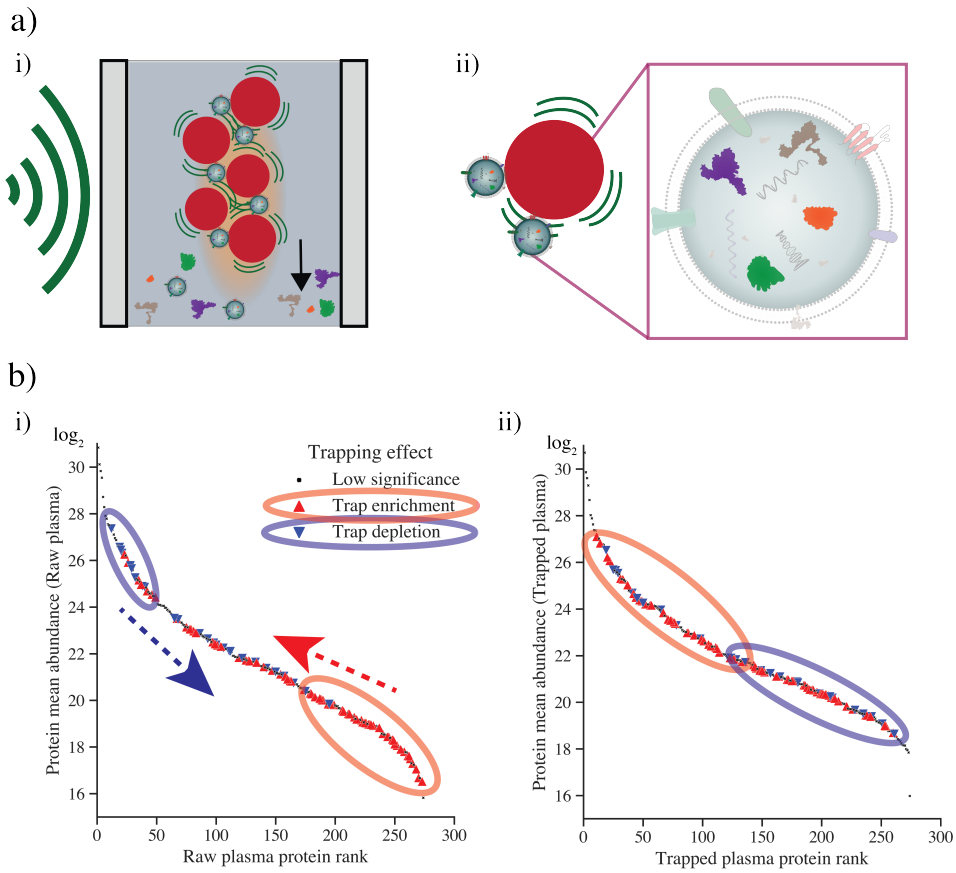

Figure 4.3: a) i) Seed particle enabled acoustic trapping used to isolate and wash EVs from 8 µL plasma (diluted to 25 µL) in 6 minutes in **Paper II**. Seed particles are shown in red - in this work polystyrene, silica, and zwitterionic silica-based seed particles were tested. ii) Trapping EVs enriches for their cargo proteins, which can be analysed by mass spectrometry. b) Mass spectrometry mean protein abundance rank plots for i) raw (N=6) and ii) trapped (N=12) plasma samples. Proteins that are significantly depleted (blue) and enriched (red) by trapping are indicated with up or down triangles. The large ovals and arrows stress that many less abundant plasma proteins are enriched to higher ranks by trapping as well as some of the top ranked proteins being reduced in relative abundance by trapping. Adapted from **Paper II.**

Paper III: Phosphorylated tau in cerebrospinal fluid-derived extracellular vesicles in Alzheimer's disease: a pilot study

Aim: Can acoustic trapping aid the investigation of the cargo of extracellular vesicles in the cerebrospinal fluid of Alzheimer's patients? *(Addressing Hypothesis 3)*

Paper III employed acoustic trapping of CSF to investigate a role of EVs in Alzheimer's disease, specifically looking into their transportation of proteins used as AD biomarkers. In this work, we used silica seed particles to trap 75 μL of CSF from a patient cohort of 40. Following acoustic isolation, we characterised the size, surface markers and p-tau cargo of these EVs. The size of the isolated EVs was not found to differ between those with and without the disease, Fig. 4.4a. Furthermore, trapped EVs were identified by TEM and immunogold labelling confirmed the presence of several markers, Fig. 4.4b. More general EV markers CD9, CD63 and CD81 were present, as well as a brain-derived marker: ATP1A3.

In this work, a lysis strategy was devised and used to investigate the internalised p-tau cargo of EVs. This work specifically focused on two phosphorylates p-tau181 and p-tau217 previously found to be important Alzheimer's biomarkers by the research group of our collaborators in Clinical Memory Research, Lund University. As Fig. 4.4c shows, we were able to detect more p-tau217 when the trapped EVs were lysed with Tween 20X, suggesting that the protein is transported inside the vesicles. Finally, we found interesting results regarding the ratio of two markers *p-tau181/217* in trapped EVs; the ratio was significantly higher in the AD cohort compared with the cognitively unimpaired group, Fig. 4.4d. This was a novel finding and differs to the results found for free floating levels in CSF.

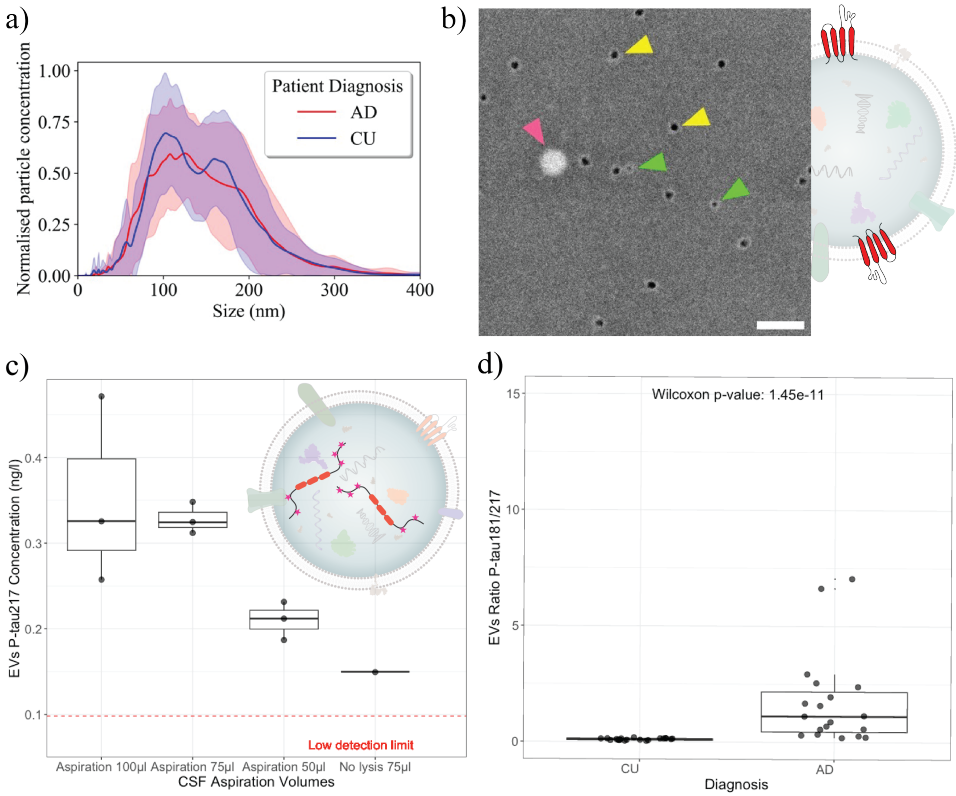

Figure 4.4: a) NTA analysis of trapped EVs from the CSF of Alzheimer's disease (AD) affected and cognitively unimpaired (CU) patients. b) TEM image of small extracellular vesicles in trapped CSF. EV surface markers have been labelled with primary antibodies against CD9 and ATP1A3, followed by 15 nm and 10 nm gold-conjugated secondary antibodies, with yellow arrows highlighting CD9 positive, green ATP1A3 positively stained EVs. The pink arrow indicates a non-labelled EV. The scale bar is 100 nm. c) Meso Scale Discovery quantification of p-tau217 in trapped, lysed EVs from 100, 75 or 50 µL of CSF and the lower signal detected without Tween 20X lysis of EVs trapped from 75 µL of CSF. Note that the difference between the p-tau217 detected is increased by lysis, implying it is internalised in the EVs. d) The patient cohort (N=40) revealed an unexpected difference in p-tau181/217 ratio between cognitively unimpaired individuals and those with Alzheimer's disease. Adapted from **Paper III**, [5], in accordance with the (CC BY 4.0) licence.

Paper IV: Immuno-acoustic trapping: towards extracellular vesicle sub-population

Aim: Is it possible to couple immunoaffinity isolation with acoustic trapping, for the isolation of sub-populations of extracellular vesicles? *(Addressing Hypothesis 4)*

One limitation of traditional seed particle acoustic trapping of EVs is that it isolates a whole population and is not able to distinguish between exosomes, microvesicles, or sub-populations of EVs derived from a specific cell type. In **Paper IV**, we addressed this by adapting the traditional method of acoustic trapping to what we have called *immuno-acoustic* isolation - combining it with immunoaffinity beads. Our method was able to isolate EVs from 17 µL human blood plasma in only 8 minutes and simultaneously trap two fractions of EVs, Fig. 4.5a. We compared our method with a manual bench-top 90 minute incubation, with centrifugation to wash. The novel automated methodology is outlined in Fig. 4.5b.

The two fractions that we isolated in our acoustic method both had EVs, confirmed by NTA and immunogold TEM. The fraction captured by acoustic trapping, separated from the anti-CD9 captured beads, contained many $CD9^-$ EVs. Whilst the specifically isolated immuno-acoustic fraction of EVs was confirmed by TEM to contain more $CD9^+$ EVs. There was some overlap in the proteomic profiles of the immuno-acoustic EV fractions, compared to both the acoustic fractions and samples isolated with the manual immunoaffinity method. EVs isolated by immuno-acoustic trapping rather than acoustics or immunoaffinity alone, yielded more proteins strongly associated with CD9.

The design of the immuno-acoustic method we used incorporated protein A coated silica seed particles. We used silica-based seed particles to minimise the processing time, as previously discussed. We developed our method using protein A in order to keep flexibility for capturing specific EV populations using different antibodies, or a mixture, in the future.

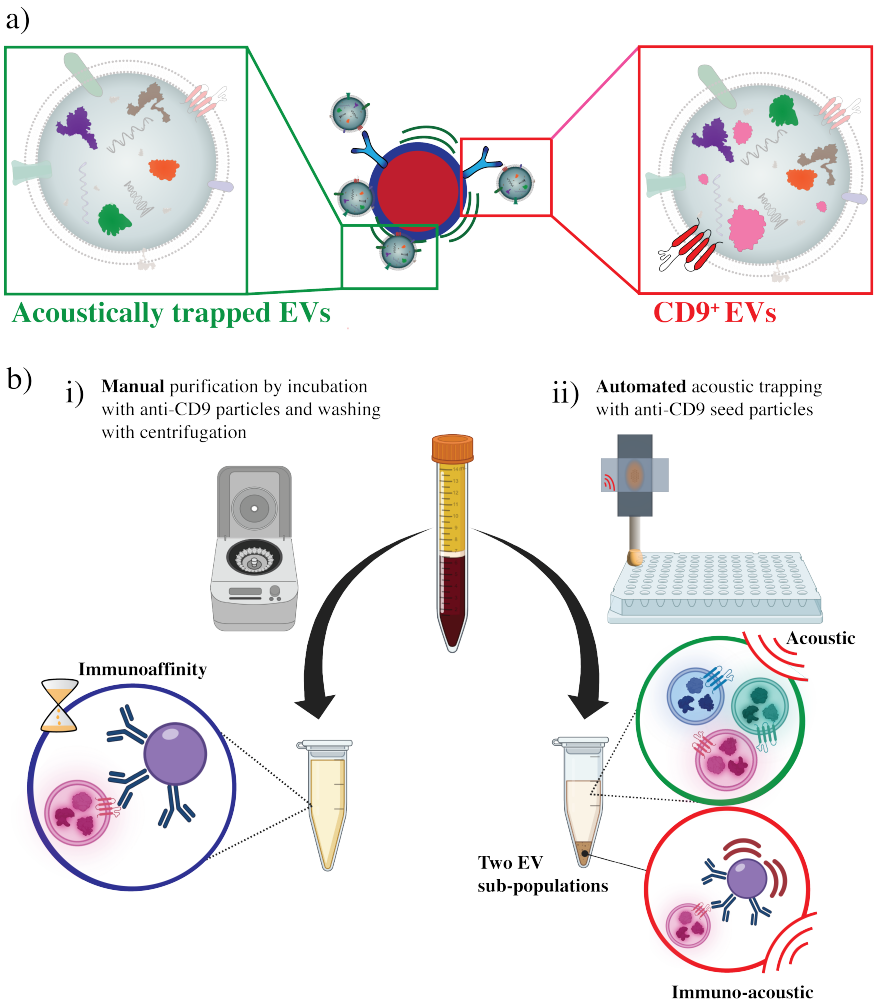

Figure 4.5: a) Schematic of acoustic trapping mechanisms taking place in the combined immuno-acoustic approach. b) Overview of methods used for the processing of plasma in this work: i) manual and ii) automated. As indicated, the acoustic fraction is separated from the immuno-acoustic fraction by sedimenting the silica seed particles with the antibody-captured EVs. Reproduced from **Paper IV**. Some parts of this figure were created in Biorender.com.

Chapter 5
Outlook

Extracellular vesicles have been hailed by many as the key to understanding, diagnosing and treating medical conditions of many kinds, if they can be isolated. This thesis focused on the development of the acoustic trapping technique to isolate these biological nanoparticles from plasma and CSF more rapidly and from smaller volumes than previously. Before this work began, it was standard to use polystyrene seed particles as sound-scatterers to trap nanoparticles, including EVs from plasma and urine. All of the papers included in this thesis use silica-based seed particles which scatter sound more strongly than polystyrene.

Acoustic trapping, whilst being discovered over a decade ago, is still poorly understood in terms of which mechanisms drive the trapping of extracellular vesicles. One problem has been the lack of measurement tools to enable robust comparison when investigating the effect of different parameters. The work in **Paper I** introduced fluorescent polystyrene nanoparticles of 270 nm as a model nanoparticles which could be monitored with a fluorescent microscope. This enabled the demonstration of silica seed particles as a preferable seed particle material to the standard polystyrene seed particles. The remaining **Papers II-IV** utilised silica seed particles and increased flow rate protocols to isolate EVs from biofluids faster than before. We also demonstrated immuno-acoustic trapping, isolating two populations of EVs in the acoustic trap for the first time; one general population and one surface marker specific population.

As hinted by its title, *'Sowing the seeds of acoustic trapping: Towards rapid isolation of extracellular vesicles'*, this thesis focuses on the *method* of EV trapping in addition to taking steps towards the ultimate goal of unveiling the cargo of these particles.

This chapter addresses several important outcomes of this work in relation to the hypotheses proposed in the introduction of this thesis, as well as limitations, opportunities, and sustainable development implications. Finally, some open questions are raised which could be important to address in future work.

5.1 The seeds of understanding

Overarching question: What are the mechanisms behind acoustic trapping of nanoparticles?

The question of the potential mechanisms behind acoustic trapping of nanoparticles was discussed in Section 2.3.3. What has been clear for a long time is that sub-micron particles cannot easily be trapped directly against high flow rates, this was understood by the size dependence of the acoustic forces on an individual particle being overcome by the drag forces. It was also evident that seed particle clusters make it possible to trap nanoparticles. The primary mechanisms thought to play a role in nanoparticle trapping using seed particles are: interparticle forces originating from scattered sound (amplified by seed particles), electrostatic attraction (depending on the nanoparticle and seed particle surfaces), hydrodynamic shielding, and micro-streaming.

In **Paper I**, the mechanism of acoustic trapping is not stated, however the increase in nanoparticle trapping efficiency by using denser seed particles does imply a role of interparticle forces, as previously assumed. On the other hand, there was a deviation from this effect when the nanoparticles had very high concentration - they trapped similarly well with silica and polystyrene seed particles. It is possible that other factors became more important at such a high nanoparticle concentration, for example electrostatic attraction between polystyrene nanoparticles and seed particles.

However, changing seed particle density and charge was found not to significantly affect the proteome of EVs enriched, in **Paper II**. The hydrodynamic shielding and micro-streaming effects have not been thoroughly explored, however preliminary evidence does suggest that the spacial distribution of seed particles within trapping capillaries has an effect on the nanoparticle trapping efficiency. Acoustic streaming might not induce any trapping forces, but the recirculation of the sample may allow nanoparticles more time to be trapped within the cluster.

5.1.1 Limitations: decoupling forces in acoustic trapping

Perhaps the most notable limitation of this work is that we have failed to experimentally decouple all of the physical properties and measure the contribution of the different forces driving acoustic trapping. This is in part due to the interlinked nature of the forces making it challenging to study one force at a time. Theoretically, it is possible to model some of these forces, such as the hydrodynamics or the acoustic forces, however, the seed particle cluster arrangement is a major unknown in these models and significant simplifications would be required. The effects of media properties, flow, actuated frequency, and voltage on the arrangements of seed particles in the capillary have been qualitatively observed, but these would be extremely tedious and complex to reproduce in simulations. Some complications with interpreting the experimental results of parameter changes are:

1. *Increasing media density* with the aim to make the interparticle forces tend to zero, Eq. 2.16, would require the media having *exactly* the same density as the nanoparticles - matching the densities enough for the buoyancy force to balance the gravitational force on the nanoparticles is achievable, but there will likely always be a non-zero difference between the two densities. The higher density media will also affect resonance frequency and possibly viscosity (as is the case for most density-modifying additives such as iodixanol) which may also influence hydrodynamic effects.
2. *Increasing media salt concentration* with the aim to shield electrostatic attraction or *using neutrally charged particles* may have an effect on how close the nanoparticles can get to the seed particles, and as such reduce the chance of trapping by interparticle forces.
3. *Increasing voltage* may enhance both the interparticle forces and the micro-streaming, however, it will also increase temperature and acoustic streaming in the system, which could give an opposing effect. Changing voltage has also been shown in some systems to drastically change the seed particle cluster size and shape. This may be due to a differing acoustic field and increased interparticle forces between the seed particles - which would also affect hydrodynamic forces experienced by nanoparticles when they pass through the seed particle cluster.

Furthermore, we tend to explore the effect of trapping parameters by using synthetic fluorescent nanoparticles (as with polystyrene nanoparticles used in **Paper I**). Other nanoparticles tend to have more than one difference compared to these model nanoparticles: density, compressibility, size, surface charge, or stability. This makes it difficult to quantify the effect of one variable. For instance, EVs are denser, smaller, and more negatively charged than polystyrene NPs. Some studies were performed with gold nanoparticles and synthetic lipid nanoparticles, looking into the effect of nanoparticle density and size. However, the results were complex to interpret due to the affinity of some nanoparticles to the surfaces of the seed particles, as well as the aggregation of some nanoparticles resulting in quantification issues. For gold nanoparticles, the nanoparticles appeared to coalesce into one much larger gold lump, that could not be disassembled easily for measurement by NTA.

5.1.2 Opportunities: future system optimisation

Decoupling the mechanisms behind acoustic trapping could be hugely beneficial for the intelligent design of future systems. For example, if micro-streaming is found to be a major contributor, then resources would be diverted to optimising the system design: such as capillary geometry, frequency of operation, and seed particle size, shape, material, and packing. On the other hand, if interparticle forces driven by sound scattering can be the main contributor, this creates opportunities for more density-selective control of nanoparticle trapping, such as has been demonstrated for binary trapping of microparticles [156]. The secondary acoustic radiation forces suggest that by matching the density of the media with the nanoparticles, we should eliminate nanoparticle trapping all together. If this can be shown, then perhaps a cut-off in EVs at a particular density can be implemented, analogous to density gradient ultracentrifugation.

5.2 Towards rapid isolation of nanoparticles

Hypothesis 1: Increasing the density of seed particles can improve the throughput and efficiency of acoustic trapping of nanoparticles.

Paper I answers this hypothesis for two different densities of seed particles, studying the case of trapped 270 nm polystyrene nanoparticles. This work

demonstrates that, at least from nanoparticle concentrations below 10^{11} particles/mL, using silica seed particles instead of the standard polystyrene seed particles does indeed increase the nanoparticle trapping efficiency. The efficiency of acoustic trapping with silica seed particles was addressed for the first time in **Paper I**, while **Papers II-IV** all implement this and demonstrate the value of increased EV isolation speeds for a number of biological applications.

Paper III implemented acoustic trapping of EVs from CSF using silica seed particles with a washing flow rate of 100 µL/min. **Paper II** explored acoustic trapping with zwitterionic silica seed particles, showing that trapped EVs from plasma revealed the same proteome with both 30 µL/min and 200 µL/min washing flow rates. Before this publication, almost no papers (except [169], as previously discussed) had explored the used of a seed particle material other than polystyrene. As demonstrated in **Paper I**, polystyrene seed particles clusters could not be retained in the acoustic field at 200 µL/min.

5.2.1 Limitations: nanoparticle quantification

Unfortunately, there are also issues with the reliability of techniques measuring nanoparticle concentration, see Section 3.2.2. This makes quantifying the effect of changing factors extremely challenging, and the reason that relative performance of silica seed particles was evaluated with fluorescent nanoparticles, in **Paper I**. The challenge remains that we have no accurate way of determining extracellular vesicle concentration, it is for this reason that we do not discuss EV trapping recovery in terms of percentages, which could have been misleading. Recovery in EV trapping is also likely to be highly dependent on the capacity of the acoustic trap, if we trapped EVs from 1 mL of raw plasma, we would expect very low recovery percentage, whereas trapping from a small volume or more dilute sample could allow higher recovery. With this in mind, we do not mention the number of particles trapped but focus on the downstream analysis of cargo. It is worth noting that despite previous studies reporting a difference in the EV concentration of CSF between patients with and without Alzheimer's disease [95], we did not find this to be the case in **Paper III** [5]. Furthermore, other factors have been discussed in relation to their effect on EV concentration, such as exercise [60], thus this is not a specific biomarker.

5.2.2 Opportunities: scaling down and speeding up

Paper I outlined a method of measuring relative performance for trapping fluorescent nanoparticles. We have used this to demonstrate the effect of seed particle density and increasing the washing flow rate. This method could, however, be applied for investigating the effect of different acoustic trapping parameters, for example those discussed in Section 5.1.1.

From a chemical consumption point of view, microfluidics in general offers possibilities for working towards sustainability goal 12: *to ensure sustainable consumption and production patterns*. The medical research field is challenged by this target, as the methodologies employed are currently consuming vast quantities of resources (reagents, antibodies, single-use plastic etc.) and producing excessive waste. By transitioning to lab-on-a-chip devices, the volumes of fluid (both in terms of reagents and waste) may be dramatically reduced. Speeding up the acoustic trapping process by using silica seed particles has also sparked some interest outside of biomedical applications. After publishing **Paper I**, more research groups are exploring the advantage of silica: Costa *et al.* have used silica seed particles for acoustic trapping of microplastics, for water quality monitoring [174].

5.3 Unveiling extracellular vesicles' cargo

In brief, rapid EV isolation by acoustic trapping using seed particles provides an invaluable tool to researchers wanting to investigate the content of EVs from any biofluid. The work in this thesis demonstrates the isolation of intact EVs in 6-10 minutes (**Paper II-IV**). In **Paper III** we also demonstrate that lysis of EVs can enable assay measurement of their internal cargo, providing evidence of pathological transport mechanisms. **Paper II** and **IV** use mass spectrometry to analyse the content of trapped EVs on a broader level, in healthy plasma, with the aim to demonstrate the value for embarking on larger cohort studies.

Hypothesis 2: Extracellular vesicles can be isolated by acoustic trapping from less than 10 µL of blood plasma.

Paper II demonstrates it is indeed possible to isolate EVs from as little as 8 µL of blood plasma, by acoustically trapping EVs and washing off free protein. This work also demonstrated the value of EV enrichment and washing

by acoustic trapping, showing that it enables access to less abundant EV proteins via shotgun proteomics. Comparing with raw plasma, we show unique detection of proteins in acoustically trapped samples, that were below the detection limit in raw plasma. This study was performed from a single blood draw from a healthy individual, which is a valuable move towards personalised medicine via diagnosis using EV-associated biomarkers. Other work looking at proteins in EVs via ultracentrifugation required pooling of samples, and although this may have value in biomarker discovery it reduces the value of the information gained on an individual level [99]. Further work to improve the richness of proteomic information gained from the isolation of EVs could include more advanced mass spectrometry purification and separation steps, however part of the value of the method laid out is the relatively simple sample handling.

Hypothesis 3: Acoustic trapping can aid the investigation of the cargo of extracellular vesicles in the cerebrospinal fluid of Alzheimer's patients.

Paper III not only demonstrates acoustic trapping of EVs from CSF for the first time, but thoroughly explores the surface markers and internalised phosphorylated tau cargo of the isolated EVs. A medium-sized cohort of Alzheimer's patients (N=20) and healthy controls (N=20) were included in this pilot study, with 6 technical replicates of the acoustic trapping. In this collaboration, we used a p-tau217 MSD assay to assess the optimal volume of CSF to process - finding that 75 µL maximised signal as well as the number of repeats from the precious biobanked samples (500 µL aliquots). The post-trapping lysis protocol which was developed was critical to investigating the EV cargo. By performing NTA and the p-tau217 assay we confirmed that Tween 20X was effective at opening the EVs and that phosphorylated tau is internalised by EVs.

Moreover, we can detect different relative levels of p-tau181 and p-tau217 in the cargo of trapped EVs, compared to in the unprocessed CSF. This was a major and surprising finding to those in the field of Alzheimer's disease. Although good diagnostic assays have already been developed for CSF [204, 205], the involvement of EVs in AD progression may help to understand disease biology and possibly offer useful information for future therapies. To develop the answer to this research question, it would be valuable to apply a more specific isolation method which allows us to look at the p-tau content of EVs from a specific cell type.

5.3.1 Limitations: EV markers

One current issue with EV isolation techniques is the lack of universal EV markers. Although tetraspanins CD9, CD81, and CD63 are *common* to find on the surface of EVs, not all EVs posses them [206]. Since EVs can be produced by any cell, they can differ widely in the surface proteins they inherit. Unfortunately, there is not yet one perfect antibody which binds to all EVs and nothing else. To add insult to injury, these common tetraspanins are strongly anchored in the plasma membrane, which makes them notoriously difficult to digest and detect via mass spectrometry [207, 208]. It would be valuable to find better generic EV markers and/or more specific markers for sub-populations of EVs, ideally ones which help to elucidate their biogenesis.

5.3.2 Opportunities: intercepting critical cargo

The path forwards from an applications point of view is striving towards the sustainability goal 3: *to ensure healthy lives and promote well-being for all at all ages*. As the medical field as a whole aims for this, one of the major challenges is developing tools that enable early diagnosis and monitoring of diseases, in order to treat patients effectively and in a timely fashion. Liquid biopsies are an ideal form of disease monitoring, as they are less invasive than solid biopsies and less expensive than advanced imaging techniques.

Biofluid samples are often taken when ill patients come to the clinic, because there is a wealth of information available in them: from relative cell counts to macromolecules and chemistry. Some of these biological messages are easy to read, however others need more involved techniques to intercept them. Intercepting specific cargo in extracellular vesicles may unveil a valuable biomarker of disease progression, or even help us uncover the mechanism behind diseases. Such a biomarker could advise future therapies from childhood cancer to Alzheimer's disease.

The number of unique samples which can be processed by acoustic trapping is a great strength demonstrated by this work. The small volume handling demonstrated in this work provides opportunities to analyse 'left-overs' in biobanks without mixing samples together or even perform animal studies which would not otherwise be feasible. These aspects are useful across research into cancers, sepsis, neurodegenerative diseases, and countless other urgent risks

to human health.

At the time of writing, our EV isolation method, from **Paper II**, was shown capable of being applied for processing some mouse tumour model plasma samples that had only 50 µL frozen aliquots remaining. The volume was too little for them to perform more ultracentrifugation, but sufficient even for replicates when using acoustic trapping. All 6 samples were processed, with technical replicates, easily within a couple of hours. The aim of this work was to aid a collaborator who aims to find tumour biomarkers within EVs using mass spectrometry.

5.4 Integrating specific subpopulation

Hypothesis 4: Immunoaffinity isolation coupled with acoustic trapping enables the isolation of sub-populations of extracellular vesicles.

Paper IV demonstrates a novel method of immuno-acoustic isolation in parallel with acoustic trapping to isolate two sub-populations of EVs from plasma, using anti-CD9 functionalised silica seed particles. This study compared this method with a manual incubation with the same immunoaffinity beads and centrifugation. The manual incubation method took 90 minutes, whereas the immuno-acoustic method could be performed in 8 minutes per sample in an automated system. TEM and proteomics analysis revealed some differences between the groups of EVs, which shows that the protocol holds value in revealing more information than acoustic trapping alone. Furthermore, the immuno-acoustic fraction isolated $CD9^+$ EVs and MS identified proteins more strongly associated with CD9 than the fractions isolated by acoustics or bench-top incubation.

However, CD9 is very common on EVs so the immuno-acoustic technique didn't isolate a wholly distinct population. To better judge the applicability of this technique, a rarer surface marker that is specific to EVs derived from one cell-type should be targeted. This would create two more different sub-populations and may reveal more about which cells are responsible for particular EV cargo. For now, we have only applied this technique to isolate EVs from blood plasma, however performing a similar isolation from CSF with a brain-specific marker such as ATP1A3 [209, 210] might elucidate valuable medical insight in downstream analysis.

5.4.1 Limitations: heterogeneity

Extracellular vesicles are challenging to analyse but, more significantly, they are heterogeneous. As it stands today, most analysis is performed on a population-wide basis, which is known to depend on the isolation method. Sub-populating EVs, as done in **Paper IV**, may still not be sufficient to access nuances in EV characteristics. EV protein expression of surface markers may not define discrete sub-populations [52, 206], and the protein corona also introduces some complexity in defining the functionality of EVs [43, 211, 212]. Single-EV analysis methods do exist [50, 213–215], but the throughput is a major limitation.

5.4.2 Opportunities: flexible targeting

In the final paper, **Paper IV**, we introduce a new versatile method for isolating two fractions of EVs from a biofluid which could be applied to any potential future EV membrane biomarkers. A particularly interesting opportunity this offers up is to isolate brain-derived EVs (for example, via *ATP1A3*) from the blood of patients with Alzheimer's disease. This would be groundbreaking for early diagnosis, where doctors currently rely on expensive brain scans which cannot be frequently used and cognitive tests which tend to pick up the disease when it has progressed significantly. A blood test for AD could provide a tool for a minimally invasive diagnostic and monitoring methodology [76, 77].

There are many conditions that can progress quickly and become fatal, pre-eclampsia and sepsis are two examples of this. In pre-eclampsia, it is thought that EVs are produced by the placenta, and finding these specific EVs in a mother's blood could be an early warning sign of a high-risk pregnancy. EVs derived from trophoblast cells could be targeted via placenta-specific enzyme placental alkaline phosphatase (*PLAP*) [59]. In sepsis, bacteria can spread through the blood to multiple organs and lead to fatality within hours, unless the appropriate treatment is given [216]. Proteomic analysis of the EV proteome alone, rather than the plasma proteome, may better aid the identification of organ dysfunction and sepsis stratification. One way that immuno-acoustic trapping could help with this is to target EVs expressing the *M1* protein that has been found on EVs produced by activated platelets in a mouse infected with specific bacteria [133].

5.5 Questions that remain

The context of this thesis spans multiple fields of work, this is exemplified by the range of conferences where this work has been presented: nano and micro engineering (*MNE 2022*), microfluidics (*μTAS 2021/2023*), acoustofluidics (*Acoustofluidics 2020/2024*), extracellular vesicles (*DSEV 2022*, *Gordon Conference on EVs 2024*), and proteomics (*NPS 2023*). Some interesting questions arose from discussions there, that are still hotly debated:

1. What is the relative contribution of different trapping mechanisms in the acoustic trapping system?
2. Is the protein corona an important part of EV function and what does that mean for isolation techniques?
3. Is there a correlation between EV surface markers and their internalised content?
4. Can we develop tools which can accurately measure nanoparticle concentration?

New and improved methods for measuring EVs, such as microfluidics-based single-EV analysis tools, will likely prove to be critical for answering these questions in the future.

Reflection

Whilst I initially thought I would be entering one new field - acoustofluidics - as I embarked on my doctoral degree, the years that followed additionally took me into the challenging field of extracellular vesicle isolation. On top of that, I gained contact with the fairly broad field of proteomics and collaborated with researchers working to uncover mechanism of Alzheimer's disease. Not to mention the nanoparticle fabrication experiments with gold and synthetic lipid vesicles, which never made it into this thesis!

It's clear to me that there is enormous potential for microfluidics-based devices to contribute to diagnostic and medical research, improving human health, diagnostic efficiency, and reagent waste reduction. Transitioning from technology development to implementation by those who need it is not without friction. Nevertheless, more robust and faster methodologies for handling small volumes of biofluids, such as has been presented in this thesis, is where I believe research supporting personalised medicine is headed. I hope in the future, that we can harness extracellular vesicles for more precise diagnostics and therapeutics. If my work in the lab with Roman contributes in any small way to reducing the suffering of someone with Alzheimer's disease in the future, that would make my efforts through this PhD education worth it.

With all of this said, what I've learnt the most conclusively is that there is still so much we don't understand. It is truly a privilege to experience the joy of the unknown, complex, and the unpredictability in the world on the nano/micro-scale, or as Thomas once aptly put it *"the beautiful science"*.

References

[1] H. Bruus, *Theoretical Microfluidics*, vol. 18. Oxford University Press, 2007.

[2] L. D. Landau and E. M. Lifshitz, *Fluid Mechanics*, vol. 6. Pergamon Press, 2 ed., 1987.

[3] T. Laurell and A. Lenshof, eds., *Microscale Acoustofluidics*. The Royal Society of Chemistry, 2014.

[4] M. Havers, A. Broman, A. Lenshof, and T. Laurell, "Advancement and obstacles in microfluidics-based isolation of extracellular vesicles," *Analytical and Bioanalytical Chemistry*, vol. 415, pp. 1265–1285, 2023.

[5] R. Sattarov, M. Havers, C. Orbjörn, E. Stomrud, S. Janelidze, T. Laurell, and N. Mattsson-Carlgren, "Phosphorylated tau in cerebrospinal fluid-derived extracellular vesicles in Alzheimer's disease: a pilot study," *Scientific Reports*, vol. 14, no. 25419, pp. 1–18, 2024.

[6] A. Manz, N. Graber, and H. M. Widmer, "Miniaturized Total Chemical Analysis Systems: a Novel Concept for Chemical Sensing," *Sensors and Actuators B*, vol. 1, no. 1-6, pp. 244–248, 1990.

[7] E. Delamarche, A. Bernard, H. Schmid, B. Michel, and H. Biebuyck, "Patterned delivery of immunoglobulins to surfaces using microfluidic networks," *Science*, vol. 276, no. 5313, pp. 779–781, 1997.

[8] S. Shqji, M. Esashi, and T. Matsuo, "Protege miniature blood gas analyser fabricated on a silicon wafer," *Sensors and Actuators*, vol. 14, no. 2, pp. 101–107, 1988.

[9] E. Gal-Or, Y. Gershoni, G. Scotti, S. M. Nilsson, J. Saarinen, V. Jokinen, C. J. Strachan, G. Boije Af Gennäs, J. Yli-Kauhaluoma, and T. Kotiaho, "Chemical analysis using 3D printed glass microfluidics," *Analytical Methods*, vol. 11, no. 13, pp. 1802–1810, 2019.

[10] P. J. Kitson, M. H. Rosnes, V. Sans, V. Dragone, and L. Cronin, "Configurable 3D-Printed millifluidic and microfluidic 'lab on a chip' reactionware devices," *Lab on a Chip*, vol. 12, no. 18, pp. 3267–3271, 2012.

[11] M. Asghari, X. Cao, B. Mateescu, D. Van Leeuwen, M. K. Aslan, S. Stavrakis, and A. J. Demello, "Oscillatory Viscoelastic Microfluidics for Efficient Focusing and Separation of Nanoscale Species," *ACS Nano*, vol. 14, no. 1, pp. 422–433, 2020.

[12] J. C. Giddings, "Field-Flow Fractionation: Analysis of Macromolecular, Colloidal, and Particulate Materials," *Science*, vol. 260, no. 5113, pp. 1456–1465, 1993.

[13] L. R. Huang, P. Silberzan, J. O. Tegenfeldt, E. C. Cox, J. C. Sturm, R. Austin, and H. Craighead, "Role of molecular size in ratchet fractionation," *Physical Review Letters*, vol. 89, no. 17, pp. 1–178301, 2002.

[14] L. G. Liang, M. Q. Kong, S. Zhou, Y. F. Sheng, P. Wang, T. Yu, F. Inci, W. P. Kuo, L. J. Li, U. Demirci, and S. Q. Wang, "An integrated double-filtration microfluidic device for isolation, enrichment and quantification of urinary extracellular vesicles for detection of bladder cancer," *Scientific Reports*, vol. 7, no. 46224, pp. 1–10, 2017.

[15] J. Zhang, S. Yan, D. Yuan, Q. Zhao, S. H. Tan, N. T. Nguyen, and W. Li, "A novel viscoelastic-based ferrofluid for continuous sheathless microfluidic separation of non-magnetic microparticles," *Lab on a Chip*, vol. 16, no. 20, pp. 3947–3956, 2016.

[16] H. Zhang and D. Lyden, "Asymmetric-flow field-flow fractionation technology for exomere and small extracellular vesicle separation and characterization," *Nature Protocols*, vol. 14, pp. 1027–1053, 2019.

[17] M. Evander, O. Gidlöf, B. Olde, D. Erlinge, and T. Laurell, "Non-contact acoustic capture of microparticles from small plasma volumes," *Lab on a Chip*, vol. 15, no. 12, pp. 2588–2596, 2015.

[18] S. Ayala-Mar, V. H. Perez-Gonzalez, M. A. Mata-Gómez, R. C. Gallo-Villanueva, and J. González-Valdez, "Electrokinetically Driven Exosome Separation and Concentration Using Dielectrophoretic-Enhanced PDMS-Based Microfluidics," *Analytical Chemistry*, vol. 91, no. 23, pp. 14975–14982, 2019.

[19] J. Yang, B. Pan, F. Zeng, B. He, Y. Gao, X. Liu, and Y. Song, "Magnetic Colloid Antibodies Accelerate Small Extracellular Vesicles Isolation for Point-of-Care Diagnostics," *Nano Letters*, vol. 21, no. 5, pp. 2001–2009, 2021.

[20] O. Reynolds, "An experimental investigation of the circumstances which determine whether the motion of water shall be direct or sinuous, and of the law of resistance in parallel channels," *Philosophical Transactions of the Royal Society of London*, vol. 174, pp. 935–982, 1883.

[21] M. Van Dyke, *An album of fluid motion*. Parabolic Press, 1982.

[22] H. Bruus, "Acoustofluidics 1: Governing equations in microfluidics," *Lab on a Chip*, vol. 11, no. 22, pp. 3742–3751, 2011.

[23] M. W. Ley and H. Bruus, "Three-dimensional numerical modeling of acoustic trapping in glass capillaries," *Physical Review Applied*, vol. 8, no. 024020, pp. 1–15, 2017.

[24] M. Havers, T. Baasch, A. Lenshof, M. Evander, and T. Laurell, "Silica seed particles improve the efficiency and throughput of nanoparticle acoustic trapping," *Physical Review Applied*, vol. 21, no. 034016, pp. 1–16, 2024.

[25] A. Einstein, *Investigations on the theory of the Brownian movement*. Dover Publications, Inc., 1956.

[26] R. Feynman, R. B. Leighton, and M. Sands, *The Feynman Lectures on Physics*, vol. 1. Perseus (Basic Books), new millennium ed., 1963.

[27] M. E. Schimpf, K. Caldwell, and J. C. Giddings, *Field-Flow Fractionation Handbook*. John Wiley & Sons, 2000.

[28] C. Bajo-Santos, M. Priedols, P. Kaukis, G. Paidere, R. Gerulis-Bergmanis, G. Mozolevskis, A. Abols, and R. Rimsa, "Extracellular Vesicles Isolation from Large Volume Samples Using a Polydimethylsiloxane-Free Microfluidic Device," *International Journal of Molecular Sciences*, vol. 24, no. 9, pp. 1–7971, 2023.

[29] S. R. Springston, M. N. Myers, and J. C. Giddings, "Continuous Particle Fractionation Based on Gravitational Sedimentation in Split-Flow Thin Cells," *Analytical Chemistry*, vol. 59, no. 2, pp. 344–350, 1987.

[30] F. Petersson, A. Nilsson, C. Holm, H. Jönsson, and T. Laurell, "Separation of lipids from blood utilizing ultrasonic standing waves in microfluidic channels," *Analyst*, vol. 129, no. 10, pp. 938–943, 2004.

[31] A. Nilsson, F. Petersson, H. Jönsson, and T. Laurell, "Acoustic control of suspended particles in micro fluidic chips," *Lab on a Chip*, vol. 4, no. 2, pp. 131–135, 2004.

[32] M. Evander, L. Johansson, T. Lilliehorn, J. Piskur, M. Lindvall, S. Johansson, M. Almqvist, T. Laurell, and J. Nilsson, "Noninvasive acoustic cell trapping in a microfluidic perfusion system for online bioassays," *Analytical Chemistry*, vol. 79, no. 7, pp. 2984–2991, 2007.

[33] B. Hammarström, T. Laurell, and J. Nilsson, "Seed particle-enabled acoustic trapping of bacteria and nanoparticles in continuous flow systems," *Lab on a Chip*, vol. 12, no. 21, pp. 4296–4304, 2012.

[34] C. Harding, J. Heuser, and P. Stahl, "Receptor-mediated Endocytosis of Transferrin and of the Transferrin Receptor in Rat Reticulocytes Recycling," *The Journal of Cell Biology*, vol. 97, pp. 329–339, 1983.

[35] R. M. Johnstone, M. Adam, J. R. Hammonds, L. Orro, and C. Turbide, "Vesicle Formation during Reticulocyte Maturation," *The Journal of Biological Chemistry*, vol. 262, no. 19, pp. 9412–9420, 1987.

[36] E. Cocucci and J. Meldolesi, "Ectosomes and exosomes: Shedding the confusion between extracellular vesicles," *Trends in Cell Biology*, vol. 25, no. 6, pp. 364–372, 2015.

[37] G. Raposo, H. W. Nijman, W. Stoorvogel, R. Leijendekker, C. Harding, C. Melief, and H. Geuze, "B Lymphocytes Secrete Antigen-presenting Vesicles," *Journal of Experimental Medicine*, vol. 183, pp. 1161–1172, 1996.

[38] H. Valadi, K. Ekström, A. Bossios, M. Sjöstrand, J. J. Lee, and J. O. Lötvall, "Exosome-mediated transfer of mRNAs and microRNAs is a novel mechanism of genetic exchange between cells," *Nature Cell Biology*, vol. 9, no. 6, pp. 654–659, 2007.

[39] M. Toyofuku, N. Nomura, and L. Eberl, "Types and origins of bacterial membrane vesicles," *Nature Reviews Microbiology*, vol. 17, pp. 13–24, 2019.

[40] A. J. Szempruch, S. E. Sykes, R. Kieft, L. Dennison, A. C. Becker, A. Gartrell, W. J. Martin, E. S. Nakayasu, I. C. Almeida, S. L. Hajduk, and J. M. Harrington, "Extracellular Vesicles from Trypanosoma brucei Mediate Virulence Factor Transfer and Cause Host Anemia," *Cell*, vol. 164, no. 1, pp. 246–257, 2016.

[41] H. I. Choi, J. P. Choi, J. Seo, B. J. Kim, M. Rho, J. K. Han, and J. G. Kim, "Helicobacter pylori-derived extracellular vesicles increased in the gastric juices of gastric adenocarcinoma patients and induced inflammation mainly via specific targeting of gastric epithelial cells," *Experimental and Molecular Medicine*, vol. 49, no. e330, pp. 1–13, 2017.

[42] R. Kalluri and V. S. LeBleu, "The biology, function, and biomedical applications of exosomes," *Science*, vol. 367, no. 640, pp. 1–16, 2020.

[43] M. Wolf, R. W. Poupardin, P. Ebner-Peking, A. C. Andrade, C. Blöchl, A. Obermayer, F. G. Gomes, B. Vari, N. Maeding, E. Eminger, H. M. Binder, A. M. Raninger, S. Hochmann, G. Brachtl, A. Spittler, T. Heuser, R. Ofir, C. G. Huber, Z. Aberman, K. Schallmoser, H. D. Volk, and D. Strunk, "A functional corona around extracellular vesicles enhances angiogenesis, skin regeneration and immunomodulation," *Journal of Extracellular Vesicles*, vol. 11, no. e12207, pp. 1–20, 2022.

[44] E. Tóth, L. Turiák, T. Visnovitz, C. Cserép, A. Mázló, B. W. Sódar, A. I. Försönits, G. Petővári, A. Sebestyén, Z. Komlósi, L. Drahos, A. Kittel, G. Nagy, A. Bácsi, A. Dénes, Y. S. Gho, K. Szabó-Taylor, and E. I. Buzás, "Formation of a protein corona on the surface of extracellular vesicles in blood plasma," *Journal of Extracellular Vesicles*, vol. 10, no. e12140, pp. 1–26, 2021.

[45] M. Heidarzadeh, A. Zarebkohan, R. Rahbarghazi, and E. Sokullu, "Protein corona and exosomes: new challenges and prospects," *Cell Communication and Signaling*, vol. 21, no. 64, pp. 1–15, 2023.

[46] A. V. Vlassov, S. Magdaleno, R. Setterquist, and R. Conrad, "Exosomes: Current knowledge of their composition, biological functions, and diagnostic and therapeutic potentials," *Biochimica et Biophysica Acta*, vol. 1820, no. 7, pp. 940–948, 2012.

[47] S. Charrin, S. Jouannet, C. Boucheix, and E. Rubinstein, "Tetraspanins at a glance," *Journal of Cell Science*, vol. 127, no. 17, pp. 3641–3648, 2014.

[48] M. P. Caby, D. Lankar, C. Vincendeau-Scherrer, G. Raposo, and C. Bonnerot, "Exosomal-like vesicles are present in human blood plasma," *International Immunology*, vol. 17, no. 7, pp. 879–887, 2005.

[49] J. M. Escola, M. J. Kleijmeer, W. Stoorvogel, J. M. Griffith, O. Yoshie, and H. J. Geuze, "Selective enrichment of tetraspan proteins on the internal vesicles of multivesicular endosomes and on exosomes secreted by human B-lymphocytes," *The Journal of Biological Chemistry*, vol. 273, no. 32, pp. 20121–20127, 1998.

[50] L. C. Mcilvenna, H.-J. Parker, A. P. Seabright, B. Sale, G. Anghileri, S. R. C. Weaver, S. J. E. Lucas, and M. Whitham, "Single vesicle analysis reveals the release of tetraspanin positive extracellular vesicles into circulation with high intensity intermittent exercise," *The Journal of Physiology*, vol. 601, no. 22, pp. 5093–5106, 2023.

[51] C. Théry *et. al.*, "Minimal information for studies of extracellular vesicles 2018 (MISEV2018): a position statement of the International Society for Extracellular Vesicles and update of the MISEV2014 guidelines," *Journal of Extracellular Vesicles*, vol. 7, pp. 1–43, 2018.

[52] J. Kowal, G. Arras, M. Colombo, M. Jouve, J. P. Morath, B. Primdal-Bengtson, F. Dingli, D. Loew, M. Tkach, and C. Théry, "Proteomic comparison defines novel markers to characterize heterogeneous populations of extracellular vesicle subtypes," *Proceedings of the National Academy of Sciences of the United States of America*, vol. 113, no. 8, pp. E968–E977, 2016.

[53] P. Wolf, "The Nature and Significance of Platelet Products in Human Plasma," *British Journal of Haematology*, vol. 13, no. 3, pp. 269–288, 1967.

[54] E. N. M. Nolte-'t Hoen, S. I. Buschow, S. M. Anderton, W. Stoorvogel, and M. H. M. Wauben, "Activated T cells recruit exosomes secreted by dendritic cells via LFA-1," *Blood*, vol. 113, no. 9, pp. 1977–1981, 2009.

[55] C. Théry, L. Duban, E. Segura, P. Væron, O. Lantz, and S. Amigorena, "Indirect activation of naïve CD4+ T cells by dendritic cell-derived exosomes," *Nature Immunology*, vol. 3, no. 12, pp. 1156–1162, 2002.

[56] Y. Ren, J. Yang, R. Xie, L. Gao, Y. Yang, H. Fan, and K. Qian, "Exosomal-like vesicles with immune-modulatory features are present in human plasma and can induce CD4+ T-cell apoptosis in vitro," *Transfusion*, vol. 51, no. 5, pp. 1002–1011, 2011.

[57] A. Jalabert, G. Vial, C. Guay, O. P. Wiklander, J. Z. Nordin, H. Aswad, A. Forterre, E. Meugnier, S. Pesenti, R. Regazzi, E. Danty-Berger, S. Ducreux, H. Vidal, S. El-Andaloussi, J. Rieusset, and S. Rome, "Exosome-like vesicles released from lipid-induced insulin-resistant muscles modulate gene expression and proliferation of beta recipient cells in mice," *Diabetologia*, vol. 59, no. 5, pp. 1049–1058, 2016.

[58] M. Knight, C. W. Redman, E. A. Linton, and I. L. Sargent, "Shedding of syncytiotrophoblast microvilli into the maternal circulation in pre-eclamptic pregnancies," *British Journal of Obstetrics and Gynaecology*, vol. 105, no. 6, pp. 632–640, 1998.

[59] A. F. Orozco, C. J. Jorgez, W. D. Ramos-Perez, E. J. Popek, X. Yu, C. A. Kozinetz, F. Z. Bischoff, and D. E. Lewis, "Placental Release of Distinct DNA-associated Microparticles into Maternal Circulation: Reflective of Gestation Time and Preeclampsia," *Placenta*, vol. 30, no. 10, pp. 891–897, 2009.

[60] P. Bryl-Górecka, R. Sathanoori, M. Al-Mashat, B. Olde, J. Jögi, M. Evander, T. Laurell, and D. Erlinge, "Effect of exercise on the plasma vesicular proteome: A methodological study comparing acoustic trapping and centrifugation," *Lab on a Chip*, vol. 18, no. 20, pp. 3101–3111, 2018.

[61] L. Ayers, R. Nieuwland, M. Kohler, N. Kraenkel, B. Ferry, and P. Leeson, "Dynamic microvesicle release and clearance within the cardiovascular system: Triggers and mechanisms," *Clinical Science*, vol. 129, no. 11, pp. 915–931, 2015.

[62] M. Sossdorf, G. P. Otto, R. A. Claus, H. H. Gabriel, and W. Lösche, "Cell-derived microparticles promote coagulation after moderate exercise," *Medicine and Science in Sports and Exercise*, vol. 43, no. 7, pp. 1169–1176, 2011.

[63] T. R. Doeppner, J. Herz, A. Görgens, J. Schlechter, A.-K. Ludwig, S. Radtke, K. de Miroschedji, P. A. Horn, B. Giebel, and D. M. Hermann, "Extracellular Vesicles Improve Post-Stroke Neuroregeneration and Prevent Postischemic Immunosuppression," *Stem Cells Translational Medicine*, vol. 4, no. 10, pp. 1131–1143, 2015.

[64] A. G. Yates, R. C. Pink, U. Erdbrügger, P. R. Siljander, E. R. Dellar, P. Pantazi, N. Akbar, W. R. Cooke, M. Vatish, E. Dias-Neto, D. C. Anthony, and Y. Couch, "In sickness and in health: The functional role of extracellular vesicles in physiology and pathology in vivo: Part II: Pathology," *Journal of Extracellular Vesicles*, vol. 11, no. e12190, pp. 1–18, 2022.

[65] B. Costa-Silva, N. M. Aiello, A. J. Ocean, S. Singh, H. Zhang, B. K. Thakur, A. Becker, A. Hoshino, M. T. Mark, H. Molina, J. Xiang, T. Zhang, T. M. Theilen, G. García-Santos, C. Williams, Y. Ararso, Y. Huang, G. Rodrigues, T. L. Shen, K. J. Labori, I. M. B. Lothe, E. H. Kure, J. Hernandez, A. Doussot, S. H. Ebbesen, P. M. Grandgenett, M. A. Hollingsworth, M. Jain, K. Mallya, S. K. Batra, W. R. Jarnagin, R. E. Schwartz, I. Matei, H. Peinado, B. Z. Stanger, J. Bromberg, and D. Lyden, "Pancreatic cancer exosomes initiate pre-metastatic niche formation in the liver," *Nature Cell Biology*, vol. 17, no. 6, pp. 816–826, 2015.

[66] N. Amabile, S. Cheng, J. M. Renard, M. G. Larson, A. Ghorbani, E. McCabe, G. Griffin, C. Guerin, J. E. Ho, S. Y. Shaw, K. S. Cohen, R. S. Vasan, A. Tedgui, C. M. Boulanger, and T. J. Wang, "Association of circulating endothelial microparticles with cardiometabolic risk factors in the Framingham Heart Study," *European Heart Journal*, vol. 35, no. 42, pp. 2972–2979, 2014.

[67] H. Sheng, S. Hassanali, C. Nugent, L. Wen, E. Hamilton-Williams, P. Dias, and Y. D. Dai, "Insulinoma-Released Exosomes or Microparticles Are Immunostimulatory and Can Activate Autoreactive T Cells Spontaneously Developed in Nonobese Diabetic Mice," *The Journal of Immunology*, vol. 187, no. 4, pp. 1591–1600, 2011.

[68] K. Esposito, M. Ciotola, B. Schisano, R. Gualdiero, L. Sardelli, L. Misso, G. Giannetti, and D. Giugliano, "Endothelial microparticles correlate with endothelial dysfunction in obese women," *Journal of Clinical Endocrinology and Metabolism*, vol. 91, no. 9, pp. 3676–3679, 2006.

[69] B. Aulston, Q. Liu, M. Mante, J. Florio, R. A. Rissman, and S. H. Yuan, "Extracellular Vesicles Isolated from Familial Alzheimer's Disease Neuronal Cultures Induce Aberrant Tau Phosphorylation in the Wild-Type Mouse Brain," *Journal of Alzheimer's Disease*, vol. 72, no. 2, pp. 575–585, 2019.

[70] B. M. Coleman and A. F. Hill, "Extracellular vesicles - Their role in the packaging and spread of misfolded proteins associated with neurodegenerative diseases," *Seminars in Cell and Developmental Biology*, vol. 40, pp. 89–96, 2015.

[71] A. J. Atkinson, W. A. Colburn, V. G. DeGruttola, D. L. DeMets, G. J. Downing, D. F. Hoth, J. A. Oates, C. C. Peck, R. T. Schooley, B. A. Spilker, J. Woodcock, and S. L. Zeger, "Biomarkers and surrogate endpoints: Preferred definitions and conceptual framework," *Clinical Pharmacology and Therapeutics*, vol. 69, no. 3, pp. 89–95, 2001.

[72] P. Gomes, F. Tzouanou, K. Skolariki, A. Vamvaka-Iakovou, C. Noguera-Ortiz, K. Tsirtsaki, C. L. Waites, P. Vlamos, N. Sousa, B. Costa-Silva, D. Kapogiannis, and I. Sotiropoulos, "Extracellular vesicles and Alzheimer's disease in the novel era of Precision Medicine: implications for disease progression, diagnosis and treatment," *Experimental Neurology*, vol. 358, no. 114183, pp. 1–17, 2022.

[73] A. Gustavsson, N. Norton, T. Fast, L. Frölich, J. Georges, D. Holzapfel, T. Kirabali, P. Krolak-Salmon, P. M. Rossini, M. T. Ferretti, L. Lanman, A. S. Chadha, and W. M. van der Flier, "Global estimates on the number of persons across the Alzheimer's disease continuum," *Alzheimer's and Dementia*, vol. 19, no. 2, pp. 658–670, 2023.

[74] "2023 Alzheimer's disease facts and figures," *Alzheimer's and Dementia*, vol. 19, no. 4, pp. 1598–1695, 2023.

[75] M. A. Busche and B. T. Hyman, "Synergy between amyloid-β and tau in Alzheimer's disease," *Nature Neuroscience*, vol. 23, no. 10, pp. 1183–1193, 2020.

[76] S. Mankhong, S. Kim, S. Lee, H. B. Kwak, D. H. Park, K. L. Joa, and J. H. Kang, "Development of Alzheimer's Disease Biomarkers: From CSF-to Blood-Based Biomarkers," *Biomedicines*, vol. 10, no. 850, pp. 1–19, 2022.

[77] E. H. Thijssen *et. al.*, "Plasma phosphorylated tau 217 and phosphorylated tau 181 as biomarkers in Alzheimer's disease and frontotemporal lobar degeneration: a retrospective diagnostic performance study," *The Lancet Neurology*, vol. 20, no. 9, pp. 739–752, 2021.

[78] H. Asai, S. Ikezu, S. Tsunoda, M. Medalla, J. Luebke, T. Haydar, B. Wolozin, O. Butovsky, S. Kügler, and T. Ikezu, "Depletion of microglia and inhibition of exosome synthesis halt tau propagation," *Nature Neuroscience*, vol. 18, no. 11, pp. 1584–1593, 2015.

[79] Z. Ruan, D. Pathak, S. Venkatesan Kalavai, A. Yoshii-Kitahara, S. Muraoka, N. Bhatt, K. Takamatsu-Yukawa, J. Hu, Y. Wang, S. Hersh, M. Ericsson, S. Gorantla, H. E. Gendelman, R. Kayed, S. Ikezu, J. I. Luebke, and T. Ikezu, "Alzheimer's disease brain-derived extracellular vesicles spread tau pathology in interneurons," *Brain*, vol. 144, no. 1, pp. 288–309, 2021.

[80] S. Muraoka, A. M. DeLeo, M. K. Sethi, K. Yukawa-Takamatsu, Z. Yang, J. Ko, J. D. Hogan, Z. Ruan, Y. You, Y. Wang, M. Medalla, S. Ikezu, M. Chen, W. Xia, S. Gorantla, H. E. Gendelman, D. Issadore, J. Zaia, and T. Ikezu, "Proteomic and biological profiling

of extracellular vesicles from Alzheimer's disease human brain tissues," *Alzheimer's and Dementia*, vol. 16, no. 6, pp. 896–907, 2020.

[81] M. S. Fiandaca, D. Kapogiannis, M. Mapstone, A. Boxer, E. Eitan, J. B. Schwartz, E. L. Abner, R. C. Petersen, H. J. Federoff, B. L. Miller, and E. J. Goetzl, "Identification of preclinical Alzheimer's disease by a profile of pathogenic proteins in neurally derived blood exosomes: A case-control study," *Alzheimer's and Dementia*, vol. 11, no. 6, pp. 600–607, 2015.

[82] Y. Wang, V. Balaji, S. Kaniyappan, L. Krüger, S. Irsen, K. Tepper, R. Chandupatla, W. Maetzler, A. Schneider, E. Mandelkow, and E. M. Mandelkow, "The release and trans-synaptic transmission of Tau via exosomes," *Molecular Neurodegeneration*, vol. 12, no. 5, pp. 1–25, 2017.

[83] M. Iba, J. L. Guo, J. D. McBride, B. Zhang, J. Q. Trojanowski, and V. M. Lee, "Synthetic tau fibrils mediate transmission of neurofibrillary tangles in a transgenic mouse model of alzheimer's-like tauopathy," *The Journal of Neuroscience*, vol. 33, no. 3, pp. 1024–1037, 2013.

[84] F. Delgado-Peraza, C. J. Nogueras-Ortiz, O. Volpert, D. Liu, E. J. Goetzl, M. P. Mattson, N. H. Greig, E. Eitan, and D. Kapogiannis, "Neuronal and astrocytic extracellular vesicle biomarkers in blood reflect brain pathology in mouse models of alzheimer's disease," *Cells*, vol. 10, no. 993, pp. 1–15, 2021.

[85] S. Palmqvist, P. Tideman, N. Mattsson-Carlgren, S. E. Schindler, R. Smith, R. Ossenkoppele, S. Calling, T. West, M. Monane, P. B. Verghese, J. B. Braunstein, K. Blennow, S. Janelidze, E. Stomrud, G. Salvadó, and O. Hansson, "Blood Biomarkers to Detect Alzheimer Disease in Primary Care and Secondary Care," *JAMA*, vol. 332, no. 15, pp. 1245–1257, 2024.

[86] L. Alvarez-Erviti, Y. Seow, H. Yin, C. Betts, S. Lakhal, and M. J. Wood, "Delivery of siRNA to the mouse brain by systemic injection of targeted exosomes," *Nature Biotechnology*, vol. 29, no. 4, pp. 341–345, 2011.

[87] D. M. Morales-Prieto, J. M. Murrieta-Coxca, M. Stojiljkovic, C. Diezel, P. E. Streicher, J. A. Henao-Restrepo, F. Röstel, J. Lindner, O. W. Witte, S. Weis, C. Schmeer, and M. Marz, "Small Extracellular Vesicles from Peripheral Blood of Aged Mice Pass the Blood-Brain Barrier and Induce Glial Cell Activation," *Cells*, vol. 11, no. 625, pp. 1–14, 2022.

[88] A. M. Dickens, L. B. Tovar-Y-Romo, S.-W. Yoo, A. L. Trout, M. Bae, M. Kanmogne, B. Megra, D. W. Williams, K. W. Witwer, M. Gacias, N. Tabatadze, R. N. Cole, P. Casaccia, J. W. Berman, D. C. Anthony, and N. J. Haughey, "Astrocyte-shed extracellular vesicles regulate the peripheral leukocyte response to inflammatory brain lesions," *Science Signaling*, vol. 10, no. eaai7696, pp. 1–12, 2017.

[89] A. G. Yates, R. C. Pink, U. Erdbrügger, P. R. Siljander, E. R. Dellar, P. Pantazi, N. Akbar, W. R. Cooke, M. Vatish, E. Dias-Neto, D. C. Anthony, and Y. Couch, "In sickness and in health: The functional role of extracellular vesicles in physiology and pathology

in vivo: Part I: Health and Normal Physiology," *Journal of Extracellular Vesicles*, vol. 11, no. e12151, pp. 1–19, 2022.

[90] M. Colombo, G. Raposo, and C. Théry, "Biogenesis, secretion, and intercellular interactions of exosomes and other extracellular vesicles," *Annual Review of Cell and Developmental Biology*, vol. 30, pp. 255–289, 2014.

[91] E. Willms, H. J. Johansson, I. Mäger, Y. Lee, K. E. M. Blomberg, M. Sadik, A. Alaarg, C. I. Smith, J. Lehtiö, S. El Andaloussi, M. J. Wood, and P. Vader, "Cells release subpopulations of exosomes with distinct molecular and biological properties," *Scientific Reports*, vol. 6, no. 22519, pp. 1–12, 2016.

[92] D. K. Jeppesen, Q. Zhang, J. L. Franklin, and R. J. Coffey, "Extracellular vesicles and nanoparticles: emerging complexities," *Trends in Cell Biology*, vol. 33, no. 8, pp. 667–681, 2023.

[93] T. Liangsupree, E. Multia, and M. L. Riekkola, "Modern isolation and separation techniques for extracellular vesicles," *Journal of Chromatography A*, vol. 1636, no. 461773, pp. 1–17, 2021.

[94] G. Midekessa, K. Godakumara, J. Ord, J. Viil, F. Lättekivi, K. Dissanayake, S. Kopanchuk, A. Rinken, A. Andronowska, S. Bhattacharjee, T. Rinken, and A. Fazeli, "Zeta Potential of Extracellular Vesicles: Toward Understanding the Attributes that Determine Colloidal Stability," *ACS Omega*, vol. 5, no. 27, pp. 16701–16710, 2020.

[95] A. Longobardi, R. Nicsanu, S. Bellini, R. Squitti, M. Catania, P. Tiraboschi, C. Saraceno, C. Ferrari, R. Zanardini, G. Binetti, G. Di Fede, L. Benussi, and R. Ghidoni, "Cerebrospinal Fluid EV Concentration and Size Are Altered in Alzheimer's Disease and Dementia with Lewy Bodies," *Cells*, vol. 11, no. 462, pp. 1–11, 2022.

[96] M. Auber and P. Svenningsen, "An estimate of extracellular vesicle secretion rates of human blood cells," *Journal of Extracellular Biology*, vol. 1, no. e46, pp. 1–9, 2022.

[97] F. A. Alzahrani and I. M. Saadeldin, eds., *Role of Exosomes in Biological Communication Systems*. Springer Nature Singapore, 2021.

[98] R. Linares, S. Tan, C. Gounou, N. Arraud, and A. R. Brisson, "High-speed centrifugation induces aggregation of extracellular vesicles," *J. Extracell. Vesicles*, vol. 4, no. 1, p. 29509, 2015.

[99] I. Metatla, K. Roger, C. Chhuon, S. Ceccacci, M. Chapelle, Pierre-Olivier Schmit, V. Demichev, and I. C. Guerrera, "Neat plasma proteomics: getting the best out of the worst," *Clinical Proteomics*, vol. 21, no. 22, pp. 1–12, 2024.

[100] R. Khanabdali, M. Mandrekar, R. Grygiel, P.-A. Vo, C. Palma, S. Nikseresht, S. Barton, M. Shojaee, S. Bhuiyan, K. Asari, S. Belzer, K. Ansari, J. I. Coward, L. Perrin, J. Hooper, D. Guanzon, A. Lai, C. Salomon, K. Kershner, C. Newton, D. Horejsh, and G. Rice, "High throughput Surface Epitope Immunoaffinity Isolation of Extracellular Vesicles and Downstream Analysis," *Biology Methods and Protocols*, vol. 9, no. 1, pp. 1–11, 2024.

[101] C. Chen, J. Skog, C. H. Hsu, R. T. Lessard, L. Balaj, T. Wurdinger, B. S. Carter, X. O. Breakefield, M. Toner, and D. Irimia, "Microfluidic isolation and transcriptome analysis of serum microvesicles," *Lab on a Chip*, vol. 10, no. 4, pp. 505–511, 2010.

[102] Z. Zhao, Y. Yang, Y. Zeng, and M. He, "A microfluidic ExoSearch chip for multiplexed exosome detection towards blood-based ovarian cancer diagnosis," *Lab on a Chip*, vol. 16, no. 3, pp. 489–496, 2016.

[103] M. Sancho-Albero, V. Sebastián, J. Sesé, R. Pazo-Cid, G. Mendoza, M. Arruebo, P. Martín-Duque, and J. Santamaría, "Isolation of exosomes from whole blood by a new microfluidic device: proof of concept application in the diagnosis and monitoring of pancreatic cancer," *Journal of Nanobiotechnology*, vol. 18, no. 150, pp. 1–15, 2020.

[104] S. S. Kanwar, C. J. Dunlay, D. M. Simeone, and S. Nagrath, "Microfluidic device (ExoChip) for on-chip isolation, quantification and characterization of circulating exosomes," *Lab on a Chip*, vol. 14, no. 11, pp. 1891–1900, 2014.

[105] P. Zhang, M. He, and Y. Zeng, "Ultrasensitive microfluidic analysis of circulating exosomes using a nanostructured graphene oxide/polydopamine coating," *Lab on a Chip*, vol. 16, no. 16, pp. 3033–3042, 2016.

[106] T. W. Lo, Z. Zhu, E. Purcell, D. Watza, J. Wang, Y. T. Kang, S. Jolly, D. Nagrath, and S. Nagrath, "Microfluidic device for high-throughput affinity-based isolation of extracellular vesicles," *Lab on a Chip*, vol. 20, no. 10, pp. 1762–1770, 2020.

[107] Q. Yang, L. Cheng, L. Hu, D. Lou, T. Zhang, J. Li, Q. Zhu, and F. Liu, "An integrative microfluidic device for isolation and ultrasensitive detection of lung cancer-specific exosomes from patient urine," *Biosensors and Bioelectronics*, vol. 163, no. 112290, pp. 1–8, 2020.

[108] J. Wang, W. Li, L. Zhang, L. Ban, P. Chen, W. Du, X. Feng, and B. F. Liu, "Chemically Edited Exosomes with Dual Ligand Purified by Microfluidic Device for Active Targeted Drug Delivery to Tumor Cells," *ACS Applied Materials and Interfaces*, vol. 9, no. 33, pp. 27441–27452, 2017.

[109] N. Kamyabi, R. Abbasgholizadeh, A. Maitra, A. Ardekani, S. L. Biswal, and K. J. Grande-Allen, "Isolation and mutational assessment of pancreatic cancer extracellular vesicles using a microfluidic platform," *Biomedical Microdevices*, vol. 22, no. 23, pp. 1–11, 2020.

[110] F. Liu, O. Vermesh, V. Mani, T. J. Ge, S. J. Madsen, A. Sabour, E. C. Hsu, G. Gowrishankar, M. Kanada, J. V. Jokerst, R. G. Sierra, E. Chang, K. Lau, K. Sridhar, A. Bermudez, S. J. Pitteri, T. Stoyanova, R. Sinclair, V. S. Nair, S. S. Gambhir, and U. Demirci, "The Exosome Total Isolation Chip," *ACS Nano*, vol. 11, no. 11, pp. 10712–10723, 2017.

[111] H. K. Woo, V. Sunkara, J. Park, T. H. Kim, J. R. Han, C. J. Kim, H. I. Choi, Y. K. Kim, and Y. K. Cho, "Exodisc for Rapid, Size-Selective, and Efficient Isolation and Analysis of Nanoscale Extracellular Vesicles from Biological Samples," *ACS Nano*, vol. 11, no. 2, pp. 1360–1370, 2017.

[112] Z. Wang, H. J. Wu, D. Fine, J. Schmulen, Y. Hu, B. Godin, J. X. Zhang, and X. Liu, "Ciliated micropillars for the microfluidic-based isolation of nanoscale lipid vesicles," *Lab on a Chip*, vol. 13, no. 15, pp. 2879–2882, 2013.

[113] Y. T. Yeh, Y. Zhou, D. Zou, H. Liu, H. Yu, H. Lu, V. Swaminathan, Y. Mao, and M. Terrones, "Rapid Size-Based Isolation of Extracellular Vesicles by Three-Dimensional Carbon Nanotube Arrays," *ACS Applied Materials and Interfaces*, vol. 12, no. 11, pp. 13134–13139, 2020.

[114] S. Shin, D. Han, M. C. Park, J. Y. Mun, J. Choi, H. Chun, S. Kim, and J. W. Hong, "Separation of extracellular nanovesicles and apoptotic bodies from cancer cell culture broth using tunable microfluidic systems," *Scientific Reports*, vol. 7, no. 9907, pp. 1–8, 2017.

[115] A. Liga, A. D. Vliegenthart, W. Oosthuyzen, J. W. Dear, and M. Kersaudy-Kerhoas, "Exosome isolation: A microfluidic road-map," *Lab on a Chip*, vol. 15, no. 11, pp. 2388–2394, 2015.

[116] L. R. Huang, E. C. Cox, R. H. Austin, and J. C. Sturm, "Continuous Particle Separation Through Deterministic Lateral Displacement," *Science*, vol. 304, no. 5673, pp. 983–987, 2004.

[117] J. T. Smith, B. H. Wunsch, N. Dogra, M. E. Ahsen, K. Lee, K. K. Yadav, R. Weil, M. A. Pereira, J. V. Patel, E. A. Duch, J. M. Papalia, M. F. Lofaro, M. Gupta, A. K. Tewari, C. Cordon-Cardo, G. Stolovitzky, and S. M. Gifford, "Integrated nanoscale deterministic lateral displacement arrays for separation of extracellular vesicles from clinically-relevant volumes of biological samples," *Lab on a Chip*, vol. 18, no. 24, pp. 3913–3925, 2018.

[118] C. Liu, B. Ding, C. Xue, Y. Tian, G. Hu, and J. Sun, "Sheathless focusing and separation of diverse nanoparticles in viscoelastic solutions with minimized shear thinning," *Analytical Chemistry*, vol. 88, no. 24, pp. 12547–12553, 2016.

[119] I. De Santo, G. D'Avino, G. Romeo, F. Greco, P. A. Netti, and P. L. Maffettone, "Microfluidic lagrangian trap for brownian particles: Three-dimensional focusing down to the nanoscale," *Physical Review Applied*, vol. 2, no. 064001, pp. 1–9, 2014.

[120] C. Liu, J. Zhao, F. Tian, L. Cai, W. Zhang, Q. Feng, J. Chang, F. Wan, Y. Yang, B. Dai, Y. Cong, B. Ding, J. Sun, and W. Tan, "Low-cost thermophoretic profiling of extracellular-vesicle surface proteins for the early detection and classification of cancers," *Nature Biomedical Engineering*, vol. 3, no. 3, pp. 183–193, 2019.

[121] F. Tian, W. Zhang, L. Cai, S. Li, G. Hu, Y. Cong, C. Liu, T. Li, and J. Sun, "Microfluidic co-flow of Newtonian and viscoelastic fluids for high-resolution separation of microparticles," *Lab on a Chip*, vol. 17, no. 18, pp. 3078–3085, 2017.

[122] W. Nakai, T. Yoshida, D. Diez, Y. Miyatake, T. Nishibu, N. Imawaka, K. Naruse, Y. Sadamura, and R. Hanayama, "A novel affinity-based method for the isolation of highly purified extracellular vesicles," *Scientific Reports*, vol. 6, no. 33935, pp. 1–11, 2016.

[123] T. N. T. Dao, M. G. Kim, B. Koo, H. Liu, Y. O. Jang, H. J. Lee, Y. Kim, Y. Park, H. S. Kim, C. Kim, and Y. Shin, "Chimeric nanocomposites for the rapid and simple isolation of urinary extracellular vesicles," *Journal of Extracellular Vesicles*, vol. 11, no. e12195, pp. 1–20, 2022.

[124] S. Jeong, J. Park, D. Pathania, C. M. Castro, R. Weissleder, and H. Lee, "Integrated Magneto-Electrochemical Sensor for Exosome Analysis," *ACS Nano*, vol. 10, no. 2, pp. 1802–1809, 2016.

[125] L. Liu, K. Chen, N. Xiang, and Z. Ni, "Dielectrophoretic manipulation of nanomaterials: A review," *Electrophoresis*, vol. 40, no. 6, pp. 873–889, 2019.

[126] Y. Liu, W. Zhao, R. Cheng, M. Logun, M. D. M. Zayas-Viera, L. Karumbaiah, and L. Mao, "Label-free ferrohydrodynamic separation of exosome-like nanoparticles," *Lab on a Chip*, vol. 20, no. 17, pp. 3187–3201, 2020.

[127] H. Chen, T. Yamakawa, M. Inaba, M. Nakano, and J. Suehiro, "Characterization of Extra-Cellular Vesicle Dielectrophoresis and Estimation of Its Electric Properties," *Sensors*, vol. 22, no. 9, 2022.

[128] S. Marczak, K. Richards, Z. Ramshani, E. Smith, S. Senapati, R. Hill, D. B. Go, and H. C. Chang, "Simultaneous isolation and preconcentration of exosomes by ion concentration polarization," *Electrophoresis*, vol. 39, no. 15, pp. 2029–2038, 2018.

[129] A. Ku, H. C. Lim, M. Evander, H. Lilja, T. Laurell, S. Scheding, and Y. Ceder, "Acoustic Enrichment of Extracellular Vesicles from Biological Fluids," *Analytical Chemistry*, vol. 90, no. 13, pp. 8011–8019, 2018.

[130] A. Ku, N. Ravi, M. Yang, M. Evander, T. Laurell, H. Lilja, and Y. Ceder, "A urinary extracellular vesicle microRNA biomarker discovery pipeline; from automated extracellular vesicle enrichment by acoustic trapping to microRNA sequencing," *PLOS ONE*, vol. 14, no. 5, pp. 1–13, 2019.

[131] M. Rezeli, O. Gidlöf, M. Evander, P. Bryl-Górecka, R. Sathanoori, P. Gilje, K. Pawłowski, P. Horvatovich, D. Erlinge, G. Marko-Varga, and T. Laurell, "Comparative Proteomic Analysis of Extracellular Vesicles Isolated by Acoustic Trapping or Differential Centrifugation," *Analytical Chemistry*, vol. 88, no. 17, pp. 8577–8586, 2016.

[132] A. Broman, A. Lenshof, M. Evander, L. Happonen, A. Ku, J. Malmström, and T. Laurell, "Multinodal Acoustic Trapping Enables High Capacity and High Throughput Enrichment of Extracellular Vesicles and Microparticles in miRNA and MS Proteomics Studies," *Analytical Chemistry*, vol. 93, pp. 3929–3937, 2021.

[133] F. Palm, A. Broman, G. Marcoux, J. W. Semple, T. L. Laurell, J. Malmström, and O. Shannon, "Phenotypic Characterization of Acoustically Enriched Extracellular Vesicles from Pathogen-Activated Platelets," *Journal of Innate Immunity*, vol. 15, pp. 599–613, 2023.

[134] R. Habibi and A. Neild, "Sound wave activated nano-sieve (SWANS) for enrichment of nanoparticles," *Lab on a Chip*, vol. 19, no. 18, pp. 3032–3044, 2019.

[135] K. Lee, H. Shao, R. Weissleder, and H. Lee, "Acoustic purification of extracellular microvesicles," *ACS Nano*, vol. 9, no. 3, pp. 2321–2327, 2015.

[136] M. Wu, Y. Ouyang, Z. Wang, R. Zhang, P. H. Huang, C. Chen, H. Li, P. Li, D. Quinn, M. Dao, S. Suresh, Y. Sadovsky, and T. J. Huang, "Isolation of exosomes from whole blood by integrating acoustics and microfluidics," *Proceedings of the National Academy of Sciences of the United States of America*, vol. 114, no. 40, pp. 10584–10589, 2017.

[137] D. J. Collins, T. Alan, and A. Neild, "Particle separation using virtual deterministic lateral displacement (vDLD)," *Lab on a Chip*, vol. 14, no. 9, pp. 1595–1603, 2014.

[138] M. Wiklund and H. M. Hertz, "Ultrasonic enhancement of bead-based bioaffinity assays," *Lab on a Chip*, vol. 6, no. 10, pp. 1279–1292, 2006.

[139] N. R. Harris, M. Hill, S. Beeby, Y. Shen, N. M. White, J. J. Hawkes, and W. T. Coakley, "A silicon microfluidic ultrasonic separator," *Sensors and Actuators B*, vol. 95, no. 1-3, pp. 425–434, 2003.

[140] H. Bruus, "Acoustofluidics 2: Perturbation theory and ultrasound resonance modes," *Lab on a Chip*, vol. 12, no. 1, pp. 20–28, 2012.

[141] F. Petersson, A. Nilsson, H. Jönsson, and T. Laurell, "Carrier medium exchange through ultrasonic particle switching in microfluidic channels," *Analytical Chemistry*, vol. 77, no. 5, pp. 1216–1221, 2005.

[142] L. E. Kinsler, A. R. Frey, A. B. Coppens, and J. V. Sanders, *Fundamentals of Acoustics*. John Wiley & Sons, Inc., 1950.

[143] K. Yosioka and Y. Kawasima, "Acoustic radiation pressure on a compressible sphere," *Acustica*, vol. 5, pp. 167–173, 1955.

[144] L. P. Gor'kov, "On the forces acting on a small particle in an acoustical field in an ideal fluid," *Soviet Physics*, vol. 6, pp. 773–775, 1962.

[145] M. Settnes and H. Bruus, "Forces acting on a small particle in an acoustical field in a viscous fluid," *Physical Review E*, vol. 85, no. 016327, pp. 1–12, 2012.

[146] P. Augustsson, J. T. Karlsen, H. W. Su, H. Bruus, and J. Voldman, "Iso-acoustic focusing of cells for size-insensitive acousto-mechanical phenotyping," *Nature Communications*, vol. 7, no. 11556, pp. 1–9, 2016.

[147] J. T. Karlsen and H. Bruus, "Forces acting on a small particle in an acoustical field in a thermoviscous fluid," *Physical Review E*, vol. 92, no. 4, 2015.

[148] T. Laurell, F. Petersson, and A. Nilsson, "Chip integrated strategies for acoustic separation and manipulation of cells and particles," *Chemical Society Reviews*, vol. 36, no. 3, pp. 492–506, 2007.

[149] K. Cushing, E. Undvall, Y. Ceder, H. Lilja, and T. Laurell, "Reducing WBC background in cancer cell separation products by negative acoustic contrast particle immuno-acoustophoresis," *Analytica Chimica Acta*, vol. 1000, pp. 256–264, 2018.

[150] W. Qiu, T. Baasch, and T. Laurell, "Enhancement of Acoustic Energy Density in Bulk-Wave-Acoustophoresis Devices Using Side Actuation," *Physical Review Applied*, vol. 17, no. 044043, pp. 1–14, 2022.

[151] M. Antfolk, P. B. Muller, P. Augustsson, H. Bruus, and T. Laurell, "Focusing of sub-micrometer particles and bacteria enabled by two-dimensional acoustophoresis," *Lab on a Chip*, vol. 14, no. 15, pp. 2791–2799, 2014.

[152] D. Van Assche, E. Reithuber, W. Qiu, T. Laurell, B. Henriques-Normark, P. Mellroth, P. Ohlsson, and P. Augustsson, "Gradient acoustic focusing of sub-micron particles for separation of bacteria from blood lysate," *Scientific Reports*, vol. 10, no. 1, 2020.

[153] Y. Tsuyama, B. Xu, K. Hattori, S. Baek, Y. Yoshioka, R. Kojima, Y. Cho, T. Laurell, S. Kim, S. Ota, and S. W. Lee, "A 50 μm acoustic resonator microchannel enables focusing 100 nm polystyrene beads and sub-micron bioparticles," *Sensors and Actuators B*, vol. 376, no. 132918, pp. 1–8, 2023.

[154] B. Hammarström, M. Evander, H. Barbeau, M. Bruzelius, J. Larsson, T. Laurell, and J. Nilsson, "Non-contact acoustic cell trapping in disposable glass capillaries," *Lab on a Chip*, vol. 10, no. 17, pp. 2251–2257, 2010.

[155] B. Hammarström, M. Evander, J. Wahlström, and J. Nilsson, "Frequency tracking in acoustic trapping for improved performance stability and system surveillance," *Lab on a Chip*, vol. 14, no. 5, pp. 1005–1013, 2014.

[156] A. Fornell, T. Baasch, C. Johannesson, J. Nilsson, and M. Tenje, "Binary acoustic trapping in a glass capillary," *Journal of Physics D: Applied Physics*, vol. 54, no. 355401, pp. 1–9, 2021.

[157] M. Gröschl, "Ultrasonic Separation of Suspended Particles-Part I: Fundamentals," *Acta Acustica*, vol. 84, pp. 432–447, 1998.

[158] G. T. Silva and H. Bruus, "Acoustic interaction forces between small particles in an ideal fluid," *Physical Review E*, vol. 90, no. 6, 2014.

[159] T. Baasch, W. Qiu, and T. Laurell, "Gap Distance between Pearl Chains in Acoustic Manipulation," *Physical Review Applied*, vol. 18, no. 014021, pp. 1–10, 2022.

[160] A. R. Mohapatra, S. Sepehrirahnama, and K. M. Lim, "Experimental measurement of interparticle acoustic radiation force in the Rayleigh limit," *Physical Review E*, vol. 97, no. 5, 2018.

[161] S. Sepehrirahnama, F. S. Chau, and K. M. Lim, "Effects of viscosity and acoustic streaming on the interparticle radiation force between rigid spheres in a standing wave," *Physical Review E*, vol. 93, no. 2, 2016.

[162] S. Sepehrirhnama and K. M. Lim, "Generalized potential theory for close-range acoustic interactions in the Rayleigh limit," *Physical Review E*, vol. 102, no. 4, pp. 1–15, 2020.

[163] S. Sepehrirahnama, A. Ray Mohapatra, S. Oberst, Y. K. Chiang, D. A. Powell, and K. M. Lim, "Acoustofluidics 24: theory and experimental measurements of acoustic interaction force," *Lab on a Chip*, vol. 22, no. 18, pp. 3290–3313, 2022.

[164] J. H. Joergensen and H. Bruus, "Theory of pressure acoustics with thermoviscous boundary layers and streaming in elastic cavities," *Journal of the Acoustical Society of America*, vol. 149, no. 5, pp. 3599–3610, 2021.

[165] W. Cui, L. Mu, X. Duan, W. Pang, and M. A. Reed, "Trapping of sub-100 nm nanoparticles using gigahertz acoustofluidic tweezers for biosensing applications," *Nanoscale*, vol. 11, no. 31, pp. 14625–14634, 2019.

[166] D. J. Collins, Z. Ma, J. Han, and Y. Ai, "Continuous micro-vortex-based nanoparticle manipulation via focused surface acoustic waves," *Lab on a Chip*, vol. 17, no. 1, pp. 91–103, 2017.

[167] S. Yazdi and A. M. Ardekani, "Bacterial aggregation and biofilm formation in a vortical flow," *Biomicrofluidics*, vol. 6, no. 4, 2012.

[168] S. Gupta and D. L. Feke, "Acoustically driven collection of suspended particles within porous media," *Ultrasonics*, vol. 35, pp. 131–139, 1997.

[169] B. Hammarström, B. Nilson, T. Laurell, J. Nilsson, and S. Ekström, "Acoustic trapping for bacteria identification in positive blood cultures with MALDI-TOF MS," *Analytical Chemistry*, vol. 86, no. 21, pp. 10560–10567, 2014.

[170] P. Ohlsson, M. Evander, K. Petersson, L. Mellhammar, A. Lehmusvuori, U. Karhunen, M. Soikkeli, T. Seppä, E. Tuunainen, A. Spangar, P. Von Lode, K. Rantakokko-Jalava, G. Otto, S. Scheding, T. Soukka, S. Wittfooth, and T. Laurell, "Integrated Acoustic Separation, Enrichment, and Microchip Polymerase Chain Reaction Detection of Bacteria from Blood for Rapid Sepsis Diagnostics," *Analytical Chemistry*, vol. 88, no. 19, pp. 9403–9411, 2016.

[171] O. Gidlöf, M. Evander, M. Rezeli, G. Marko-Varga, T. Laurell, and D. Erlinge, "Proteomic profiling of extracellular vesicles reveals additional diagnostic biomarkers for myocardial infarction compared to plasma alone," *Scientific Reports*, vol. 9, no. 8991, pp. 1–13, 2019.

[172] P. Bryl-Górecka, R. Sathanoori, L. Arevström, R. Landberg, C. Bergh, M. Evander, B. Olde, T. Laurell, O. Fröbert, and D. Erlinge, "Bilberry Supplementation after Myocardial Infarction Decreases Microvesicles in Blood and Affects Endothelial Vesiculation," *Molecular Nutrition and Food Research*, vol. 64, no. 2000108, pp. 1–10, 2020.

[173] A. Ku, J. Fredsøe, K. D. Sørensen, M. Borre, M. Evander, T. Laurell, H. Lilja, and Y. Ceder, "High-Throughput and Automated Acoustic Trapping of Extracellular Vesicles to Identify microRNAs With Diagnostic Potential for Prostate Cancer," *Frontiers in Oncology*, vol. 11, no. 631021, pp. 1–13, 2021.

[174] M. Costa, B. Hammarström, L. van der Geer, S. Tanriverdi, H. N. Joensson, M. Wiklund, and A. Russom, "EchoGrid: High-Throughput Acoustic Trapping for Enrichment of Environmental Microplastics," *Analytical Chemistry*, vol. 96, no. 23, pp. 9493–9502, 2024.

[175] S. Lu, K. Zhu, W. Song, G. Song, D. Chen, T. Hayat, N. S. Alharbi, C. Chen, and Y. Sun, "Impact of water chemistry on surface charge and aggregation of polystyrene microspheres suspensions," *Science of the Total Environment*, vol. 630, pp. 951–959, 2018.

[176] W. Jiang and Irgum Knut, "United Sates Patent Application Publication: Zwitterionic stationary phase as well as method for using and producing said phase," 2010.

[177] E. Wikberg, J. J. Verhage, C. Viklund, and K. Irgum, "Grafting of silica with sulfobetaine polymers via aqueous reversible addition fragmentation chain transfer polymerization and its use as a stationary phase in HILIC," *Journal of Separation Science*, vol. 32, no. 12, pp. 2008–2016, 2009.

[178] W. Jiang and K. Irgum, "Tentacle-Type Zwitterionic Stationary Phase Prepared by Surface-Initiated Graft Polymerization of 3-[N,N-Dimethyl-N-(Methacryloyloxyethyl)-ammonium] Propanesulfonate through Peroxide Groups Tethered on Porous Silica," *Analytical Chemistry*, vol. 74, no. 18, pp. 4682–4687, 2002.

[179] W. Jiang and K. Irgum, "Covalently bonded polymeric zwitterionic stationary phase for simultaneous separation of inorganic cations and anions," *Analytical Chemistry*, vol. 71, no. 2, pp. 333–344, 1999.

[180] D. D. Carlo, L. Y. Wu, and L. P. Lee, "Dynamic single cell culture array," *Lab on a Chip*, vol. 6, no. 11, pp. 1445–1449, 2006.

[181] M. Tayebi, Y. Zhou, P. Tripathi, R. Chandramohanadas, and Y. Ai, "Exosome Purification and Analysis Using a Facile Microfluidic Hydrodynamic Trapping Device," *Analytical Chemistry*, vol. 92, no. 15, pp. 10733–10742, 2020.

[182] S. S. Sadhal, "Acoustofluidics 13: Analysis of acoustic streaming by perturbation methods," *Lab on a Chip*, vol. 12, no. 13, pp. 2292–2300, 2012.

[183] T. Baasch, A. Pavlic, and J. Dual, "Acoustic radiation force acting on a heavy particle in a standing wave can be dominated by the acoustic microstreaming," *Physical Review E*, vol. 100, no. 061102, pp. 1–5, 2019.

[184] B. G. Winckelmann and H. Bruus, "Acoustic radiation force on a spherical thermoviscous particle in a thermoviscous fluid including scattering and microstreaming," *Physical Review E*, vol. 107, no. 6, 2023.

[185] G. Zhang, W. Cui, W. Pang, S. Liu, S. Ning, X. Li, and M. Reed, "Programmable and Parallel Trapping of Submicron/Nanoscale Particles Using Acoustic Micro-Pillar Array Chip," *Advanced Materials Interfaces*, vol. 8, no. 24, 2021.

[186] A. Surolia, D. Pain, and M. I. Khan, "Protein A: nature's universal anti-antibody," *Elsevier Biomedical Press*, vol. 6, no. 03, pp. 74–76, 1982.

[187] V. Filipe, A. Hawe, and W. Jiskoot, "Critical evaluation of nanoparticle tracking analysis (NTA) by NanoSight for the measurement of nanoparticles and protein aggregates," *Pharmaceutical Research*, vol. 27, no. 5, pp. 796–810, 2010.

[188] R. Vogel, J. Savage, J. Muzard, G. D. Camera, G. Vella, A. Law, M. Marchioni, D. Mehn, O. Geiss, B. Peacock, D. Aubert, L. Calzolai, F. Caputo, and A. Prina-Mello, "Measuring particle concentration of multimodal synthetic reference materials and extracellular vesicles with orthogonal techniques: Who is up to the challenge?," *Journal of Extracellular Vesicles*, vol. 10, no. e12052, pp. 1–28, 2021.

[189] D. Bachurski, M. Schuldner, P. H. Nguyen, A. Malz, K. S. Reiners, P. C. Grenzi, F. Babatz, A. C. Schauss, H. P. Hansen, M. Hallek, and E. Pogge von Strandmann, "Extracellular vesicle measurements with nanoparticle tracking analysis–An accuracy and repeatability comparison between NanoSight NS300 and ZetaView," *Journal of Extracellular Vesicles*, vol. 8, no. 1596016, pp. 1–18, 2019.

[190] A. Bateman *et. al.*, "UniProt: the Universal Protein Knowledgebase in 2023," *Nucleic Acids Research*, vol. 51, no. D1, pp. D523–D531, 2023.

[191] P. A. Dalgarno, J. Juan-Colás, G. J. Hedley, L. Piñeiro, M. Novo, C. Perez-Gonzalez, I. D. Samuel, M. C. Leake, S. Johnson, W. Al-Soufi, J. C. Penedo, and S. D. Quinn, "Unveiling the multi-step solubilization mechanism of sub-micron size vesicles by detergents," *Scientific Reports*, vol. 9, no. 12897, pp. 1–11, 2019.

[192] P. K. Smith, R. I. Krohn, G. T. Hermanson, A. K. Mallia, F. H. Gartner, M. D. Provenzano, E. K. Fujimoto, N. M. Goeke, B. J. Olson, and D. C. Klenk, "Measurement of Protein Using Bicinchoninic Acid," *Analytical Biochemistry*, vol. 150, pp. 76–85, 1985.

[193] A. Makarov, "Electrostatic axially harmonic orbital trapping: A high-performance technique of mass analysis," *Analytical Chemistry*, vol. 72, no. 6, pp. 1156–1162, 2000.

[194] T. Guo, J. A. Steen, and M. Mann, "Mass-spectrometry-based proteomics: from single cells to clinical applications.," *Nature*, vol. 638, no. 8052, pp. 901–911, 2025.

[195] R. Aebersold and M. Mann, "Mass spectrometry-based proteomics," *Nature*, vol. 422, pp. 198–207, 2003.

[196] L. C. Gillet, P. Navarro, S. Tate, H. Röst, N. Selevsek, L. Reiter, R. Bonner, and R. Aebersold, "Targeted data extraction of the MS/MS spectra generated by data-independent acquisition: A new concept for consistent and accurate proteome analysis," *Molecular and Cellular Proteomics*, vol. 11, no. 6, 2012.

[197] S. Eliuk and A. Makarov, "Evolution of Orbitrap Mass Spectrometry Instrumentation," *Annual Review of Analytical Chemistry*, vol. 8, pp. 61–80, 2015.

[198] J. K. Eng, A. L. Mccormack, and J. R. Yates, "An Approach to Correlate Tandem Mass Spectral Data of Peptides with Amino Acid Sequences in a Protein Database," *Journal of American Society for Mass Spectrometry*, vol. 5, pp. 976–989, 1994.

[199] V. Demichev, C. B. Messner, S. I. Vernardis, K. S. Lilley, and M. Ralser, "DIA-NN: neural networks and interference correction enable deep proteome coverage in high throughput," *Nature Methods*, vol. 17, no. 1, pp. 41–44, 2020.

[200] C. C. Wu, K. A. Tsantilas, J. Park, D. Plubell, P. Naicker, I. Govender, S. Buthelezi, S. Stoychev, J. Jordaan, G. Merrihew, E. Huang, E. D. Parker, M. Riffle, A. N. Hoofnagle, and M. J. Maccoss, "Mag-Net: Rapid enrichment of membrane-bound particles enables high coverage quantitative analysis of the plasma proteome," *bioRxiv preprint doi: https://doi.org/10.1101/2023.06.10.544439*, 2023.

[201] S. Janelidze, D. Bali, N. J. Ashton, N. R. Barthelemy, J. Vanbrabant, E. Stoops, E. Vanmechelen, Y. He, A. O. Dolado, G. Triana-Baltzer, M. J. Pontecorvo, H. Zetterberg, H. Kolb, M. Vandijck, K. Blennow, R. J. Bateman, and O. Hansson, "Head-to-head comparison of 10 plasma phospho-tau assays in prodromal Alzheimer's disease," *Brain*, vol. 146, no. 4, pp. 1592–1601, 2023.

[202] U. S. Sandau, S. M. Magaña, J. Costa, J. P. Nolan, T. Ikezu, L. J. Vella, H. K. Jackson, L. R. Moreira, P. L. Palacio, A. F. Hill, J. F. Quinn, K. R. Van Keuren-Jensen, T. J. McFarland, J. Palade, E. A. Sribnick, H. Su, K. Vekrellis, B. Coyle, Y. Yang, J. M. Falcón-Perez, R. Nieuwland, and J. A. Saugstad, "Recommendations for reproducibility of cerebrospinal fluid extracellular vesicle studies," *Journal of Extracellular Vesicles*, vol. 13, no. 1, 2024.

[203] R. Pyati and M. M. Richter, "ECL - Electrochemical luminescence," *Annual Reports on the Progress of Chemistry - Section C*, vol. 103, pp. 12–78, 2007.

[204] J. Hanes, A. Kovac, H. Kvartsberg, E. Kontsekova, L. Fialova, S. Katina, B. Kovacech, E. Stevens, J. Hort, M. Vyhnalek, L. Boonkamp, M. Novak, H. Zetterberg, O. Hansson, P. Scheltens, K. Blennow, C. E. Teunissen, and N. Zilka, "Evaluation of a novel immunoassay to detect p-tau Thr217 in the CSF to distinguish Alzheimer disease from other dementias," *Neurology*, vol. 95, no. 22, pp. E3026–E3035, 2020.

[205] S. Janelidze, E. Stomrud, R. Smith, S. Palmqvist, N. Mattsson, D. C. Airey, N. K. Proctor, X. Chai, S. Shcherbinin, J. R. Sims, G. Triana-Baltzer, C. Theunis, R. Slemmon, M. Mercken, H. Kolb, J. L. Dage, and O. Hansson, "Cerebrospinal fluid p-tau217 performs better than p-tau181 as a biomarker of Alzheimer's disease," *Nature Communications*, vol. 11, no. 1683, 2020.

[206] Y. Fan, C. Pionneau, F. Cocozza, P. Y. Boëlle, S. Chardonnet, S. Charrin, C. Théry, P. Zimmermann, and E. Rubinstein, "Differential proteomics argues against a general role for CD9, CD81 or CD63 in the sorting of proteins into extracellular vesicles," *Journal of Extracellular Vesicles*, vol. 12, no. 12352, pp. 1–18, 2023.

[207] A. de Menezes-Neto, M. J. Sáez, I. Lozano-Ramos, J. Segui-Barber, L. Martin-Jaular, J. M. Ullate, C. Fernandez-Becerra, F. E. Borrás, and H. A. del Portillo, "Size-exclusion chromatography as a stand-alone methodology identifies novel markers in mass spectrometry analyses of plasma-derived vesicles from healthy individuals," *Journal of Extracellular Vesicles*, vol. 4, no. 12352, pp. 1–18, 2015.

[208] T. Rabilloud, "Membrane proteins ride shotgun," *Nature Biotechnology*, vol. 21, pp. 508–510, 2003.

[209] Y. You, Z. Zhang, N. Sultana, M. Ericsson, Y. A. Martens, M. Sun, T. Kanekiyo, S. Ikezu, S. A. Shaffer, and T. Ikezu, "ATP1A3 as a target for isolating neuron-specific extracellular vesicles from human brain and biofluids," *Science Advances*, vol. 9, no. 37, 2023.

[210] Y. You, S. Muraoka, M. P. Jedrychowski, J. Hu, A. K. McQuade, T. Young-Pearse, R. Aslebagh, S. A. Shaffer, S. P. Gygi, M. Blurton-Jones, W. W. Poon, and T. Ikezu, "Human neural cell type-specific extracellular vesicle proteome defines disease-related molecules associated with activated astrocytes in Alzheimer's disease brain," *Journal of Extracellular Vesicles*, vol. 11, no. 1e12183, pp. 1–23, 2022.

[211] L. Dietz, J. Oberländer, A. Mateos-Maroto, J. Schunke, M. Fichter, E. M. Krämer-Albers, K. Landfester, and V. Mailänder, "Uptake of extracellular vesicles into immune cells is enhanced by the protein corona," *Journal of Extracellular Vesicles*, vol. 12, no. 12, 2023.

[212] A. Musicò, R. Zenatelli, M. Romano, A. Zendrini, S. Alacqua, S. Tassoni, L. Paolini, C. Urbinati, M. Rusnati, P. Bergese, G. Pomarico, and A. Radeghieri, "Surface functionalization of extracellular vesicle nanoparticles with antibodies: a first study on the protein corona "variable"," *Nanoscale Advances*, vol. 5, no. 18, pp. 4703–4717, 2023.

[213] C. Liu, X. Xu, B. Li, B. Situ, W. Pan, Y. Hu, T. An, S. Yao, and L. Zheng, "Single-Exosome-Counting Immunoassays for Cancer Diagnostics," *Nano Letters*, vol. 18, no. 7, pp. 4226–4232, 2018.

[214] Z. J. Smith, C. Lee, T. Rojalin, R. P. Carney, S. Hazari, A. Knudson, K. Lam, H. Saari, E. L. Ibañez, T. Viitala, T. Laaksonen, M. Yliperttula, and S. Wachsmann-Hogiu, "Single exosome study reveals subpopulations distributed among cell lines with variability related to membrane content," *Journal of Extracellular Vesicles*, vol. 4, no. 28533, 2015.

[215] R. P. Carney, S. Hazari, M. Colquhoun, D. Tran, B. Hwang, M. S. Mulligan, J. D. Bryers, E. Girda, G. S. Leiserowitz, Z. J. Smith, and K. S. Lam, "Multispectral Optical Tweezers for Biochemical Fingerprinting of CD9-Positive Exosome Subpopulations," *Analytical Chemistry*, vol. 89, no. 10, pp. 5357–5363, 2017.

[216] A. Kumar, D. Roberts, K. E. Wood, B. Light, J. E. Parrillo, S. Sharma, R. Suppes, D. Feinstein, S. Zanotti, L. Taiberg, D. Gurka, A. Kumar, and M. Cheang, "Duration of hypotension before initiation of effective antimicrobial therapy is the critical determinant of survival in human septic shock," *Critical Care Medicine*, vol. 34, no. 6, pp. 1589–1596, 2006.